# SYSTEMATIC ANALYSIS OF THE SIGNAL RESPONSIVE GENE REGULATORY NETWORK GOVERNING *MYXOCOCCUS XANTHUS* DEVELOPMENT

By

Shreya Saha

A DISSERTATION

Submitted to
Michigan State University
in partial fulfillment of the requirements
for the degree of

Cell and Molecular Biology – Doctor of Philosophy

2020

ABSTRACT

SYSTEMATIC ANALYSIS OF THE SIGNAL RESPONSIVE GENE REGULATORY NETWORK GOVERNING *MYXOCOCCUS XANTHUS* DEVELOPMENT

By

Shreya Saha

Studies of signal-induced gene expression in bacteria have contributed to understanding of how bacteria cope with environmental stress. As an extensively studied model, *Myxococcus xanthus* provides fascinating insights into how changes at the level of gene expression enable which bacteria to survive environmental insults such as nutrient limitation. Upon starvation *M. xanthus* cells glide into aggregates and form mounds that mature into fruiting bodies as some cells form spores. Previously, our group defined 24-30 h poststarvation as the critical period for commitment to spore formation, when cells commit to form spores despite perturbation of the starvation signal by nutrient addition. The process of multicellular development that culminates in sporulation is governed by a network of signal-responsive transcription factors that integrate signals for starvation and cellular alignment. In this dissertation I present the first systematic approach to elucidate the network dynamics during the commitment period.

In the network, MrpC is a starvation-responsive transcription factor, whereas FruA is a transcription factor that responds to cellular alignment conveyed by C-signaling. Transcription of *fruA* is dependent on MrpC binding, and FruA activity is proposed to be posttranslationally regulated by C-signaling, although the mechanism is unknown. FruA and MrpC cooperatively regulate transcription of the *dev* operon. My systematic analysis of the network dynamics supported a model in which posttranslational activation of FruA by C-signaling is critical for *dev* transcription and for commitment to spore formation.

Similar to *dev*, MrpC and C-signal-activated FruA combinatorially controlled transcription of the late-acting *fadIJ* operon involved in spore metabolism. Regulation of late-acting operons implicated in spore coat biogenesis (*exoA-I*, *nfsA-H*, *MXAN_3259-MXAN_3263*) was discovered to be under complex control by MrpC and FruA. My evidence suggests that transcription of these operons depends at least in part on a C-signal-dependent switch from negative regulation by unactivated FruA to positive regulation by activated FruA during the period leading up to and including commitment to sporulation. MrpC negatively regulated *exo* and *MXAN_3259* during mound formation, but positively regulated *nfs*. During commitment to sporulation, MrpC continued to positively regulate *nfs*, switched to positive regulation of *MXAN_3259*, and continued to negatively regulate *exo*. A third transcription factor, Nla6, appeared to be a positive regulator of all the late genes. We propose that in combination with regulation by Nla6, differential regulation by FruA in response to C-signaling and by MrpC controls late gene expression to ensure that spore resistance and surface characteristics meet environmental demands.

This dissertation is dedicated to my parents Prabir Kumar Saha and Sipra Saha, who always inspired me by their life-choices, encouraged me to follow my dreams and work sincerely to accomplish those.

ACKNOWLEDGEMENTS

Firstly, I would like to thank my mentor Dr Lee R Kroos for providing constant support throughout this journey. During this entire journey he was patient, supportive, encouraging, and most of all a devoted mentor which helped me strive and constantly grow as a scientist during my PhD. All these qualities not only make him one of the best mentors of Michigan State University, but also one of the best mentors I have come across in my research career so far. I will always look up to him as my role model for doing good science, dedication, sincerity, for taking care of my students and for supporting and respecting my colleagues.

I want to extend my gratitude to all the scientists who have worked immensely hard to nurture the field of *Myxococcus xanthus* research which has been an excellent foundation for my PhD research. I would like to acknowledge my committee members for their valuable advice, my supportive peers at Michigan State University for making the place an excellent and fun working environment.

Finally, I wish to thank my parents, my younger sister who always motivated me to pursue my dreams and to dedicate myself towards doing good work and shouldering all the challenges they faced in India regarding the health and well-being of my family. I want to thank my husband Dr Pavel Roy and his family for being supporting throughout all the thick and thins of my life.

My gratitude towards this meaningful journey of PhD at Michigan State University which added significantly towards the kind of person I am today.

TABLE OF CONTENTS

LIST OF TABLES

LIST OF FIGURES

**CHAPTER 1: Lessons from the study of signal induced gene expression in bacteria**

## Introduction

How bacteria sense environmental cues and initiate changes at the cellular and molecular level is an ever-fascinating question. In addition to environmental signals, bacteria send signals to each and respond appropriately. Bacteria integrate multiple signals from each other and from their environment to change individual and community behavior. Molecular understanding of how bacterial communities coordinate their behavior in response to signals will enable us to manipulate these communities for several applications, such as biofuel production [4] and therapeutics [5].

An example of signal-induced gene expression that has been extensively studied is the stationary-phase response in *Escherichia coli*, during which sigma factor RpoS mediates global changes in gene expression [6]. Under growth conditions, RpoS is degraded by the protease ClpXP [7] because the response regulator protein RssB specifically targets RpoS to ClpXP for degradation [8]. Upon entering the stationary phase, in response to phosphate starvation, regulation of RssB by an anti-adaptor protein IraP ensures stability of RpoS [9], promoting expression of RpoS-regulated stress response genes. Regulation of RpoS stability thus provides an example of signal-induced regulation of gene expression to promote a bacterial response.

Upon starvation for carbon, nitrogen or phosphorous, *Bacillus subtilis* undergoes endospore formation, which provides a more complicated model system to study temporal regulation of gene expression induced by starvation signals. During *B. subtilis* endosporulation, signals between the mother cell and forespore trigger differential gene expression and ensures coordination of gene regulation between the two compartments [10]. A critical step during

endospore formation is the release of active $\sigma^K$ into the mother cell by cleaving the precursor pro-$\sigma^K$ at the outer forespore membrane, in response to a signal from within the forespore [11]. This step promotes transcription of $\sigma^K$ RNA polymerase (RNAP) dependent genes in the mother cell, products of which ensure formation of the cortex and coat layers of the spore. Cleavage of pro-$\sigma^K$ serves as a critical checkpoint for forespore formation and is triggered by the interaction of pro-$\sigma^K$ with an intramembrane metalloprotease, SpoIVFB [12]. SpoIVFB is inhibited by complex formation with BofA and SpoIVFA until the signal comes from the forespore [13].

A fascinating model to study how a bacterial cell integrates multiple signals and initiates coordinated expression changes of multiple genes to alter community behavior is the multicellular developmental process of the gram-negative bacterium *Myxococcus xanthus* [2]. Upon scarcity of nutrients a developmental process gets initiated with aggregation of rod-shaped cells leading to formation of mounds followed by differentiation of cells within mounds to dormant spores, resistant to environmental insults. The majority of cells lyse during the formation of mounds [14], perhaps providing nutrients to cells which are destined to form spores. About 15% of the developmental population remain outside of fruiting bodies as peripheral rods [3, 14, 15], and only a few percent of the developing rods convert to round spores [3, 14]. The process of starvation-induced multicellular development of *M. xanthus* is governed by a signal-responsive gene regulatory network (GRN) [2, 11]. Cascades of signal-responsive transcription factors of the GRN coordinately and sequentially regulate target genes temporally and spatially [2]. Among these transcription factors, some are involved in combinatorial regulation of the target genes, providing integration of multiple signals [16-18]. An intriguing aspect is that typical prokaryotic-like signaling and mechanisms of gene regulation

appear to be insufficient to control the multicellular developmental program of *M. xanthus.* Intricate, eukaryotic-like components and mechanisms play crucial roles in reprogramming gene expression to regulate development of this bacterium [19]. For example, eukaryotic-like serine/threonine protein kinase (STPK) in bacteria was first identified in *M. xanthus* and it is required for normal development [20]. A breakthrough in the field was achieved when DNA microarray studies identified a group of $\sigma^{54}$ RNAP-dependent enhancer-binding proteins (EBPs), which are critical for fruiting body development [21]. Some of these EBPs have an N-terminal sensory domain predicted to be phosphorylated by one of the abundant STPKs in *M. xanthus*, transducing the starvation signal to activate target gene transcription at the beginning of the developmental process [22].

Despite significant advancements in the areas of signal transduction and gene regulation during *M. xanthus* fruiting body development, a systematic and quantitative understanding of gene expression changes had not yet been achieved when I began my research. Additionally, a mechanistic understanding of the regulation of genes which are transcribed late in development and lead to completion of spore formation remained to be elucidated. In particular, how these late-acting genes are controlled by the upstream transcription factors of the GRN was unknown. My work has aimed to address these questions.

***Understanding signaling and its impact on gene expression is important to enable manipulation of bacterial lifestyle and community behavior***

Intercellular communication or social interaction between bacteria allows all members of a bacterial community to function in synchrony, thus acting like a multicellular organism. In contrast to the harmonious behavior of a bacterial community, some social interactions between bacteria stimulate individuality within a group of cells, thus promoting diversity in a

bacterial community [23]. Exchange of information in the form of signaling between bacteria is primarily responsible for the social interactions between individual cells within a bacterial community. Hence, the production, release and exchange of signaling molecules is critical for formation, maintenance and function of bacterial communities. Detection and exchange of extracellular, diffusible signal molecules is a means to measure the density of a cell population (aka quorum sensing) to regulate biofilm formation in pathogenic organisms [24-26]. Early in *M. xanthus* development, A-signal provides quorum sensing to measure accumulation of a certain cell density which serves as a checkpoint for the decision to begin aggregation [27]. The other type of signaling mechanism is short-range signaling, which requires close proximity or contact between bacterial cells [23]. This intimate conversation between bacteria is seen in reciprocal C-signaling between closely-packed *M. xanthus* cells within mounds, crisscross signaling between the mother cell and the forespore within a *B. subtilis* sporangium, and contact-dependent inhibition of growth mediated by cell surface proteins CdiA and CsdiB in *E. coli* [23]. Upon association of extracellular signaling molecules with cell surface receptors, a membrane-associated protein kinase takes part in transduction of the signal via phosphorylation cascades, which eventually impact DNA-binding proteins (transcription factors) leading to regulation of the target genes as a response to the external stimuli [23].

Bacteria also respond to internal cues. The stringent response to nutrient limitation is extensively studied as a classic example of a broadly conserved reorientation of gene expression [28, 29], during which the ribosome-associated protein RelA senses amino acid starvation and stimulates production of a secondary messenger molecule (p)ppGpp in cell. Intracellular accumulation of (p)ppGpp modulates RNA polymerase activity, resulting in global

alteration of gene expression [28, 29]. The stringent response is crucial for regulation of processes like bacterial virulence [30], resistance to antimicrobial agents [31], survival of pathogens upon host invasion [32], and biofilm formation favoring environmental survival and host colonization of pathogens [33]. For example, expression of VpsT, the transcriptional activator of biofilm genes in *Vibrio cholerae*, is dependent on the stationary-phase sigma factor RpoS, which is induced by the stringent response [33]. Bacterial adaptation and lifestyle alterations with changes in the environment are also mediated by the stringent response [34], such as nutrient limitation-induced withdrawal from the biofilm lifestyle in order to switch to the free-swimming, planktonic lifestyle. This switch is mediated by a phosphodiesterase, BifA, expression of which is dependent on (p)ppGpp synthesis in *Pseudomonas putida* [35]. Progression of the starvation-induced multicellular lifestyle of *M. xanthus* is promoted by a contact-dependent, intercellular signal (C-signal) encoded by CsgA, but production of the C-signal is linked to the stringent response. Transcription of *csgA* is positively regulated by (p)ppGpp upon starvation, whereas transcription of *socE*, which is high during vegetative growth, is negatively regulated by (p)ppGpp [36]. C-signal promotes multicellularity by ensuring close proximity between developing cells in mounds before inducing gene expression that promotes further progression of the developmental process [37-39]. Hence, in this case, the starvation signal via the internal stringent response and (p)ppGpp signaling is coupled to intercellular C-signaling.

Understanding how transduction of environmental and intercellular signals re-orients gene expression is revealing how bacteria switch between lifestyles, and maintain both individual and communal lifestyles. Such understanding is important to be able to manipulate bacterial

communities for advancement of basic and applied research. For example, understanding bacterial communication within multispecies communities of gut microbiota aids probiotic intervention as a therapeutic strategy for gastrointestinal diseases [40]. Understanding signaling and gene regulation in multispecies biofilms facilitates their manipulation for biofuel production by simple, cost-effective technologies like solid-state fermentation [4]. Successful application of biofilm-mediated bioremediation to clean up toxic effluents from industrial plants or treat public waste water requires understanding of interactions within biofilm communities [41]. For example, a mixed biofilm formed by different species of *Rhodococcus* and *Pseudomonas* has been successfully used to clean up toxic chlorophenols like 2,4,6-tricholophenol, 2,3,4,6- tetrachlorophenol, pentachlorophenol [42].

***Features of signal-responsive gene regulatory networks and the significance of studying gene regulatory networks***

Bacterial two-component systems are one of the major mechanisms of bacterial signal transduction and are typically comprised of a sensor histidine kinase for receiving an input signal and a response regulator which transmits the signal to the level of gene expression [43]. Proper interaction between the sensor kinase and its partner response regulator ensures fidelity in transmission of the signal leading to changes in expression of target genes. For example, transmission of a quorum signal by the ComA/ComP two-component system promotes transcription of *srf* genes leading to development of competence under inadequate nutritional conditions in *B. subtilis* [44]. The majority of the response regulators have a DNA-binding domain, and trigger transcription of genes by direct binding to promoter regions as transcription factors [45]. Some response regulators are involved in phosphorelays involving phosphotransfer between proteins before being phosphorylated and activating target genes

[43]. Mainly two sensor kinases, KinA and KinB, initiate a multicomponent cascade of sequential phosphorylation of downstream proteins, leading to phosphorylation of the transcription factor SpoA, which initiates sporulation in *B. subtilis* by activating transcription of sporulation genes [46, 47]. In comparison to the relatively simple phosphorelay network that controls initiation of sporulation in *B. subtilis*, expression of mycobacterial $\sigma^E$-dependent stress response genes during infection is under control of a complex GRN involving transcriptional, translational and posttranslational mechanisms [48].

An added layer of complexity in gene regulation is conferred when expression of a target gene of a downstream regulatory module is dependent on the protein product from an upstream regulatory module, leading to formation of enormous GRNs comprised of multiple smaller regulatory modules. Some fascinating examples of such GRNs are those that control multicellular development of *Myxococcus xanthus* and endospore formation of *B. subtilis* [2, 11]. For example, in the *M. xanthus* GRN the phosphorylated version of a product from the EBP module, Nla28~P, activates transcription of the *mrpAB* operon, leading to synthesis of MrpC, which is the product of the Mrp module [2]. An intriguing feature of such multilayered GRNs is regulatory loops, which can be positive or negative, feed-forward or feed-back, or autoregulatory [2, 11]. During *B. subtilis* sporulation, synthesis of the mother cell sigma factor $\sigma^K$ and the forespore sigma factor $\sigma^G$ are under the control of independent positive autoregulatory loops to elevate production of the respective regulatory proteins [11]. Autoregulatory loops typically involve a single transcription factor, whereas, feed-forward loops involve at least two, where expression of one transcription factor regulates expression of a second transcription factor, and the two regulate transcription of a target gene [11]. In *B.*

*subtilis* transcription of *gerR* is activated by $\sigma^E$ RNAP, and GerR negatively regulates 14 genes of the $\sigma^E$ regulon, resulting in 14 genes being expressed in a pulse [49]. In a different kind of feed-forward loop, expression of the target gene is under positive control by both transcription factors. For example, during *B. subtilis* sporulation, $\sigma^E$ RNAP activates transcription of SpoIIID, which together with $\sigma^E$ RNAP activates transcription of the gene encoding pro-$\sigma^K$, thus delaying expression of the $\sigma^K$ regulon until sufficient SpoIIID accumulation, a strategy referred to as "AND" logic [49]. Another example of a feed-forward loop will be discussed in detail in Chapter 2, which involves MrpC and activated FruA combinatorially activating transcription of the developmental *dev* operon in the *M. xanthus* GRN [3]. Also in the *M. xanthus* GRN, a quorum sensing signal, A-signal, is produced under control of transcription factors in the EBP module, and A-signaling feeds back into the EBP module, thus forming a positive feed-back loop [2]. The regulatory loops of GRNs provide checkpoints, signal amplification, and combinatorial control of gene expression in order to ensure spatial and temporal regulation of gene expression during stress responses, including development. At the early stage of *M. xanthus* multicellular development, sequential phosphorylation of EBPs ensures stage-to-stage transition into aggregation, providing checkpoints for furthering the decision to build mounds [50]. In addition to starvation, the EBP module regulates production of (p)ppGpp and A-signal, which positively feed back into the EBP module, resulting in amplification of the signals, and providing a strategy to determine whether starvation is prolonged enough to initiate development [27, 51]. At the later stages of *B. subtilis* endospore formation, release of active $\sigma^K$ into the mother cell requires a signal from the forespore, thus ensuring that coat protein assembly around the forespore is suspended until the proper time, an example of strict

temporal regulation of gene expression [13, 52]. The regulatory loops significantly contribute to differential gene expression, a strategy to accomplish formation of two separate compartments within a sporangium (a larger mother cell and a smaller forespore), during endospore formation in *B. subtilis* [11]. Expression of distinct sigma factor cascades beginning with $\sigma^H$ and $\sigma^A$ in the forespore and mother cell, respectively, ensures progression of differential gene expression between the two compartments in *B. subtilis* [11].

Some other fascinating features of GRNs which play critical roles in spatial and temporal regulation of gene expression are ultrasensitivity (nonlinear responses), irreversibility, and bistability. A large change in the expression of a target gene (output) in response to a small change in the expression of a transcription factor (input) is considered an ultrasensitive or nonlinear response [53, 54]. In *B. subtilis* the decision to form a spore exhibits an ultrasensitive response to a threshold concentration of the KinA histidine protein kinase [54]. This is an example of expression of cell fate-determining genes exhibiting nonlinear outputs in response to a threshold level of the input sensor kinase of the phosphorelay that controls the sporulation decision [43, 47]. In bistable switches the regulatory system switches between two ultrasensitive thresholds (Off to On and On to Off), rather than resting at an intermediate state [53, 55]. The mechanism of the Off to On switch often involves positive autoregulation of the regulator leading to amplification of the input [55]. In other cases of Off to On switches, expression of a target gene is under the control of two mutually repressing repressors ($R_1$ and $R_2$), when addition of an inducer antagonizes production of $R_2$, derepressing the target gene, $R_1$ is produced ensuring repression of $R_2$, leaving the target gene on [55]. The stress response mechanism of *Mycobacterium tuberculosis* exhibits bistability, where the active form of the

sigma factor $\sigma^E$ reaches the "OFF" threshold of ultrasensitivity due to sequestration by the anti-sigma factor (RseA), leading to a switch Off mode of *mprAB* transcription. Release of active $\sigma^E$ from RseA, in combination with the positive feedback loop from MprAB to the $\sigma^E$ promoter, ensures that $\sigma^E$ reaches the "ON" threshold of ultrasensitivity, leading to an irreversible switch On mode of MprAB production until a significant change in the input signal occurs [53]. Importantly, phenomena where expression of a target gene is controlled by multiple regulatory proteins in multiple layers is not rare in bacterial systems. These systems often rely on alternative sigma factors and EBPs. The earlier discussed stringent response-induced accumulation of RpoS [6] in *E. coli* and the sporulation-specific sigma factors of *B. subtilis* are examples of alternative sigma factors, which are related to the major, housekeeping sigma factor (e.g. $\sigma^{70}$ in *E. coli*), but possess distinct promoter recognition properties. Unlike $\sigma^{70}$ and related alternative sigma factors, $\sigma^{54}$ recognizes conserved sequences centered at -12 and -24 relative to the transcriptional start site, and works in coordination with EBPs to transcribe $\sigma^{54}$ RNAP-dependent genes. A well-studied example of $\sigma^{54}$ RNAP-dependent genes are activated by the EBP NtrC in response to limited nitrogen availability of cells [56]. Why is gene regulation often multilayered and why must gene expression be so tightly regulated? Expression of large regulons is energetically costly and in some cases becomes irreversible. For example, the $\sigma^E$ regulon of *B. subtilis* includes about 270 genes and irreversibly commits the cell to endospore formation [54]. Sporulation appears to be the last resort for the cell in order to survive starvation. In order to prevent wasteful usage of the limited resources available to a bacterial cell, conditional expression of stress-responsive genes is tightly regulated and often controlled at multiple levels.

The functions of GRNs with all the features mentioned above are not limited to regulating bacterial stress responses [7], pathogenesis [33], sporulation and multicellular development [2, 11], but also community behavior and cell fate determination in bacteria. Multiple interconnected regulons of quorum-sensing genes regulate population wide gene expression, thereby enabling community-wide coordination of collective behavior in *Pseudomonas aeruginosa* [57]. This is just one example of such coordination in bacterial community behavior, which leads to biofilm formation in many species [58]. Differential gene expression regulated by GRNs govern cell fate determination in bacteria. During endospore formation of *B. subtilis*, different levels of SpoA0~P within the developing population determine cell fate by down-regulating expression of the repressor SinR and inducing expression of the sporulation genes in cells destined to form endospores [59]. There are other bacterial systems where the mechanism of cell fate determination still remains to be understood [2]. Lineage commitment and determination of cell fate are critical processes during development of multicellular organisms [60, 61]. For example, patterned expression of transcription factors under the control of HIPPO signaling determines cell fate decisions during embryonic stem cell development [60]. Understanding how GRNs govern decision during development of multicellular organisms not only advances fundamental knowledge, it also provides a foundation to tackle diseases related to erroneous development. Some of the significant challenges associated with studying relatively complicated GRNs of eukaryotes are the time-intensive genetic manipulation and comparatively higher cost, making it attractive to study simple model organisms to advance our understanding of GRNs. Additionally, understanding

GRNs regulating bacterial stress responses, development, virulence, and antibiotic resistance can directly facilitate invention of novel therapeutic strategies for infectious and other diseases.

***Myxococcus xanthus as a model for studying bacterial signaling and multicellularity***

Although many bacteria can lead a unicellular lifestyle, many bacteria spend at least part of their lives in multicellular communities and some choose a multicellular lifestyle almost exclusively. Multicellularity may arise by aggregation of single cells, chaining and clustering of cells by incomplete cell fission or filamentation from a single cell by cell division arrest [62]. Some of the examples of multicellular behavior in microbes are aerial mycelium formation during sporulation of *Streptomyces*, formation of heterocysts in chains in filamentous cyanobacteria *Anabaena*, and collective swarming of rod-shaped *M. xanthus* cells. Since formation of multicellular structures require shared and unique molecular mechanisms within the population, the process is energetically expensive. Despite the expense, bacteria can receive several benefits by forming multicellular structures, such as improved resource acquisition and resistance to predation or stress, thus offsetting the costs [62]. *M. tuberculosis* transitions from a unicellular mode of living to filamentous structures during proliferation inside macrophages as an adaptive response during phagocytosis [62]. In addition to the benefits a bacterium gains from multicellularity, the prevalence of intercellular signaling in bacterial communities makes them fascinating systems to study signal-induced gene regulation [23].

Among bacteria which predominantly lead a multicellular lifestyle, the *Myxobacteria* are extensively studied. *Myxobacteria* are a group of gram-negative, soil dwellers and are involved in social predation. The best-characterized species is *Myxococcus xanthus.* During vegetative

growth, *M. xanthus* builds a multicellular community by organizing high cell density swarms [63]. Upon availability of nutrients, *M. xanthus* exhibits collective predation by secreting extracellular digestive enzymes to lyse the prey leading to cooperative feeding [63]. When plenty of nutrients are available *M. xanthus* cells collectively spread over a solid surface to take advantage of the nutrients, a behavior referred as swarming [63]. The type IV pili-dependent motility, referred as S or social motility, and motility dependent on focal adhesion complexes [64], referred as A or adventurous motility, both are required for swarming of *M. xanthus* in the presence of nutrients [63]. Leaving behind extracellular matrix slime trails at the lagging end of a cell for other cells to follow is associated with A-motility [20]. S-motility is characterized by coordinated swarming movement of large groups of cells and occurs by extension and retraction of the type IV pili. Activation of highly coordinated S-motility requires close proximity between cells and is facilitated by exopolysaccharide [20]. S-motility is essential for coordinated predation when plenty of nutrient is around and also for multicellular development when access to nutrient is limited [20].

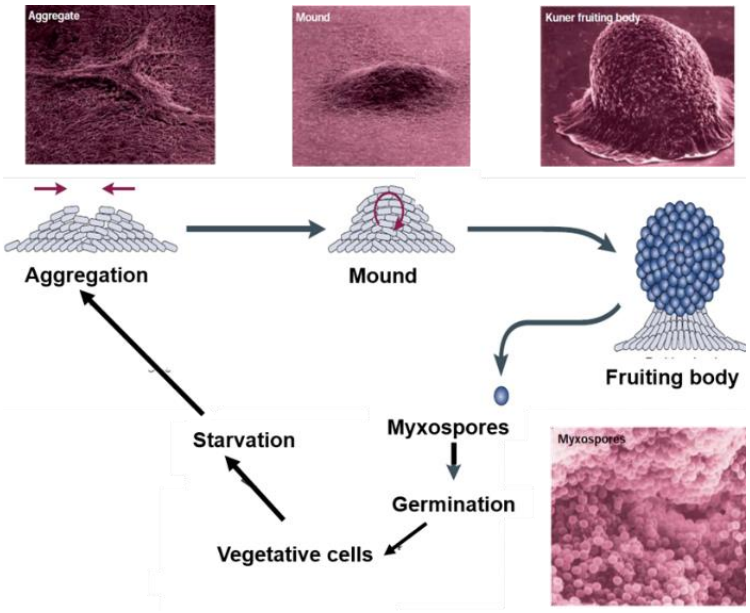


**Figure 1.1 Life cycle of *Myxococcus xanthus*.** Multicellular development is induced upon starvation. During development *M. xanthus* undergoes several morphological changes including aggregation, mound formation and maturation of fruiting bodies that involves differentiation of stress-resistant myxospores. Upon appearance of nutrients myxospores germinate and undergo vegetative growth. (Adapted from [1]).

When the supply of nutrients runs low, *M. xanthus* initiates a complex developmental program by coordinating cell movements into mounds (Fig. 1). The program culminates in the formation of multicellular fruiting bodies filled with stress-resistant spores [1]. Under starvation conditions, developing cells adhere to the solid surface by forming biofilms, within which cells participate in organized wave-like movements referred as rippling under certain conditions [1]. When two waves moving in opposite directions collide with each other, they may reflect, but imperfect reflection may cause a traffic jam, forming high cell density stationary aggregates of cells that lead to mound building. Mounds also form upon fusion of adjacent aggregates [1]. As

more cells enter mounds, they increase in size and eventually contain around $10^5$ cells [1]. Finally, signaling between closely-packed cells within mounds leads to differentiation of rods

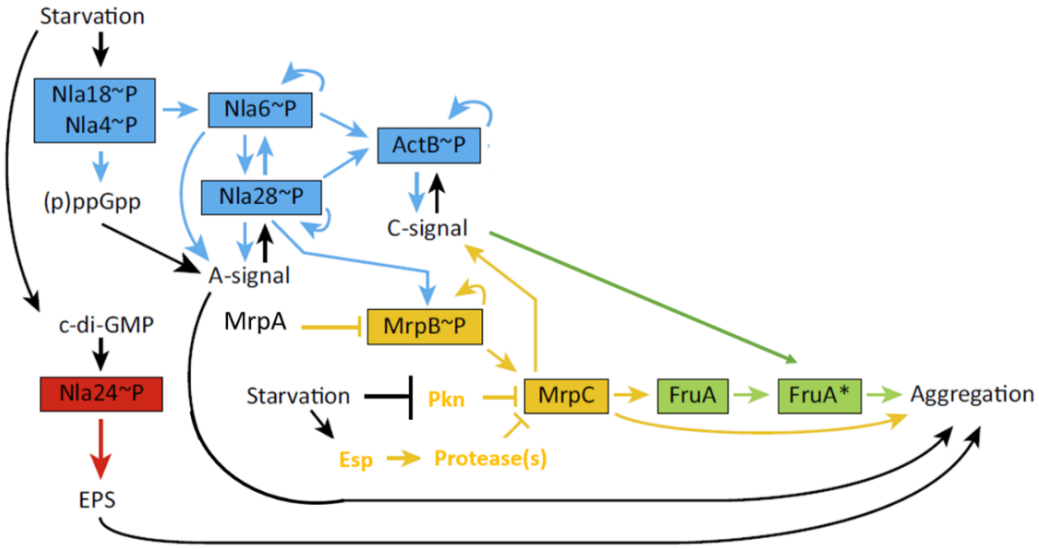


**Figure 1.2 The GRN governing changes before and during aggregation.** The four modules are shown in different colors [enhancer-binding protein cascade (blue), Nla24 module (red), MrpC module (orange), FruA module. Transcription factors are boxed. Arrows and lines with a barred end indicate positive and negative regulation, respectively (Adapter from [2]).

into round spores resistant to environmental insults [1]. The spore-filled mound is called a "fruiting body." Also during the developmental process, a majority of cells undergo lysis by a mechanism which is not completely understood [14, 65] and some cells persist as peripheral rods outside of fruiting bodies [15]. Thus, under starvation conditions, integration of intracellular and extracellular signals promotes a coordinated sequence of three highly organized multicellular structures (aggregates, mounds, fruiting bodies) and determination of three distinct cell fates (lysing cells, peripheral rods, stress-resistant spores), in some ways comparable to eukaryotic development [19]. Starvation-induced multicellular development and

cell fate determination (Fig. 1) of *M. xanthus* is governed by a highly signal-responsive GRN (Fig. 2) which is strikingly unique compared to GRNs regulating sporulation of *B. subtilis* and three species of *Streptomyces* (*coelicolor*, *griseus*, and *venezuelae*), the other commonly studied models of bacterial development. The primary distinguishing feature is that unlike the GRNs regulating sporulation in the other bacteria, in the *M. xanthus* GRN EBPs play unique roles in regulating transcription of developmental genes in coordination with $\sigma^{54}$ RNAP [2]. Compared to the sporulation GRN in *Streptomyces*, the *M. xanthus* GRN exhibits more instances of combinatorial regulation of target genes [2]. Taken together, the other GRNs appear to be comparatively less signal intensive, perhaps because they did not evolve to govern developmental processes as complex as exhibited by *M. xanthus* [2]. *M. xanthus* provides an attractive model system to decipher the complications of multicellular development and cell fate decisions. With the added advantage of genetic manipulation of *M. xanthus* being less time and cost intensive, this bacterium is considered a premium model to study signal-responsive gene regulation in bacteria.

### *The signal-responsive gene regulatory network governing multicellular development of M. xanthus*

***The GRN governing changes before and during aggregation:*** This portion of the GRN can be summarized in four regulatory modules – the EBP cascade module, the Nla24 module, the Mrp module and the FruA module [2] (Fig. 2). Upon starvation, RelA activity leads to accumulation of the secondary messenger molecules penta and tetraphosphate [(p)ppGpp], when ribosomes stall due to amino acid limitation, which is called stringent response [2]. During the stringent response in *M. xanthus* (p)ppGpp induces production of two extracellular signals, A-signal and C-signal [66]. The A-signal is a signal for quorum sensing and provides a measure of cell density

[51, 67]. When a particular quorum is reached the starving cells start expressing early developmental genes in response to A-signaling. The identity of C-signal and its mode of action is still under investigation [38, 68]. According to one model, C-signal or C-factor (p17) is a proteolytic product generated by PopC mediated N- terminal cleavage of full-length CsgA (p25) [38, 69]. An alternative model suggests that phospholipase activity of CsgA releases diacylglycerols from the inner membrane which serves a C-signal and causes cell shortening [68]. In support of this model, purified p17 failed to rescue the developmental defect of a *csgA* mutant, but addition of purified *M. xanthus* diacylglycerols induced formation of dark fruiting bodies by a *csgA* mutant [68]. During development two distinct threshold levels of C-signaling are required to achieve aggregation and sporulation [70], ensuring synchronized development [71].

**The EBP cascade module:** Within the GRN the cascade of EBPs is the first module to respond to the starvation signal. EBPs typically bind 100 bp upstream of the promoter and activate transcription of $\sigma^{54}$ RNAP-dependent genes [56]. EBPs in the cascade module are likely activated by phosphorylation in a sequential manner, with Nla18~P and Nla4~P activating transcription of the gene encoding Nla6, and Nla6~P in turn activating the gene coding for Nla28 [50, 72]. Nla6~P and Nla28~P both are involved in positive autoregulation, providing signal amplification and serving to evaluate whether starvation is persistent enough to initiate aggregation [2]. Nla6~P and Nla28~P also regulate each other, providing positive feedback within the EBP cascade and regulating production of A-signal and ActB [2]. Products of the *act* operon regulate the rise of C-signal, which eventually feeds into the FruA module and leads to aggregation and eventually fruiting body formation [73]. Nla28~P feeds into the Mrp module by

activating transcription of the *mrpAB* operon. Therefore, at the preaggregation stage expression of EBP-dependent genes ensures progression to the aggregation stage.

**The Nla24 module:** This module is a relatively recent discovery and is activated by another secondary messenger molecule, cyclic diguanylate (c-di-GMP), in response to starvation early in development. An increase in the level of c-di-GMP is essential for fruiting body formation, as c-di-GMP binds with its receptor, the EBP Nla24, leading to stimulation of exopolysaccharide (EPS) synthesis at the preaggregation stage [74].

**The Mrp module:** This module is comprised of three Mrp proteins and at least two starvation-responsive signal transduction pathways (Pkn and Esp) [2]. MrpA acts as a phosphatase of MrpB~P, which encodes an EBP, regulating transcription of *mrpC* [75]. MrpC encodes a transcription factor from the CRP (cAMP receptor protein) family and is the key output of the Mrp module [75]. The signal for starvation not only feeds into the EBP cascade but also impacts the Mrp module by posttranslationally affecting MrpC in two ways. The Pkn STPK cascade can phosphorylate MrpC, weaking its binding to DNA [76], but recently reported results suggest this has a minor effect on development [77]. Starvation also triggers proteolysis of MrpC via the Esp signaling pathway [78] [79]. During the preaggregation stage, the Esp signaling pathway determines the pace of development by regulating the concentration of MrpC in the starving cells. Addition of nutrient medium results in rapid proteolysis of MrpC and blocks commitment to sporulation, suggesting MrpC is a mediator of the starvation signal and serves as a checkpoint conveying persistent starvation [80]. MrpC accumulates to a higher level in aggregating cells than in non-aggregating cells [14]. MrpC serves as a key transcriptional regulator of genes, including genes critical for aggregation, given that an *mrpC* mutant fails to

aggregate [3, 77]. MrpC negatively autoregulates its transcription at the level of synthesis [3, 77] and upregulates or downregulates transcription of nearly 300 developmental genes by direct binding [81]. Negative autoregulation of MrpC which is a major transcriptional regulator of *M xanthus* development perhaps shortens the response time of genetic regulatory circuits and decreases variability in gene expression between cells undergoing development [77]. MrpC activates transcription of the gene encoding FruA [3, 82], another key transcription factor for developmental gene expression [3, 82].

**The FruA module:** FruA relies on C-signaling to activate it for transcription of downstream genes in the GRN [83, 84]. As described above, the mechanism of C-signaling is controversial, but it is clear that cells must be aligned to engage in C-signaling, which in turn promotes aggregation, further alignment of cells, and more C-signaling [37, 85, 86]. C-signal appears to activate FruA posttranslationally [83, 84], represented as formation of FruA$^*$ in Figure 2. FruA$^*$ is proposed to mediate cellular responses to C-signaling both individually [87] and combinatorially with MrpC [3, 18] by regulating transcription of genes whose products ensure aggregation, mound formation, and eventually sporulation as the levels of C-signaling and FruA$^*$ rise [70, 71]. How C-signaling activates FruA remains to be elucidated. Earlier work showed that FruA is similar to response regulators of two-component systems and suggested that C-signaling leads to phosphorylation of FruA [83, 84]. However, typically a response regulator is phosphorylated by a protein kinase, which has not been identified for FruA. The atypical response regulator domain of FruA lacks some aspartate residues normally required for phosphorylation. Additionally, treatment with small molecule phosphodonors failed to increase DNA-binding ability of FruA [16]. Altogether, the evidence suggested that phosphorylation was unlikely to be

the mechanism by which FruA is activated. In Chapter 2 we show additional evidence suggesting FruA is not activated by phosphorylation [3].

***The GRN governing sporulation***: Transcription factors from the modules described above ensure expression of developmental genes essential for the pre-aggregation and aggregation stages of development. In particular, MrpC and C-signal-dependent FruA$^{*}$ regulate transcription of genes whose products ensure progression of development from the stage of aggregation to the eventual completion of spore formation. MrpC and FruA integrate the two major signaling inputs, starvation and C-signal (serving as a spatial coordinator), respectively, and regulate expression of downstream genes of the GRN (Fig. 3). Combinatorial regulation by MrpC and FruA$^{*}$ integrates the signal for starvation and C-signaling, respectively, thus ensuring that only the starving cells capable of accumulating MrpC, and cells also in close proximity within mounds and therefore capable of C-signaling and accumulating FruA$^{*}$, commit to spore formation [16, 80]). Among the C-signal-dependent genes which are important for sporulation and are under combinatorial control of MrpC and FruA$^{*}$ are genes of the *dev* operon [18] (Fig. 3). The *dev* operon includes a CRISPR-Cas system and is proposed to protect *M. xanthus* cells from phage infection during multicellular development [3, 88]. Three genes of *dev* operon, *devTRS*, negatively autoregulate transcription tenfold [3, 88]. The product of the first gene, *devI*, is a small 40-residue protein that inhibits sporulation [89, 90]. Hence, the mutant lacking *devI* forms sonication-resistant spores 6 h earlier in comparison to the wild-type strain [3, 89, 90].
In contrast, mounds formed by the *devTRS* mutants do not darken and these mutants are impaired in spore formation [3, 88, 91]. These findings indicate that in *devTRS* mutants the lack

of the negative autoregulation leads to overproduction of DevI and results in a sporulation defect.

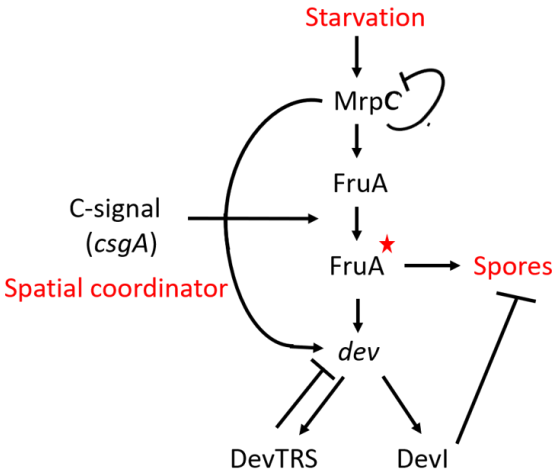


**Figure 1.3 The GRN governing sporulation with the output gene *dev*.** Figure shows GRN governing sporulation in *M. xanthus* with one of the outputs *dev*. The key transcription factors MrpC and FruA integrate starvation signal and the C-signal (the signal for spatial coordination) into the network. In response to starvation, MrpC negatively autoregulates at the level of transcription. Transcription of *fruA* is activated by MrpC. In response to C-signal, activated FruA (FruA$^{*}$) cooperatively with MrpC activate transcription of dev operon. One of the genes of dev operon, DevI, if overproduced delays spore formation, whereas, DevTRS proteins negatively autoregulate transcription. (Adapted from [3]).

In agreement, sporulation of *devTRS* mutants can be restored by a null mutation in *devI* [89]. In Chapter 2 we investigate the effects of C-signaling, FruA, and MrpC on the *dev* transcript level [3].

Other C-signal-dependent genes of the GRN act late during the sporulation stage of the developmental process. In Figure 4, *exo* and *nfs* represent nine (*exoA-I*) and eight *(nfsA-H)* gene operons whose products help build the spore coat, and hence are critical for completion of spore formation [92, 93]. The protein products of three genes of *exo* operon (*exoA*, *exoB* and *exoC*) appear to form a terminal transport complex spanning from the cytoplasmic membrane

to the outer membrane [93]. *exoC* encodes a PCP-2a-like polysaccharide copolymerase family protein likely responsible for the export of spore coat material [92-94]. Developmental transcription of *exo* appears to be activated by direct binding of FruA$^{*}$ in response to C-signaling [87]. Strikingly, the EBP Nla6 from the EBP module which regulates transcription of genes during the pre-aggregation stage, has been shown to bind to the *exo* promoter region [72]. Nla6 appears to activate transcription of *exo* at the stage when aggregation begins, but negatively regulate *exo* transcription closer to the time of sonication-resistant spore formation [72]. In Chapter 3 we report novel aspects of regulation of *exo* transcription by MrpC and FruA which has not been activated by C-signaling (Fig. 4). In Chapter 3 we also provide evidence that products of the *exo* operon are critical for sonication-resistant spore formation. Products of the *nfs* operon are critical for assembling the spore coat material once it has been exported to the cell surface [93]. In Chapter 3 we elucidate the roles of MrpC and unactivated FruA in regulating *nfs* transcription.

In Chapter 3 we also report studies of two other late-acting operons of the GRN (Fig. 4). *MXAN_3259* is predicted to encode a polysaccharide deacetylase [72] and *MXAN_5372* is predicted to encode a FadI homolog involved in fatty acid □-oxidation during spore formation [95]. Similar to *exo*, transcription of *MXAN_3259* is activated by Nla6 at the beginning of aggregation, but negatively regulated by Nla6 closer to the time of spore formation, and mutations in *MXAN_3259* [72] or *exoC* [92, 96] caused similar sporulation defects. In Chapter 3 we elucidate the roles of MrpC, unactivated FruA, and activated FruA$^{*}$ in regulating developmental transcription of *MXAN_3259* and *MXAN_5372* (*fadI* in Fig. 4). Our findings reported in Chapter 3 indicate novel roles of unactivated FruA and MrpC in negative regulation,

and together with positive regulation by FruA$^*$ produce differential control of the four late-acting operons (Fig. 4). We propose that upon reaching a distinct threshold for sporulation, C-signaling posttranslationally activates FruA, and FruA$^*$ increases transcription of genes essential for completion of spore formation.

We hypothesize that by integrating the starvation signal and the signal for spatial coordination (C-signal) the GRN (Fig. 3 and 4) governs the decision to form a spore during the commitment period. The decision to form a spore includes the molecular changes leading to spore formation. These changes are suggested to occur between 24 – 30 h after the onset of starvation. The time between 24-30 h poststarvation is defined as the commitment period, during which an increasing number of *M. xanthus* cells actively convert to spores despite perturbing the starvation signal by adding nutrients [80]. Therefore, in order to understand changes leading to spore formation, work described in this dissertation attempted to elucidate the gene expression dynamics of the GRN (Fig. 3 and 4) during the commitment period.

Previous attempts to study the GRN governing *M. xanthus* multicellular development involved usage of multiple strains, different conditions of development, and phenotypic rather than molecular approaches, without fine time resolution [75, 82, 87]. These factors made it difficult to decipher the molecular complexity of *M. xanthus* development. To overcome these challenges, systematic and quantitative experimental approaches need to be combined with computational methods to build mathematical models of GRNs that can predict novel outcomes. These outcomes are often testable by wet lab experiments, resulting in refinement of the existing mathematical models and formulation of novel testable hypotheses. Thus, systematic and quantitative experimental approaches in combination with computational

modeling are advantageous in contributing to the understanding of GRNs in a time efficient manner.

Chapter 2 describes systematic and quantitative experimental approaches coupled with a computational model designed to help elucidate GRN function during the commitment period of *M. xanthus* development. Systematic analysis was performed with fine time resolution to build a computational model where the *dev* transcript level was the output and MrpC and FruA were inputs (Fig. 3). The model was used to make predictions related to hypotheses formulated to explain an observed large change in the *dev* transcript level in a *csgA* mutant despite a much smaller change in the level of FruA [3]. Our systematic experimental analysis in combination with mathematical modeling supports the hypothesis that C-signaling activates FruA at least ninefold posttranslationally in order to increase transcription of the *dev* operon and commit cells to spore formation [3]. The project took a striking turn when our systematic analysis revealed unexpected changes in the expression levels of the late genes of the GRN (*exo, nfs, MXAN_3259* and *fadI*) in the absence of MrpC and FruA, indicating novel roles of these transcription factors in regulating the late genes during commitment (Fig. 4). These initial findings were explored the work described in Chapter 3 to elucidate potential molecular mechanisms of the late gene regulation by Nla6, FruA and MrpC. Chapter 3 provides novel insights into the function and differential regulation of the late genes.

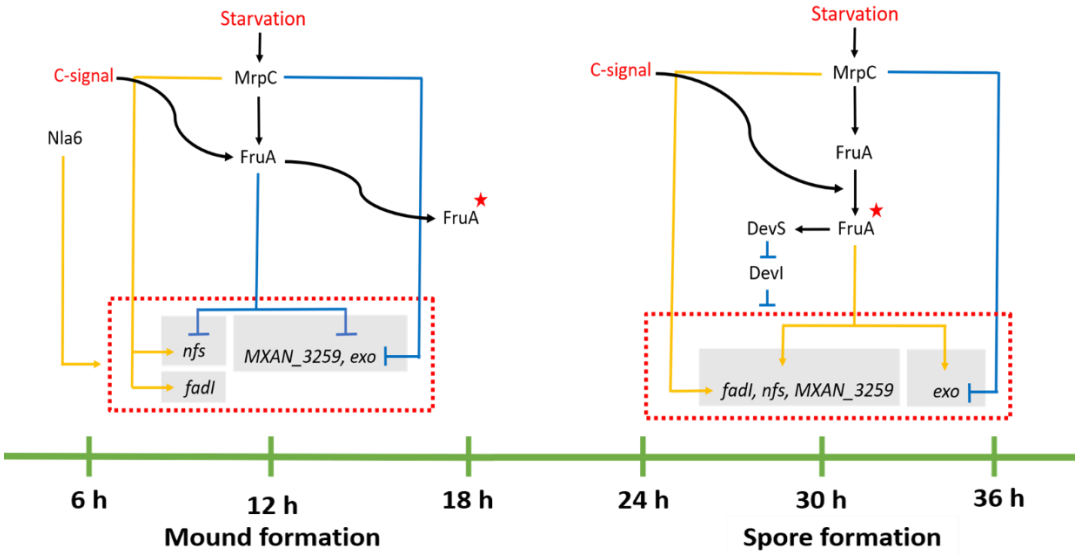


**Figure 1.4 Model of differential regulation of late genes at two different morphological stages during development.** Starvation increases the MrpC level which in turn increases the FruA level. C-signal activates FruA to FruA*. Around the time of mound formation unactivated FruA predominates and around the time of spore formation activated FruA (FruA*) predominates. Positive regulation (yellow arrows) and negative regulation (blue line with blunt) of late genes (gray boxes) is indicated. During mound formation between 6 and 18 h poststarvation, Nla6 positively regulates transcription of all four late genes (dashed box), but unactivated FruA and MrpC negatively regulate certain late genes as indicated. During spore formation between 24 and 36 h, activated FruA* induces transcription of the dev operon gene. DevS (and DevT and DevR, which are not shown) negatively autoregulates transcription of *devI*. DevI negatively regulates all four late genes (dashed box), but FruA* positively regulates their transcription, while MrpC positively or negatively regulates certain late genes as indicated.

**REFERENCES**

## REFERENCES


1. Kaiser D: Coupling cell movement to multicellular development in myxobacteria. *Nature reviews Microbiology* 2003, 1(1):45-54.

2. Kroos L: Highly Signal-Responsive Gene Regulatory Network Governing Myxococcus Development. *Trends in genetics : TIG* 2017, 33(1):3-15.

3. Saha S, Patra, P, Igoshin, O, Kroos, L.: Systematic analysis of the Myxococcus xanthus developmental gene regulatory network supports posttranslational regulation of FruA by C-signaling. *Molecular microbiology* 2019, 111(6):1732-1752.

4. Wang ZW, Chen, S.: Potential of biofilm-based biofuel production. *Applied microbiology and biotechnology* 2009, 83(1):1-18.

5. Hall-Stoodley L, Stoodley, P.: Evolving concepts in biofilm infections. *Cellular microbiology* 2009, 11(7):1034-1043.

6. Battesti A, Majdalani, N, Gottesman, S.: The RpoS-mediated general stress response in Escherichia coli. *Annual review of microbiology* 2011, 65:189-213.

7. Schweder T, Lee, K. H, Lomovskaya, O, Matin, A.: Regulation of Escherichia coli starvation sigma factor (sigma s) by ClpXP protease. *Journal of bacteriology* 1996, 178(2):470-476.

8. Zhou Y, Gottesman, S, Hoskins, J. R, Maurizi, M. R, Wickner, S.: The RssB response regulator directly targets sigma(S) for degradation by ClpXP. *Genes & development* 2001, 15(5):627-637.

9. Bougdour A, Gottesman, S.: ppGpp regulation of RpoS degradation via anti-adaptor protein IraP. *Proceedings of the National Academy of Sciences of the United States of America* 2007, 104(31):12896-12901.

10. Stragier P, Losick, R.: Molecular genetics of sporulation in Bacillus subtilis. *Annual review of genetics* 1996, 30:297-241.

11. Kroos L: The Bacillus and Myxococcus developmental networks and their transcriptional regulators. *Annual review of genetics* 2007, 41:13-39.

12. Halder S, Parrell, D, Whitten, D, Feig, M, Kroos, L.: Interaction of intramembrane metalloprotease SpoIVFB with substrate Pro-sigma(K). *Proceedings of the National Academy of Sciences of the United States of America* 2017, 114(50):E10677-E10686.

13. Cutting S, Driks, A, Schmidt, R, Kunkel, B, Losick, R.: Forespore-specific transcription of a gene in the signal transduction pathway that governs Pro-sigma K processing in Bacillus subtilis. *Genes & development* 1991, 5(3):456-466.

14. Lee B, Holkenbrink, C, Treuner-Lange, A, Higgs, P. I.: Myxococcus xanthus developmental cell fate production: heterogeneous accumulation of developmental regulatory proteins and reexamination of the role of MazF in developmental lysis. *Journal of bacteriology* 2012, 194(12):3058-3068.

15. O'Connor KA, Zusman, D. R.: Development in Myxococcus xanthus involves differentiation into two cell types, peripheral rods and spores. *Journal of bacteriology* 1991, 173(11):3318-3333.

16. Mittal S, Kroos, L.: A combination of unusual transcription factors binds cooperatively to control Myxococcus xanthus developmental gene expression. *Proceedings of the National Academy of Sciences of the United States of America* 2009, 106(6):1965-1970.

17. Mittal S, Kroos, L.: Combinatorial regulation by a novel arrangement of FruA and MrpC2 transcription factors during Myxococcus xanthus development. *Journal of bacteriology* 2009, 191(8):2753-2763.

18. Campbell A, Viswanathan, P, Barrett, T, Son, B, Saha, S, Kroos, L.: Combinatorial regulation of the dev operon by MrpC2 and FruA during Myxococcus xanthus development. *Journal of bacteriology* 2015, 197(2):240-251.

19. Kroos L: Eukaryotic-like signaling and gene regulation in a prokaryote that undergoes multicellular development. *Proceedings of the National Academy of Sciences of the United States of America* 2005, 102(8):2681-2682.

20. Munoz-Dorado J, Marcos-Torres, F. J, Garcia-Bravo, E, Moraleda-Munoz, A, Perez, J.: Myxobacteria: Moving, Killing, Feeding, and Surviving Together. *Frontiers in microbiology* 2016, 7:781.

21. Jakobsen JS, Jelsbak, L, Jelsbak, L, Welch, R. D, Cummings, C, Goldman, B, Stark, E, Slater, S, Kaiser, D.: Sigma54 enhancer binding proteins and Myxococcus xanthus fruiting body development. *Journal of bacteriology* 2004, 186(13):4361-4368.

22. Jelsbak L, Givskov, M, Kaiser, D.: Enhancer-binding proteins with a forkhead-associated domain and the sigma54 regulon in Myxococcus xanthus fruiting body development. *Proceedings of the National Academy of Sciences of the United States of America* 2005, 102(8):3010-3015.

23. Bassler BL, Losick, R.: Bacterially speaking. *Cell* 2006, 125(2):237-246.

24. Waters CM, Lu, W, Rabinowitz, J. D, Bassler, B. L.: Quorum sensing controls biofilm formation in Vibrio cholerae through modulation of cyclic di-GMP levels and repression of vpsT. *Journal of bacteriology* 2008, 190(7):2527-2536.

25. de Kievit TR: Quorum sensing in Pseudomonas aeruginosa biofilms. *Environmental microbiology* 2009, 11(2):279-288.

26. Deziel E, Gopalan, S, Tampakaki, A. P, Lepine, F, Padfield, K. E, Saucier, M, Xiao, G, Rahme, L. G.: The contribution of MvfR to Pseudomonas aeruginosa pathogenesis and quorum sensing circuitry regulation: multiple quorum sensing-regulated genes are modulated without affecting lasRI, rhlRI or the production of N-acyl-L-homoserine lactones. *Molecular microbiology* 2005, 55(4):998-1014.

27. Kuspa A, Plamann, L, Kaiser, D.: A-signalling and the cell density requirement for Myxococcus xanthus development. *Journal of bacteriology* 1992, 174(22):7360-7369.

28. Hauryliuk V, Atkinson, G. C, Murakami, K. S, Tenson, T, Gerdes, K.: Recent functional insights into the role of (p)ppGpp in bacterial physiology. *Nature reviews Microbiology* 2015, 13(5):298-309.

29. Roberts JW: Promoter-specific control of E. coli RNA polymerase by ppGpp and a general transcription factor. *Genes & development* 2009, 23(2):143-146.

30. Dalebroux ZD, Svensson, S. L, Gaynor, E. C, Swanson, M. S.: ppGpp conjures bacterial virulence. *Microbiology and molecular biology reviews : MMBR* 2010, 74(2):171-199.

31. Poole K: Bacterial stress responses as determinants of antimicrobial resistance. *The Journal of antimicrobial chemotherapy* 2012, 67(9):2069-2089.

32. Geiger T, Francois, P, Liebeke, M, Fraunholz, M, Goerke, C, Krismer, B, Schrenzel, J, Lalk, M, Wolz, C.: The stringent response of Staphylococcus aureus and its impact on survival after phagocytosis through the induction of intracellular PSMs expression. *PLoS pathogens* 2012, 8(11):e1003016.

33. He H, Cooper, J. N, Mishra, A, Raskin, D. M.: Stringent response regulation of biofilm formation in Vibrio cholerae. *Journal of bacteriology* 2012, 194(11):2962-2972.

34. Boutte CC, Crosson, S.: Bacterial lifestyle shapes stringent response activation. *Trends in microbiology* 2013, 21(4):174-180.

35. Diaz-Salazar C, Calero, P, Espinosa-Portero, R, Jimenez-Fernandez, A,, Wirebrand L, Velasco-Dominguez, M. G, Lopez-Sanchez, A, Shingler, V, Govantes, F.: The stringent response promotes biofilm dispersal in Pseudomonas putida. *Scientific reports* 2017, 7(1):18055.

36. Crawford EW, Jr, Shimkets, L. J.: The Myxococcus xanthus socE and csgA genes are regulated by the stringent response. *Molecular microbiology* 2000, 37(4):788-799.

37. Kim SK, Kaiser, D.: C-factor: a cell-cell signaling protein required for fruiting body morphogenesis of M. xanthus. *Cell* 1990, 61(1):19-26.

38. Lobedanz S, Sogaard-Andersen, L.: Identification of the C-signal, a contact-dependent morphogen coordinating multiple developmental responses in Myxococcus xanthus. *Genes & development* 2003, 17(17):2151-2161.

39. Kroos L, Kaiser, D.: Expression of many developmentally regulated genes in Myxococcus depends on a sequence of cell interactions. *Genes & development* 1987, 1(8):840-854.

40. Rauch M, Lynch, S. V.: The potential for probiotic manipulation of the gastrointestinal microbiome. *Current opinion in biotechnology* 2012, 23(2):192-201.

41. Singh R, Paul, D, Jain, R. K.: Biofilms: implications in bioremediation. *Trends in microbiology* 2006, 14(9):389-397.

42. Puhakka JA, Herwig, R. P, Koro, P. M, Wolfe, G. V, Ferguson, J. F.: Biodegradation of chlorophenols by mixed and pure cultures from a fluidized-bed reactor. *Applied microbiology and biotechnology* 1995, 42(6):951-957.

43. Mitrophanov AY, Groisman, E. A.: Signal integration in bacterial two-component regulatory systems. *Genes & development* 2008, 22(19):2601-2611.

44. Mueller JP, Bukusoglu, G, Sonenshein, A. L.: Transcriptional regulation of Bacillus subtilis glucose starvation-inducible genes: control of gsiA by the ComP-ComA signal transduction system. *Journal of bacteriology* 1992, 174(13):4361-4373.

45. Gao R, Stock, A. M.: Biological insights from structures of two-component proteins. *Annual review of microbiology* 2009, 63:133-154.

46. Sonenshein AL: Control of sporulation initiation in Bacillus subtilis. *Current opinion in microbiology* 2000, 3(6):561-566.

47. Tojo S, Hirooka, K, Fujita, Y.: Expression of kinA and kinB of Bacillus subtilis, necessary for sporulation initiation, is under positive stringent transcription control. *Journal of bacteriology* 2013, 195(8):1656-1665.

48. Manganelli R, Provvedi, R.: An integrated regulatory network including two positive feedback loops to modulate the activity of sigma(E) in mycobacteria. *Molecular microbiology* 2010, 75(3):538-542.

49. Eichenberger P, Fujita, M, Jensen, S. T, Conlon, E. M, Rudner, D. Z, Wang, S. T, Ferguson, C, Haga, K, Sato, T, Liu, J. S, Losick, R.: The program of gene transcription for a single differentiating cell type during sporulation in Bacillus subtilis. *PLoS biology* 2004, 2(10):e328.

50. Giglio KM, Caberoy, N, Suen, G, Kaiser, D, Garza, A. G.: A cascade of coregulating enhancer binding proteins initiates and propagates a multicellular developmental program. *Proceedings of the National Academy of Sciences of the United States of America* 2011, 108(32):E431-439.

51. Kuspa A, Plamann, L, Kaiser, D.: Identification of heat-stable A-factor from Myxococcus xanthus. *Journal of bacteriology* 1992, 174(10):3319-3326.

52. Dong TC, Cutting, S. M.: The PDZ domain of the SpoIVB transmembrane signaling protein enables cis-trans interactions involving multiple partners leading to the activation of the pro-sigmaK processing complex in Bacillus subtilis. *The Journal of biological chemistry* 2004, 279(42):43468-43478.

53. Ray JC, Tabor, J. J, Igoshin, O. A.: Non-transcriptional regulatory processes shape transcriptional network dynamics. *Nature reviews Microbiology* 2011, 9(11):817-828.

54. Narula J, Devi, S. N, Fujita, M, Igoshin, O. A.: Ultrasensitivity of the Bacillus subtilis sporulation decision. *Proceedings of the National Academy of Sciences of the United States of America* 2012, 109(50):E3513-3522.

55. Dubnau D, Losick, R.: Bistability in bacteria. *Molecular microbiology* 2006, 61(3):564-572.

56. Bush M, Dixon, R.: The role of bacterial enhancer binding proteins as specialized activators of sigma54-dependent transcription. *Microbiology and molecular biology reviews : MMBR* 2012, 76(3):497-529.

57. Schuster M, Greenberg, E. P.: A network of networks: quorum-sensing gene regulation in Pseudomonas aeruginosa. *International journal of medical microbiology : IJMM* 2006, 296(2-3):73-81.

58. Svenningsen SL: Small RNA-Based Regulation of Bacterial Quorum Sensing and Biofilm Formation. *Microbiology spectrum* 2018, 6(4).

59. Tan IS, Ramamurthi, K. S.: Spore formation in Bacillus subtilis. *Environmental microbiology reports* 2014, 6(3):212-225.

60. Frum T, Ralston, A.: Cell signaling and transcription factors regulating cell fate during formation of the mouse blastocyst. *Trends in genetics : TIG* 2015, 31(7):402-410.

61. Levine M, Davidson, E. H.: Gene regulatory networks for development. *Proceedings of the National Academy of Sciences of the United States of America* 2005, 102(14):4936-4942.

62. Claessen D, Rozen, D. E, Kuipers, O. P, Sogaard-Andersen, L, van Wezel, G. P.: Bacterial solutions to multicellularity: a tale of biofilms, filaments and fruiting bodies. *Nature reviews Microbiology* 2014, 12(2):115-124.

63. Kaiser D, Robinson, M, Kroos, L.: Myxobacteria, polarity, and multicellular morphogenesis. *Cold Spring Harbor perspectives in biology* 2010, 2(8):a000380.

64. Mignot T: The elusive engine in Myxococcus xanthus gliding motility. *Cellular and molecular life sciences : CMLS* 2007, 64(21):2733-2745.

65. Nariya H, Inouye, M.: MazF, an mRNA interferase, mediates programmed cell death during multicellular Myxococcus development. *Cell* 2008, 132(1):55-66.

66. Konovalova A, Lobach S, Sogaard-Andersen L: A RelA-dependent two-tiered regulated proteolysis cascade controls synthesis of a contact-dependent intercellular signal in Myxococcus xanthus. *Molecular microbiology* 2012, 84(2):260-275.

67. Kuspa A, Plamann L, Kaiser D: A-signalling and the cell density requirement for Myxococcus xanthus development. *Journal of bacteriology* 1992, 174(22):7360-7369.

68. Boynton TO, Shimkets, L. J.: Myxococcus CsgA, Drosophila Sniffer, and human HSD10 are cardiolipin phospholipases. *Genes & development* 2015, 29(18):1903-1914.

69. Rolbetzki A, Ammon, M, Jakovljevic, V, Konovalova, A, Sogaard-Andersen, L.: Regulated secretion of a protease activates intercellular signaling during fruiting body formation in M. xanthus. *Developmental cell* 2008, 15(4):627-634.

70. Kim SK, Kaiser, D.: C-factor has distinct aggregation and sporulation thresholds during Myxococcus development. *Journal of bacteriology* 1991, 173(5):1722-1728.

71. Kruse T, Lobedanz, S, Berthelsen, N. M, Sogaard-Andersen, L.: C-signal: a cell surface-associated morphogen that induces and co-ordinates multicellular fruiting body morphogenesis and sporulation in Myxococcus xanthus. *Molecular microbiology* 2001, 40(1):156-168.

72. Giglio KM, Zhu, C, Klunder, C, Kummer, S, Garza, A. G.: The enhancer binding protein Nla6 regulates developmental genes that are important for Myxococcus xanthus sporulation. *Journal of bacteriology* 2015, 197(7):1276-1287.

73. Gronewold TM, Kaiser, D.: The act operon controls the level and time of C-signal production for Myxococcus xanthus development. *Molecular microbiology* 2001, 40(3):744-756.

74. Skotnicka D, Smaldone, G. T, Petters, T, Trampari, E, Liang, J, Kaever, V., Malone JG, Singer, M, Sogaard-Andersen, L.: A Minimal Threshold of c-di-GMP Is Essential for Fruiting Body Formation and Sporulation in Myxococcus xanthus. *PLoS genetics* 2016, 12(5):e1006080.

75. Sun H, Shi, W.: Genetic studies of mrp, a locus essential for cellular aggregation and sporulation of Myxococcus xanthus. *Journal of bacteriology* 2001, 183(16):4786-4795.

76. Nariya H, Inouye, S.: A protein Ser/Thr kinase cascade negatively regulates the DNA-binding activity of MrpC, a smaller form of which may be necessary for the Myxococcus xanthus development. *Molecular microbiology* 2006, 60(5):1205-1217.

77. McLaughlin PT, Bhardwaj, V, Feeley, B. E, Higgs, P. I.: MrpC, a CRP/Fnr homolog, functions as a negative autoregulator during the Myxococcus xanthus multicellular developmental program. *Molecular microbiology* 2018.

78. Higgs PI, Jagadeesan, S, Mann, P, Zusman, D. R.: EspA, an orphan hybrid histidine protein kinase, regulates the timing of expression of key developmental proteins of Myxococcus xanthus. *Journal of bacteriology* 2008, 190(13):4416-4426.

79. Schramm A, Lee, B, Higgs, P. I.: Intra- and interprotein phosphorylation between two-hybrid histidine kinases controls Myxococcus xanthus developmental progression. *The Journal of biological chemistry* 2012, 287(30):25060-25072.

80. Rajagopalan R K, L.: Nutrient-regulated proteolysis of MrpC halts expression of genes important for commitment to sporulation during Myxococcus xanthus development. *Journal of bacteriology* 2014, 196(15):2736-2747.

81. Robinson M, Son, B, Kroos, D, Kroos, L.: Transcription factor MrpC binds to promoter regions of hundreds of developmentally-regulated genes in Myxococcus xanthus. *BMC genomics* 2014, 15:1123.

82. Ueki T, Inouye, S.: Identification of an activator protein required for the induction of fruA, a gene essential for fruiting body development in Myxococcus xanthus. *Proceedings of the National Academy of Sciences of the United States of America* 2003, 100(15):8782-8787.

83. Ogawa M, Fujitani, S, Mao, X, Inouye, S, Komano, T.: FruA, a putative transcription factor essential for the development of Myxococcus xanthus. *Molecular microbiology* 1996, 22(4):757-767.

84. Ellehauge E, Norregaard-Madsen, M, Sogaard-Andersen, L.: The FruA signal transduction protein provides a checkpoint for the temporal co-ordination of intercellular signals in Myxococcus xanthus development. *Molecular microbiology* 1998, 30(4):807-817.

85. Kim SK, Kaiser, D.: Cell motility is required for the transmission of C-factor, an intercellular signal that coordinates fruiting body morphogenesis of Myxococcus xanthus. *Genes & development* 1990, 4(6):896-904.

86. Kim SK, Kaiser, D.: Cell alignment required in differentiation of Myxococcus xanthus. *Science* 1990, 249(4971):926-928.

87. Ueki T, Inouye, S.: Identification of a gene involved in polysaccharide export as a transcription target of FruA, an essential factor for Myxococcus xanthus development. *The Journal of biological chemistry* 2005, 280(37):32279-32284.

88. Viswanathan P, Murphy, K, Julien, B, Garza, A. G, Kroos, L.: Regulation of dev, an operon that includes genes essential for Myxococcus xanthus development and CRISPR-associated genes and repeats. *Journal of bacteriology* 2007, 189(10):3738-3750.

89. Rajagopalan R, Wielgoss, S, Lippert, G, Velicer, G. J, Kroos, L.: devI is an evolutionarily young negative regulator of Myxococcus xanthus development. *Journal of bacteriology* 2015, 197(7):1249-1262.

90. Rajagopalan R, Kroos L: The dev Operon Regulates the Timing of Sporulation during Myxococcus xanthus Development. *Journal of bacteriology* 2017, 199(10).

91. Thony-Meyer L, Kaiser, D.: devRS, an autoregulated and essential genetic locus for fruiting body development in Myxococcus xanthus. *Journal of bacteriology* 1993, 175(22):7450-7462.

92. Muller FD, Schink, C. W, Hoiczyk, E, Cserti, E, Higgs, P. I.: Spore formation in Myxococcus xanthus is tied to cytoskeleton functions and polysaccharide spore coat deposition. *Molecular microbiology* 2012, 83(3):486-505.

93. Holkenbrink C, Hoiczyk, E, Kahnt, J, Higgs, P. I.: Synthesis and assembly of a novel glycan layer in Myxococcus xanthus spores. *The Journal of biological chemistry* 2014, 289(46):32364-32378.

94. Cuthbertson L, Mainprize, I. L, Naismith, J. H, Whitfield, C.: Pivotal roles of the outer membrane polysaccharide export and polysaccharide copolymerase protein families in export of extracellular polysaccharides in gram-negative bacteria. *Microbiology and molecular biology reviews : MMBR* 2009, 73(1):155-177.

95. Bhat S, Boynton, T. O, Pham, D, Shimkets, L. J.: Fatty acids from membrane lipids become incorporated into lipid bodies during Myxococcus xanthus differentiation. *PloS one* 2014, 9(6):e99622.

96. Licking E, Gorski, L, Kaiser, D.: A common step for changing cell shape in fruiting body and starvation-independent sporulation of Myxococcus xanthus. *Journal of bacteriology* 2000, 182(12):3553-3558.

## CHAPTER 2: Systematic analysis of the *Myxococcus xanthus* developmental gene regulatory network supports posttranslational regulation of FruA by C-signaling

This chapter was published in the journal of Molecular Microbiology and can be found at the following citation.

Saha, S., Patra, P, Igoshin, O, Kroos, L. (2019). "Systematic analysis of the Myxococcus xanthus developmental gene regulatory network supports posttranslational regulation of FruA by C-signaling." Mol Microbiol **111**(6): 1732-1752.

I contributed significantly to the writing, editig and preparing all the figures for the manuscript. Data from all the wet-lab experiements were acquired and analyzed by me. Dr Pintu Patra from the research group of Dr Oleg Igoshin (Rice university, Houston) prfommed all the work related to the mathematical model.

Molecular micro provides authors the right to use and reprint published work without written permission as part of a dissertaion, give the work is properly cited (see above). The publication reprint and the supplementary material is provided on the following pages.

**Abstract**

Upon starvation *Myxococcus xanthus* undergoes multicellular development. Rod-shaped cells move into mounds in which some cells differentiate into spores. Cells begin committing to sporulation at 24-30 h poststarvation, but the mechanisms governing commitment are unknown. FruA and MrpC are transcription factors that are necessary for commitment. They bind cooperatively to promoter regions and activate developmental gene transcription, including that of the *dev* operon. Leading up to and during the commitment period, *dev* mRNA increased in wild type, but not in a mutant defective in C-signaling, a short-range signaling interaction between cells that is also necessary for commitment. The C-signaling mutant exhibited ~20-fold less *dev* mRNA than wild type at 30 h poststarvation, despite a similar level of MrpC and only twofold less FruA. Boosting the FruA level twofold in the C-signaling mutant had little effect on the *dev* mRNA level, and *dev* mRNA was not less stable in the C-signaling mutant. Neither did high cooperativity of MrpC and FruA binding upstream of the *dev* promoter explain the data. Rather, our systematic experimental and computational analyses support a model in which C-signaling activates FruA at least ninefold posttranslationally in order to commit a cell to spore formation.

## Introduction

Differentiated cell types are a hallmark of multicellular organisms. Understanding how pluripotent cells become restricted to particular cell fates is a fascinating question and a fundamental challenge in biology. In general, the answer involves a complex interplay between signals and gene regulation. This is true both during development of multicellular eukaryotes [1-3] and during transitions in microbial communities that lead to different cell types [4-7]. Bacterial cells in microbial communities adopt different fates as gene regulatory networks (GRNs) respond to a variety of signals, including some generated by other cells. Moreover, we now understand that microbial communities or microbiomes profoundly impact eukaryotic organisms, and vice versa [8, 9]. Yet the daunting complexity of microbiomes and multicellular eukaryotes impedes efforts to fully understand their interactions in molecular detail. By studying simpler model systems, paradigms can be discovered that can guide investigations of more complex interactions.

A relatively simple model system is provided by the bacterium *Myxococcus xanthus*, which undergoes starvation-induced multicellular development [10]. In response to starvation, cells generate intracellular and extracellular signals that regulate gene expression [7, 11]. The rod-shaped cells alter their movements so that thousands form a mound. Within a mound, cells differentiate into ovoid spores that resist stress and remain dormant until nutrients reappear. The spore-filled mound is called a fruiting body. Other cells adopt a different fate and remain outside the fruiting body as peripheral rods [12]. A large proportion of the cells lyse during the developmental process [13]. What determines whether a given cell in the population forms a spore, remains as a peripheral rod, or undergoes lysis? *M. xanthus* provides an attractive

model system to discover how signaling between cells affects a GRN and determines cell fate. Here, we focus on a circuit that regulates commitment to sporulation.

In a recent study, cells committed to spore formation primarily between 24 and 30 h poststarvation (PS), because addition of nutrients to the starving population prior to 24 h PS blocked subsequent sporulation, addition at 24 h PS allowed a few spores to form subsequently, and addition at 30 h PS allowed about tenfold more spores to form [14]. At the molecular level, addition of nutrients before or during the commitment period caused rapid proteolysis of MrpC [14], a transcription factor required for fruiting body formation [15, 16]. MrpC appears to directly regulate more than one hundred genes involved in development [17], and one well-characterized MrpC target gene, *fruA* [18], codes for another transcription factor required for fruiting body formation [19]. FruA and MrpC bind cooperatively to the promoter regions of many genes, and appear to activate transcription [17, 20-24]. In particular, transcription of the *dev* operon appears to be activated by cooperative binding of the two transcription factors at two sites located upstream of the promoter [20]. Because mutations in three genes of the *dev* operon (*devTRS*) strongly impair sporulation [25-27], the feed-forward loop involving MrpC and FruA regulation of the *dev* operon is an attractive molecular mechanism to control spore formation (Fig. 1). Recent work revealed that products of the *dev* operon act as a timer for sporulation [28]. DevTRS negatively autoregulate expression of DevI, which inhibits sporulation if overproduced, and delays sporulation by about 6 h when produced normally [28, 29] (Fig. 1).

Expression of the *dev* operon and many other developmental genes depends on C-signaling [30], which has been proposed to activate FruA [31] and/or MrpC [22] (Fig. 1), although the

mechanism of C-signal transduction remains a mystery. Null mutations in the *csgA* gene block C-signaling and sporulation, but the mutants can be rescued by co-development with *csgA*$^{+}$ cells which supply the C-signal [32]. C-signaling appears to be a short-range signaling interaction that requires cells to move into alignment [33-35], as they do during mound formation [36]. Two theories about the identity of the C-signal have emerged. One theory states that the C-signal is a 17-kDa fragment of CsgA produced by the specific proteolytic activity of PopC at the cell surface [37-39].

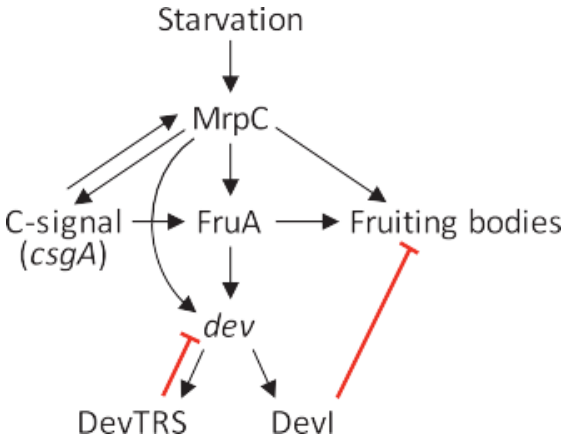


**Figure 2.1 Simplified model of the gene regulatory network governing formation of fruiting bodies.** Starvation increases the level of MrpC early in the process [40-42]. MrpC causes an increase in C-signal [41], the product of *csgA* [43, 44]. MrpC activates transcription of the gene for FruA [45] and C-signal somehow enhances FruA [46] and/or MrpC activity [47]. MrpC and FruA bind cooperatively to the promoter region of the *dev* operon and activate transcription [48]. The resulting DevTRS proteins negatively autoregulate [49-52]. DevI delays spore formation within nascent fruiting bodies [52], but if overproduced, DevI inhibits sporulation [51], which is promoted by MrpC [40] and FruA [53] activity.

The other theory is that diacylglycerols released from the inner membrane by cardiolipin phospholipase activity of intact CsgA are the C-signal [54]. However, in neither case has the signal receptor been identified, so our understanding of C-signaling is incomplete. Likewise, how C-signaling impacts recipient cells is unknown. One way that C-signaling has been proposed to affect recipient cells is to stimulate autophosphorylation of a histidine protein kinase, which would then transfer the phosphate to FruA [31]. This model was attractive because FruA is similar to response regulators of two-component signal transduction systems [19, 31]. Typically, a response regulator is phosphorylated by a histidine protein kinase in response to a signal, thus activating the response regulator to perform a function [55]. The effects of substitutions at the predicted site of phosphorylation in FruA supported the model that FruA is activated by phosphorylation on D59 [31]. However, a histidine protein kinase capable of phosphorylating FruA has not been identified. Also, several observations suggest that FruA may not be phosphorylated. Most notably, D59 of FruA is present in an atypical receiver domain that lacks a conserved metal-binding residue normally required for phosphorylation to occur, and treatment of FruA with small-molecule phosphodonors did not increase its DNA-binding activity [22]. The receiver domain of FruA was shown to be necessary for cooperative binding with MrpC to DNA, so it was proposed that C-signaling may affect activity of MrpC and/or FruA [22] (Fig. 1).

The regulation of MrpC has been reported to be complex, involving autoregulation, phosphorylation, proteolytic processing, binding to a toxin protein, and stability [14, 15, 56-60]. Also, since MrpC is similar to CRP family transcription factors that bind cyclic nucleotides [15],

MrpC activity could be modulated by nucleotide binding, so there are many ways in which C-signaling could affect MrpC activity [22].

Here, using synergistic experimental and computational approaches, we investigate the impact of C-signaling on a circuit that regulates commitment to sporulation by focusing on the feed-forward loop involving MrpC and FruA control of *dev* operon transcription (Fig. 1). We describe methods to systematically and quantitatively study the developmental process. Using these methods we measure the levels of GRN components in wild type and in mutants (e.g., a *csgA* mutant unable to produce C-signal) during the period leading up to and including commitment to spore formation. We then formulate a mathematical model for the steady-state concentration of *dev* mRNA and use the model to computationally predict the magnitude of potential regulatory effects of C-signaling that would be required to explain our data. By testing the predictions, some potential regulatory mechanisms are ruled out and at least ninefold activation of FruA by C-signaling is supported.

## Results

### *M. xanthus development can be studied systematically*

We first established quantitative assays to analyze cellular and molecular changes during *M. xanthus* development. To facilitate collection of sufficient cell numbers for counting, as well as for RNA and protein measurements, development was induced by starvation under submerged culture conditions. Cells adhere to the bottom of a plastic well or dish, and develop under a layer of buffer. Prior to cell harvest, photos were taken to document phenotypic differences between strains. As expected, wild-type strain DK1622 formed mounds by 18 h poststarvation (PS) and the mounds matured into compact, darkened fruiting bodies at 36 to 48 h PS (Fig. 2). In contrast, *csgA* and *fruA* null mutants failed to progress beyond forming loose aggregates. A *devI* null mutant was similar to wild type (WT), whereas a *devS* null mutant formed mounds slowly and they failed to darken. Developing populations were harvested at the times indicated in Figure 2 to measure cellular and molecular changes in the same populations. To quantify changes at the cellular level, we counted the total number of cells (after fixation and dispersal, so that rod-shaped cells, spores, and cells in transition between the two were counted) and the number of sonication-resistant spores in the developing populations.

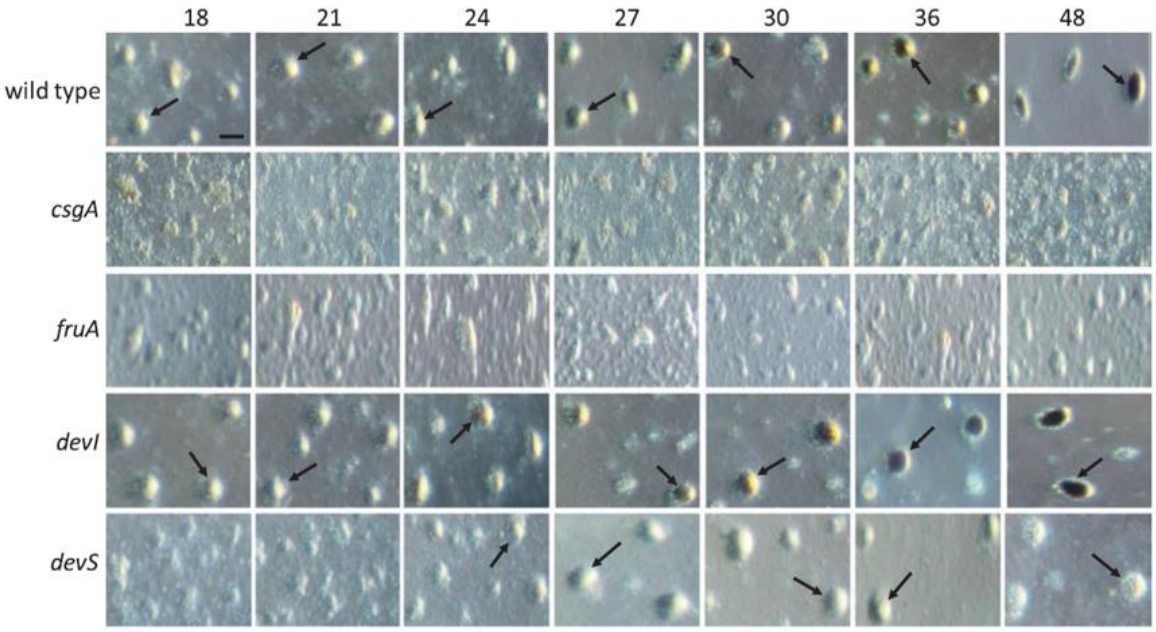


**Figure 2.2 Development of *M. xanthus* strains.** Wild-type DK1622 and its indicated mutant derivatives were subjected to starvation under submerged culture conditions and images were obtained at the indicated number of hours poststarvation (PS). DK1622 formed mounds by 18 h PS (an arrow points to one). The *csgA* and *fruA* mutants failed to form mounds, the *devI* mutant was similar to DK1622 and the *devS* mutant formed mounds later, by 24 h PS, but the mounds failed to darken at later times. Bar, 100 µm. Similar results were observed in at least three biological replicates.

We also counted the number of rod-shaped cells at the time when development was initiated by starvation ($T_0$). By subtracting the number of sonication-resistant spores from the total cell number, we determined the number of sonication-sensitive cells. About 30% of the wild-type cells present at $T_0$ remained as sonication-sensitive cells at 18 h PS (Fig. S1A), consistent with the suggestion that the majority of cells lyse early during development under submerged culture conditions, which was based on the decrease in the total protein concentration of developing cultures [14]. The number of sonication-sensitive cells continued to decline after 18

h PS, reaching ~4% of the $T_0$ number by 48 h PS (Fig. S1A). Spores were first observed at 27 h PS and the number rose to ~1% of the $T_0$ number by 48 h PS (Fig. S1B). The *devI* mutant was similar to WT, except spores were first observed 6 h earlier at 21 h PS, as reported recently [28]. The *csgA*, *fruA*, and *devS* mutants failed to make a detectable number of spores (at a detection limit of 0.01% of the $T_0$ number) and appeared to be slightly delayed relative to WT and the *devI* mutant in terms of the declining number of sonication-sensitive cells (Fig. S1). We conclude that at the cellular level during the time between 18 and 30 h PS (when we measured RNA and protein levels as described below), the developing populations decline from ~30-40% to ~10-20% of the initial rod number and only ~0.5% (WT, *devI*) or <0.01% (*csgA*, *fruA*, *devS*) of the cells form sonication-resistant spores (from which the RNAs and proteins we measured would not be recovered based on control experiments). We stopped collecting samples at 30 PS because thereafter the number of sonication-sensitive cells continues to decline and the spore number continues to rise, making RNA and protein more difficult to recover quantitatively, yet many cells are committed at 30 h PS to make spores by 36 h PS even if nutrients are added [14]. Hence, we focused on changes at the molecular level between 18 and 30 h PS, the period leading up to and including the time that many cells commit to spore formation.

To measure RNA levels of a large number of samples, we adapted methods described previously [14] to a higher-throughput robotic platform for RT-qPCR analysis. Reproducibility of the analysis was tested among biological replicates and two types of technical replicates as illustrated in Figure S2A, for each RNA to be measured, at 24 h PS, the midpoint of our focal period. No normalization was done in this experiment. Each transcript number was derived from a standard curve of genomic DNA subjected to qPCR. For each RNA, we found that the

average transcript number and the standard deviation for three cDNA technical replicates from a single RNA sample, three RNA technical replicates from a single biological replicate, and three biological replicates, was not significantly different (single factor ANOVA, $\alpha = 0.05$) (Fig. S2B-S2E). These results suggest that biological variation in RNA levels at 24 h PS is comparable to technical variation in preparing RNA and cDNA. In subsequent experiments, we measured RNA for at least three biological replicates and we did not perform RNA or cDNA technical replicates. We also note the high abundance of the *mrpC* transcript (~10%) relative to 16S rRNA, and the lower relative abundance of the *fruA* (~1%) and *dev* (~0.1%) transcripts.

We have typically used 16S rRNA as an internal standard for RT-qPCR analysis during *M. xanthus* development [14]. The high abundance of *mrpC* transcript relative to 16S rRNA at 24 h PS (Fig. S2B and S2E) raised the possibility that rRNA decreases relative to total RNA at 18 to 30 h PS. To test this possibility, we measured the 16S rRNA level per 1μg of total RNA from 18 to 30 h PS. Figure S3A shows that the level does not change significantly (single factor ANOVA, $\alpha = 0.05$), validating 16S rRNA as an internal standard for subsequent experiments. We also found that the total RNA yield per cell does not change significantly from 18 to 30 h PS (single factor ANOVA, $\alpha = 0.05$) (Fig. S3B), consistent with the finding that the 16S rRNA level does not change significantly, since the majority of total RNA is rRNA.

To measure protein levels, a portion of each well-mixed developing population was immediately added to sample buffer, boiled, and frozen for subsequent semi-quantitative immunoblot analysis [28]. The rest of the population was used for cell counting and RNA analysis as described above and in the Experimental Procedures.

***Levels of MrpC and FruA fail to account for the low level of dev mRNA in a* csgA *mutant***

By systematically quantifying protein and mRNA levels during the period leading up to and including the time that cells commit to spore formation, we investigated whether the GRN shown in Figure 1 could account for observed changes over time in WT and in mutants. In particular, we were interested in whether changes in the levels of MrpC and/or FruA proteins could account for the observed changes in the level of *dev* mRNA, since MrpC and FruA bind cooperatively to the *dev* promoter region and activate transcription [20]. In WT, we found that the MrpC level decreased about 1.5-fold on average from 18 to 30 h PS (Fig. 3A) and the FruA level rose about 1.5-fold on average (Fig. 3B), whereas the *dev* mRNA level rose about threefold on average (Fig. 4A). In each case, the fold-change was small and the variation between biological replicates was large, so the result of a single factor ANOVA ($\alpha = 0.05$) for each time course did not support a significant difference. We reasoned that cooperative binding of MrpC and FruA could easily account for the threefold rise on average in *dev* mRNA. We also measured the levels of *mrpC* and *fruA* mRNA. The *mrpC* mRNA level changed very little on average (Fig. 4B), but the *fruA* mRNA level decreased about twofold on average after 18 h PS (Fig. 4C), in contrast to the 1.5-fold rise on average in the FruA protein level (Fig. 3B), suggesting weak positive posttranscriptional regulation of the FruA level during the period of commitment to spore formation.

To investigate how C-signaling affects the GRN shown in Figure 1, we measured protein and mRNA levels in the *csgA* null mutant. In agreement with earlier studies suggesting that C-signaling activates FruA [31] and/or MrpC [22], we found very little *dev* mRNA in the *csgA* mutant (Fig. 4A). Notably, the large decrease in the level of *dev* mRNA in the *csgA* mutant

compared with WT could not be accounted for by a large decrease in the level of MrpC or FruA. The MrpC level was elevated about 1.5-fold on average in the *csgA* mutant relative to WT at most time points (Fig. 3A), but the differences were not statistically significant ($p > 0.05$ in Student's two-tailed *t*-tests comparing mutant to WT at each time point). The FruA level was diminished in the *csgA* mutant relative to WT, but only about twofold on average (Fig. 3B). The differences in the FruA level were statistically significant ($p < 0.05$ in Student's two-tailed *t*-tests) at each time point except 21 h PS ($p = 0.12$), but alone the twofold lower levels of FruA in the *csgA* mutant fail to account for the very low levels of *dev* mRNA.

We also investigated if CsgA regulates *dev* transcription via LadA instead of FruA. LadA is a LysR type of transcriptional activator, which was earlier shown to activate *dev* transcription by direct binding. In a *ladA* mutant, developmental expression of *dev* was shown to be impaired from a *lacZ* transcriptional fusion, *dev* transcription is dependent on LadA during development. In contradiction to the earlier findings, in our laboratory conditions, in the absence of LadA, *dev* expression was found to be unchanged in comparison to the wild type during commitment. Hence, in our laboratory condition developmental expression of *dev* does not appear to be dependent on LadA. Though earlier in commitment the *ladA* mutant was delayed in mound formation compared to the wild type, by 48 h PS the mutant formed dark fruiting bodies and 50% of the wild type sonication resistant spores. We compared the levels of *fmg* genes between wild type and *ladA* mutant. During the commitment period, the level of *fmgE* transcript was consistently low in the *ladA* mutant compared to the wild type. Both *fmgA* and *fmgD* showed significant decrease at 18 h PS, whereas, *fmgB* was significantly low at 18 h and 24 h PS in ladA mutant compared to wild type.

The *mrpC* and *fruA* mRNA levels were diminished about twofold and 1.5-fold on average, respectively, in the *csgA* mutant relative to WT (Fig. 4B and 4C), but at nearly all time points the differences were not statistically significant ($p > 0.05$ in Student's two-tailed *t*-tests, except $p = 0.02$ at 27 h for *mrpC* mRNA).

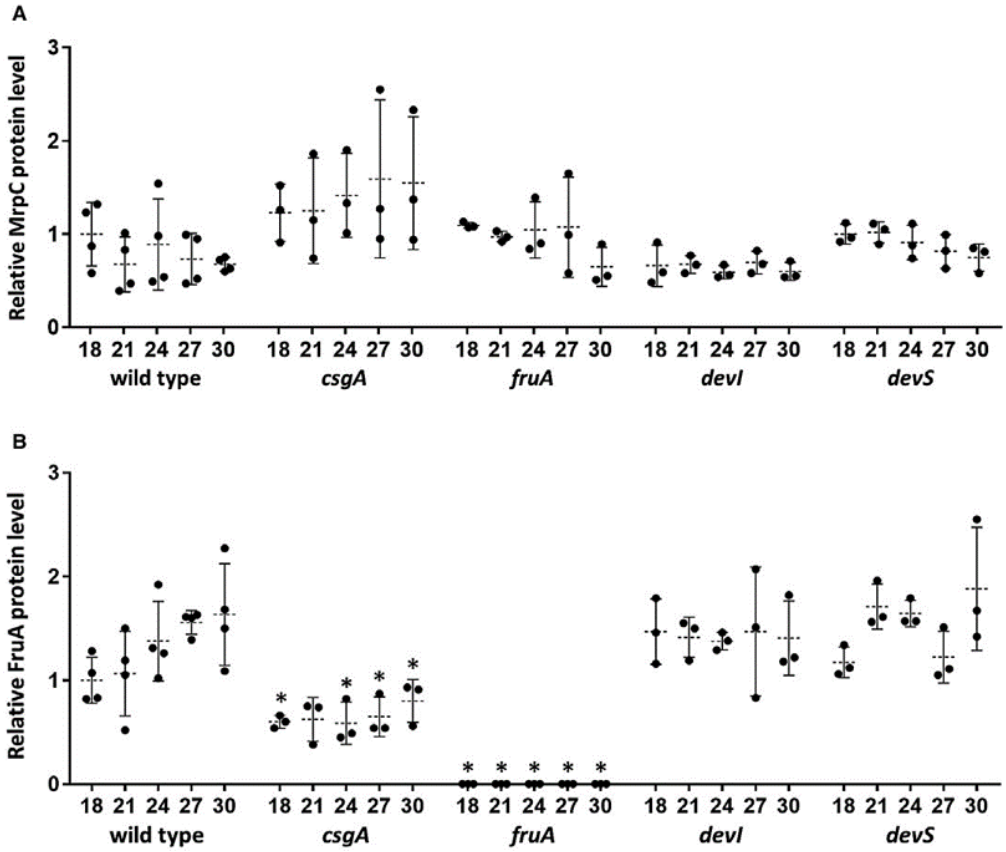


**Figure 2.3 Levels of MrpC and FruA during *M. xanthus* development.** Wild-type DK1622 and its indicated mutant derivatives were subjected to starvation under submerged culture conditions and samples were collected at the indicated number of hours poststarvation (PS) for measurement of MrpC (A) and FruA (B) by immunoblot. Graphs show the data points and average of at least three biological replicates, relative to wild-type DK1622 at 18 h PS, and error bars show one standard deviation. Asterisks indicate a significant difference ($p < 0.05$ in Student's two-tailed t-tests) from wild type at the corresponding time PS.

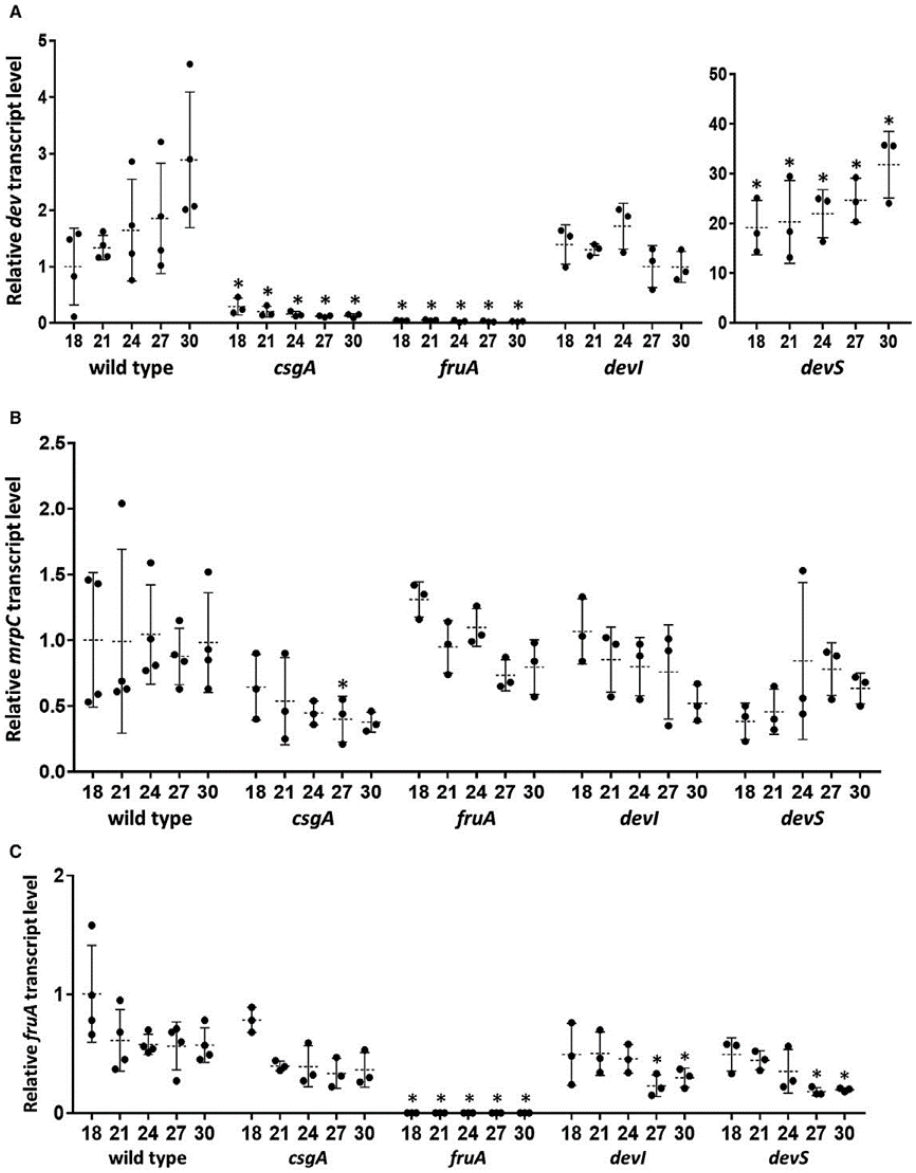


**Figure 2.4 Transcript levels during *M. xanthus* development.** Wild-type DK1622 and its indicated mutant derivatives were subjected to starvation under submerged culture conditions and samples were collected at the indicated number of hours poststarvation (PS) for measurement of *dev* (A), *mrpC* (B) and *fruA* (C) transcript levels by RT-qPCR. Graphs show the data points and average of at least three biological replicates, relative to wild-type DK1622 at 18 h PS and error bars show one standard deviation. Asterisks indicate a significant difference ($p < 0.05$ in Student's two-tailed *t*-tests) from wild type at the corresponding time PS.

The small differences in the level of *fruA* mRNA in the *csgA* mutant relative to WT are especially noteworthy, since they imply that C-signaling has little or no effect on MrpC activity. The results of our *fruA* mRNA measurements agree with published reports using *fruA*-*lacZ* fusions [31, 61]. Furthermore, we found that *fruA* mRNA stability is similar in the *csgA* mutant and in WT at 30 h PS (Fig. S4), indicating that the similar steady-state *fruA* mRNA level we observed (Fig. 4C) reflects a similar rate of synthesis, rather than altered synthesis compensated by altered stability. We conclude that C-signaling does not affect MrpC activity. Therefore, the low level of *dev* mRNA in a *csgA* mutant (Fig. 4A) could be due to failure to activate FruA or to *dev*-specific regulatory mechanisms.

To begin to characterize potential *dev*-specific regulatory mechanisms during the period leading up to and including commitment to sporulation, we measured protein and mRNA levels in the *devS* and *devI* null mutants. The MrpC and FruA levels were similar to WT (Fig. 3). The *dev* mRNA level ranged from 20-fold higher in the *devS* mutant than in WT at 18 h PS, to 10-fold higher at 30 h PS (Fig. 4A), consistent with negative autoregulation by DevS (and DevT and DevR) reported previously [28, 29]. Unexpectedly, the *dev* mRNA level in the *devI* mutant was about threefold lower than in WT at 30 h PS (Fig. 4A), suggesting that DevI feeds back positively on accumulation of *dev* mRNA, although the difference was not quite statistically significant at the 95% confidence level ($p = 0.06$ in Student's two-tailed *t*-test). Other differences were that the *fruA* mRNA levels in the *devI* and *devS* mutants were about twofold lower than in WT at 27 and 30 h PS (Fig. 4C), and these were statistically significant ($p < 0.05$ in Student's two-tailed *t*-tests comparing mutant to WT at each time point). Since the FruA levels in these mutants were

similar to those in WT (Fig. 3B), positive posttranscriptional regulation of FruA appeared to occur in the mutants, as well as in WT.

To complete our characterization of the GRN shown in Figure 1, we also measured protein and mRNA levels in the *fruA* and *mrpC* null mutants. We did not collect samples of the *mrpC* mutant at as many time points since we expected little or no expression of GRN components. As expected, neither MrpC nor FruA were detected in the *mrpC* mutant (Fig. S5). In the *fruA* mutant, the MrpC level was similar to WT and, as expected, FruA was not detected (Fig. 3). Also as expected, in the *fruA* mutant the *fruA* mRNA was not detected, the *dev* mRNA level was very low, and the *mrpC* mRNA level was similar to WT (Fig. 4). Since the *mrpC* mutant had an in-frame deletion of codons 74 to 229 [15], we were able to design primers for RT-qPCR analysis that should detect the shorter *mrpC* transcript. Surprisingly, the *mrpC* mutant exhibited an elevated level of *mrpC* transcript compared with WT at 18 and 24 h PS (Fig. S6A). The result was surprising since expression of an *mrpC-lacZ* fusion had been reported to be abolished in the *mrpC* mutant, which had led to the conclusion that MrpC positively autoregulates [15]. We considered the possibility that the shorter transcript in the *mrpC* mutant is more stable than the WT transcript, but the transcript half-lives after addition of rifampicin did not differ significantly (Fig. S7). We conclude that MrpC negatively regulates the *mrpC* transcript level. While this work was in progress, McLaughlin *et al*. reached the same conclusion [60]. In all other respects, the *mrpC* mutant yielded expected results. The *fruA* and *dev* transcripts were very low (Fig. S6B and S6C), consistent with the expectations that MrpC is required to activate *fruA* transcription [18] and that MrpC and FruA are required to activate *dev* transcription [20, 31, 62]. Also, the *mrpC* mutant failed to progress beyond forming loose aggregates (Fig. S8),

appeared to be slightly delayed relative to WT in terms of the declining number of sonication-sensitive cells (Fig. S9A), and failed to make a detectable number of spores (at a detection limit of 0.01% of the $T_0$ number) (Fig. S9B).

Taken together, our systematic, quantitative measurements of components of the GRN shown in Figure 1 imply that failure to activate FruA and/or *dev*-specific regulatory mechanisms may account for the low level of *dev* mRNA in a *csgA* mutant. Given the complex feedback architecture of *dev* regulation (i.e., strong negative feedback by DevTRS and weak positive feedback by DevI at 30 h PS), delineating the effects of C-signaling on the *dev* transcript level requires a mathematical modeling approach.

### *Mathematical modeling suggests several mechanisms that could explain the low level of dev mRNA in the* csgA *mutant*

The observed small differences in the levels of MrpC and FruA in the *csgA* mutant relative to WT do not account for the very low level of *dev* mRNA in the *csgA* mutant. To evaluate plausible mechanisms that may explain these experimental findings, we quantitatively analyzed transcriptional regulation of *dev* by formulating a mathematical model that expresses the *dev* mRNA concentration as a function of the regulators MrpC, FruA, DevI, and DevS. MrpC and FruA bind cooperatively to the *dev* promoter region and activate transcription [20]. Our results suggest that DevI is a weak positive regulator and DevS is a strong negative regulator of *dev* transcription by 30 h PS (Fig. 4A). Incorporating these effects into a transcriptional regulation model, we express the concentration of *dev* mRNA as a product of three regulation functions ($\Pi_{\mathrm{FM}}, \Pi_{\mathrm{I}}, \Pi_{\mathrm{S}}$) divided by the transcript degradation rate $\delta_{dev}$ (see Experimental Procedures for detailed explanation):

$$[\mathrm{mRNA}_{dev}] = \frac{1}{\delta_{dev}} \underbrace{\left( \alpha_{\mathrm{FM}} \frac{\left(\frac{[\mathrm{FruA}][\mathrm{MrpC}]}{\mathrm{K_{FM}}}\right)^{a}}{1+\left(\frac{[\mathrm{FruA}][\mathrm{MrpC}]}{\mathrm{K_{FM}}}\right)^{a}} \right)}_{\Pi_{\mathrm{FM}}} \underbrace{\left( 1+\alpha_{\mathrm{I}} \frac{\left(\frac{[\mathrm{DevI}]}{\mathrm{K_I}}\right)^{b}}{1+\left(\frac{[\mathrm{DevI}]}{\mathrm{K_I}}\right)^{b}} \right)}_{\Pi_{\mathrm{I}}} \underbrace{\left( \frac{1}{1+\left(\frac{[\mathrm{DevS}]}{\mathrm{K_S}}\right)^{c}} \right)}_{\Pi_{\mathrm{S}}}$$

Here, we use a quasi-steady state approximation for the mRNA levels by taking advantage of the fact that mRNA decay (with half-lives typically in minutes) is much faster than our experimental measurement times (in hours). This allows us to assume a rapid equilibrium between the rate of *dev* transcription and the decay of its mRNA, which leads to the above equation, in which $\alpha_{\mathrm{FM}}, \alpha_{\mathrm{I}}, \delta_{\mathrm{dev}}, \mathrm{a}, \mathrm{b}, \mathrm{c}, \mathrm{K_{FM}}, \mathrm{K_I}$ and $\mathrm{K_S}$ are parameters characterizing promoter regulation. We assume that these biochemical parameters are not a function of the genetic background and, therefore, in the strains in which *dev* mRNA was measured (e.g., the *csgA* mutant), the concentration of *dev* mRNA is determined by the concentrations of proteins (indicated by square brackets in the equation), more specifically the concentrations of their transcriptionally active forms (in case there is a posttranslational regulation). To estimate how the different regulation parameters (such as transcription rate, degradation rate, cooperativity constant, etc.) affect the *dev* mRNA level, we first constrain the model parameters by the experimental result shown in Figure 3B, $[\mathrm{FruA}]_{\mathrm{WT}}/[\mathrm{FruA}]_{csgA} \cong 2$, and search for parameters that can result in the observed 22-fold difference in $[\mathrm{mRNA}_{dev}]$ in WT relative to the *csgA* mutant at 30 h PS (Fig. 4A).

To estimate the contribution of autoregulation by Dev proteins to their own transcription (i.e., the terms $\Pi_{\mathrm{I}}, \Pi_{\mathrm{S}}$) in WT and the *csgA* mutant, we employ the data from the *devI* and *devS* mutants (Fig. 4A). Specifically, we take the ratio of the *dev* mRNA level in WT to that in *devI* and *devS* mutants to estimate the feedback regulation from DevI and DevS, respectively (see

Experimental Procedures for details). We find the contribution from DevI and DevS feedback regulation in WT to be $\Pi_{\mathrm{I,WT}} = 2.9$ and $\Pi_{\mathrm{S,WT}} = 0.091$, respectively. Using these values, we find the contribution from FruA and MrpC regulation to be $\Pi_{\mathrm{FM,WT}}/\delta_{dev,\mathrm{WT}} = 11$. In the *csgA* mutant, since the *dev* mRNA level is very low, we assume the DevI and DevS protein levels to be low. This gives the contribution of different regulation functions as $\Pi_{\mathrm{I},csgA} \approx 1$, $\Pi_{\mathrm{S},csgA} \approx 1$, and $\Pi_{\mathrm{FM},csgA}/\delta_{dev,csgA} = 0.13$. In summary, this analysis reveals that the twofold reduction of FruA protein observed in the *csgA* mutant (Fig. 3B) leads to a change of $(\Pi_{\mathrm{FM,WT}}/\Pi_{\mathrm{FM},csgA})(\delta_{dev,csgA}/\delta_{dev,\mathrm{WT}}) \approx 84$-fold in the FruA- and MrpC-dependent transcript regulation term. We reasoned that the observed 22-fold reduction in *dev* transcript in the *csgA* mutant relative to WT at 30 h PS (Fig. 4A) could result from a reduction in the FruA- and MrpC-dependent activation rate $\Pi_{\mathrm{FM}}$ and/or an increase in the transcript degradation rate $\delta_{dev}$. In what follows we use the mathematical model to predict the magnitude of these effects that would be necessary to explain the observed 22-fold difference in $[\mathrm{mRNA}_{dev}]$.

- **Hypothesis 1: Increase in *dev* transcript degradation rate in the *csgA* mutant**

First, we estimate the difference in *dev* transcript degradation rate necessary to explain the observed difference in transcript level between WT and the *csgA* mutant. For this, we make two assumptions. First, we assume that MrpC and FruA bind to the *dev* promoter region with a Hill cooperativity coefficient $a = 2$ (i.e., the maximum for a single cooperative binding site). Second, we assume that the observed twofold difference in FruA protein level results in a twofold difference in transcriptionally active FruA. Under these assumptions, we vary the remaining unknown parameters to compute the required fold difference in transcript degradation rate for different values of promoter saturation. Our results plotted in Figure 5A

show that at least a 20-fold difference in transcript degradation rate is required to explain the transcript data. This experimentally testable prediction will be assessed in a subsequent section.

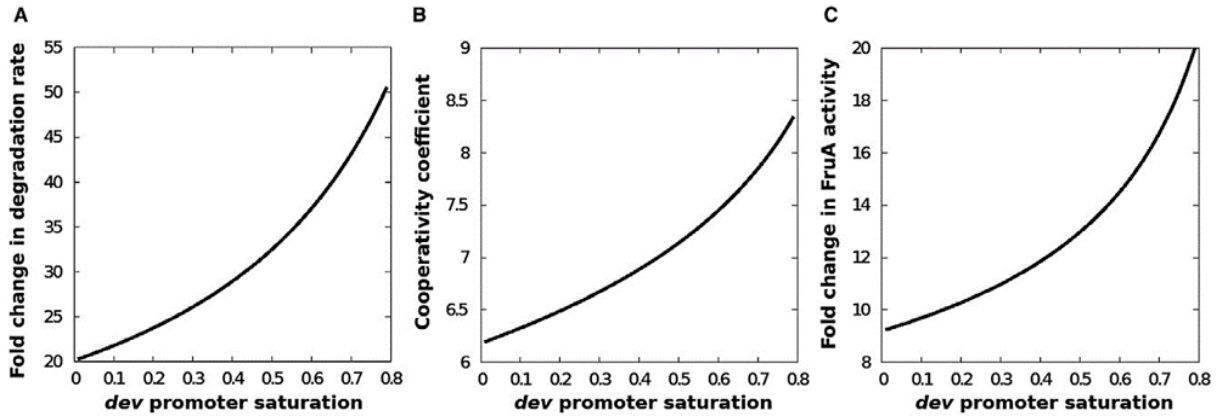


**Figure 2.5 Mathematical modeling of different hypotheses to explain the low *dev* transcript level in a *csgA* mutant.** Plots showing the required fold change in *dev* transcript degradation rate in the *csgA* mutant in comparison to wild type (A), cooperativity coefficient for MrpC and FruA binding to the *dev* promoter region (B) and reduction in FruA activity in the *csgA* mutant in comparison to wild type (C), to explain the experimental data for different values of promoter saturation.

If the results are inconsistent with this prediction, we must conclude that at least one of the two assumptions above is invalid, resulting in the following two alternative hypotheses: the Hill coefficient of MrpC and FruA binding to the *dev* promoter region is much higher than $a = 2$ and/or the amount of transcriptionally active FruA does not scale with the measured FruA protein level (e.g., if *csgA*-dependent C-signaling is also involved in posttranslational activation of FruA).

- **Hypothesis 2: High cooperativity of MrpC and FruA binding to the *dev* promoter region**

Next, we test if a higher binding cooperativity can explain the difference in *dev* transcript level between WT and the *csgA* mutant. We compute the required cooperativity coefficient by assuming the degradation rate does not change between the two strains. Our results plotted in Figure 5B show that the minimum cooperativity coefficient required to explain the experimental results is six for low promoter saturation. In biologically realistic conditions, where promoter saturation is higher; the required cooperativity is even higher. Such a large cooperativity can only be explained if there is more than one site in the promoter region where MrpC and FruA bind with high cooperativity. We know that the *dev* promoter region has at least two MrpC and FruA cooperative binding sites; one is proximal upstream, whereas the other is distal upstream [20]. Interaction between the proximal and distal upstream binding sites by DNA looping may contribute to high cooperativity coefficient predicted by the model. The distal upstream binding site appeared to boost *dev* promoter activity after 24 h PS, based on β-galactosidase activity from a *lacZ* reporter. Hence, in a subsequent section, we study the impact of a distal site deletion on different transcripts (*mrpC, fruA, dev*) and proteins (MrpC, FruA) to test if presence of the distal site contributes to higher cooperativity. If the results are

not consistent with the model predictions, we must conclude that the fold difference in active FruA exceeds that observed for the total concentration of each protein (i.e., *csgA*-dependent C-signaling is involved in posttranslational activation of FruA).

- **Hypothesis 3: Posttranslational regulation of FruA activity**

To assess the difference in active FruA level required to explain the observed difference in *dev* transcript level, in the absence of other effects, we fix the cooperativity coefficient at $a = 2$ and assume the transcript degradation rate to be unchanged between WT and the *csgA* mutant. We then use our model to compute the fold difference in active FruA required to achieve a 22-fold reduction in *dev* transcript in the *csgA* mutant relative to WT. Our results plotted in Figure 5C show that at least a ninefold reduction in active FruA is needed in the *csgA* mutant. The reduction in active FruA in the *csgA* mutant would presumably be due to the absence of C-signal-dependent posttranslational activation of FruA, not due to the twofold lower level of FruA protein we observed in the *csgA* mutant relative to WT (Fig. 3B). The reduction in active FruA may be considerably greater than ninefold if the *dev* promoter region approaches saturation (e.g., 20-fold at 80% saturation in Fig. 5C). Also, mathematical modeling of our data at each time point from 18 to 30 h PS yields a similar result (Fig. S10), suggesting that in WT, FruA has already been activated by C-signaling at least ninefold by 18 h PS, and perhaps as much as 30-fold if the *dev* promoter region approaches saturation (righthand panel in Fig. S10).

***Stability of the* dev *transcript is unchanged in a* csgA *mutant***

To measure the *dev* transcript degradation rate in WT and the *csgA* mutant, we compared the *dev* transcript levels after addition of rifampicin to block transcription at 30 h PS. The average half-life of the *dev* transcript in three biological replicates was 11 ± 6 min in WT and 7 ± 1 min in

the *csgA* mutant (Fig. 6), which is not a statistically significant difference ($p = 0.36$ in a Student's two-tailed *t*-test). We conclude that elevated turnover does not account for the low level of *dev* transcript in the *csgA* mutant. These results allow us to rule out Hypothesis 1.

### *The distal upstream binding site for MrpC and FruA has little impact on the* dev *transcript level*

In a previous study, weak cooperative binding of MrpC and FruA to a site located between positions -254 and -229 upstream of the *dev* promoter appeared to boost β-galactosidase activity from a *lacZ* transcriptional fusion about twofold between 24 and 30 h PS, but deletion of the distal upstream site did not impair spore formation [20]. These findings suggested that the distal site has a modest impact on *dev* transcription that is inconsequential for sporulation. However, β-galactosidase activity from *lacZ* fused to *dev* promoter segments with different amounts of upstream DNA and integrated ectopically may not accurately reflect the contribution of the distal site to the *dev* transcript level. Therefore, we measured the *dev* transcript level in a mutant lacking the distal site (i.e., DNA between positions -254 and -228 was deleted from the *M. xanthus* chromosome). The level of *dev* transcript in the distal site mutant was similar to WT measured in the same experiment, in this case increasing about twofold from 18 to 30 h PS (Fig. 7). Likewise, there were no significant differences between the distal site mutant and WT in the levels of *mrpC* or *fruA* transcripts (Fig. S6) or the corresponding proteins (Fig. S5) ($p > 0.05$ in Student's two-tailed *t*-tests comparing mutant to WT at each time point). The distal site mutant formed mounds by 18 h PS, which matured into compact, darkened fruiting bodies at later times, similar to WT (Fig. S8), and the percentages of sonication-sensitive cells and sonication-resistant spores observed for the distal site mutant were similar to WT (Fig. S9). We conclude that the distal site has little or no impact on the

developmental process. In particular, the distal site does not contribute to high cooperativity of MrpC and FruA binding to the *dev* promoter region that could explain the higher level of *dev*

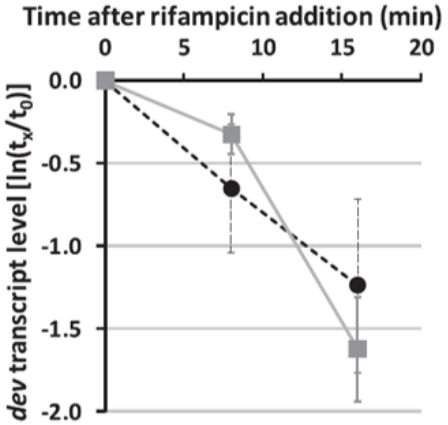


**Figure 2.6 *dev* transcript stability.** Wild-type DK1622 and the *csgA* mutant were subjected to starvation under submerged culture conditions for 30 h. The overlay was replaced with fresh starvation buffer containing rifampicin (50 μg/ml) and samples were collected immediately ($t_0$) and at the times indicated ($t_x$) for measurement of the *dev* transcript level by RT-qPCR. Transcript levels at $t_x$ were normalized to that at $t_0$ for each of three biological replicates and used to determine the transcript half-life for each replicate. The average half-life and one standard deviation are reported in the text. The graph shows the average $\ln(t_x/t_0)$ and one standard deviation for the three biological replicates of wild type (black dashed line) and the *csgA* mutant (gray solid line).

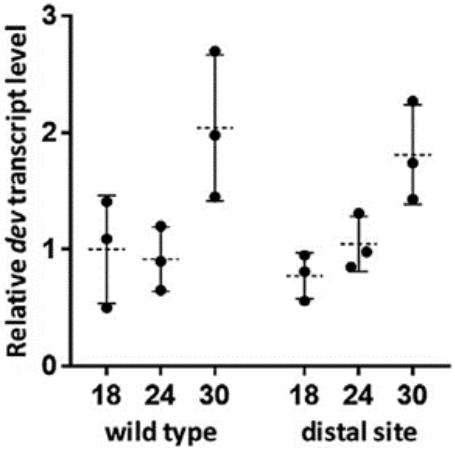


**Figure 2.7 *dev* transcript levels in wild type and *distal site* mutant.**

**Figure 2.7 (cont'd)**

Wild-type DK1622 and its indicated mutant derivative were subjected to starvation under submerged culture conditions and samples were collected at the indicated number of hours poststarvation (PS) for measurement of *dev* transcript levels by RT-qPCR. Graphs show the data points and average of three biological replicates, relative to wild-type DK1622 at 18 h PS and error bars show one standard deviation.

transcript in WT than in the *csgA* mutant. These results allow us to rule out Hypothesis 2.

***Boosting the FruA level in the* csgA *mutant has no effect on the dev transcript level***

Having ruled out the first two hypotheses, our modeling predicts that the only viable option to explain the effect of the *csgA* null mutation on the *dev* transcript level is Hypothesis 3: at least a ninefold reduction in active FruA is needed in the *csgA* mutant as compared with WT. Specifically, our model showed that the low *dev* transcript level in the *csgA* mutant is not due to its twofold lower FruA level (Fig. 3B), but rather due to a failure to activate FruA in the absence of C-signaling (Fig. 5C and S10). As a result, the model predicts that in the *csgA* mutant most of the FruA remains inactive. To test this prediction, we integrated *fruA* transcriptionally fused to a vanillate-inducible promoter ectopically in the *csgA* mutant. Upon induction the *csgA* $P_{van}$-*fruA* strain accumulated a similar level of FruA as WT (Fig. 8A), but the *dev* transcript level

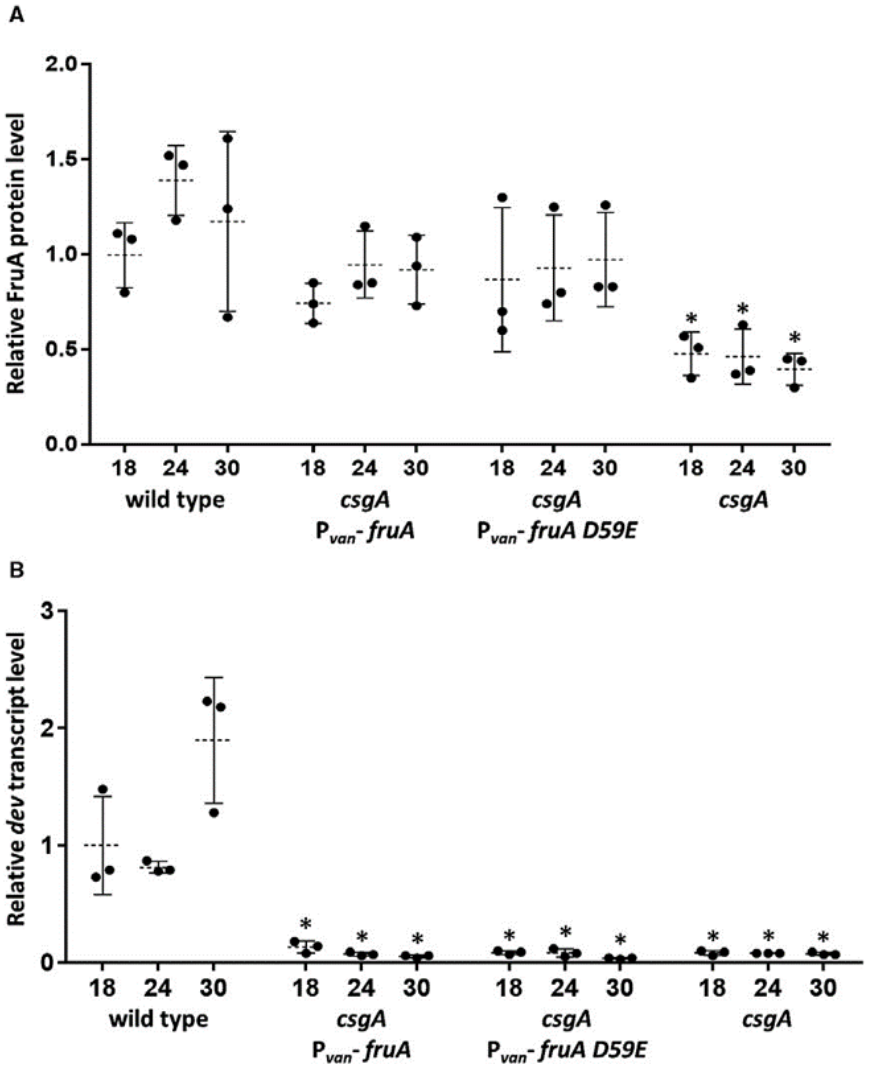


**Figure 2.8 FruA protein and *dev* transcript levels.** Wild-type DK1622 and its indicated mutant derivatives were subjected to starvation under submerged culture conditions and samples were collected at the indicated number of hours poststarvation (PS) for measurement of FruA levels by immunoblot (A) and *dev* transcript levels by RT-qPCR (B). Graphs show the data points and average of three biological replicates, relative to wild-type DK1622 at 18 h PS and error bars show one standard deviation. Asterisks indicate a significant difference ($p < 0.05$ in Student's two-tailed *t*-tests) from wild type at the corresponding time PS.

remained as low as in the *csgA* mutant (Fig. 8B). Hence, boosting the FruA level in the *csgA* mutant had no effect on the *dev* transcript level.

Additionally, we tested the previously proposed idea of phosphorylation to be a potential mechanism of CsgA dependent activation of FruA. FruA was earlier suggested to be phosphorylated on the residue D59. We created a phosphomimetic form of FruA by substituting E for D at residue 59. We ectopically expressed the phosphomimetic form of FruA (*fruA(*D59E) by transcriptionally fusing it to a vanillate-inducible promoter in the *csgA* mutant background. Upon induction the *csgA* $P_{van}$*-fruA (D59E)* strain accumulated a similar level of FruA as WT and *csgA* $P_{van}$*-fruA*. (Fig. 8A), but the *dev* transcript level remained as low as observed in *csgA* mutant and *csgA* $P_{van}$*-fruA* strain (Fig. 8B), consistent with our prediction and supporting the hypothesis that C-signaling activates FruA at least ninefold. Additionally, boosting the level of the phosphomimetic form of FruA (FruA-D59E), in the *csgA* mutant fails to recover the level of *dev* transcript, suggesting phosphorylation not to be a mechanism for CsgA dependent activation of FruA.

The boost in FruA level correlated with a boost in *fruA* transcript level in the *csgA* $P_{van}$*-fruA and csgA* $P_{van}$*-fruA (D59E)* strain(Fig. S11A). As expected, the *mrpC* transcript (Fig. S11B) and MrpC protein (Fig. S12) levels were similar in the *csgA* $P_{van}$*-fruA and csgA* $P_{van}$*-fruA (D59E)* strain as in the *csgA* mutant at 18 and 24 h Post starvation. Induction of the *csgA* $P_{van}$*-fruA* strain did not rescue its development since it failed to progress beyond forming loose aggregates (Fig. S13), failed to make a detectable number of spores by 48 h PS (at a detection limit of 0.01% of the $T_0$ number; data not shown), and appeared to be slightly delayed relative to WT in terms of the declining number of sonication-sensitive cells, like the *csgA* mutant (Fig. S14).

As a control, $P_{van}$-*fruA and* $P_{van}$-*fruA (D59E)* were integrated ectopically in the *fruA* mutant. Upon induction the *fruA* $P_{van}$-*fruA* strain formed mounds by 18 h PS and the mounds matured into compact, darkened fruiting bodies at later times, similar to WT without or with vanillate added (Fig. S15). Also, the induced *fruA* $P_{van}$-*fruA* strain exhibited a similar number of sonication-resistant spores as WT at 36 h PS (data not shown). *fruA Pvan-fruA (D59E)* was delayed in mound formation by 6 h PS, but eventually formed darkened fruiting bodies by 30 h PS followed by similar number of sonication resistant spores as wild type by 36 h PS. These results show that ectopic induction of the *fruA* and *fruA (D59E)* from P*van-fruA* rescued development of a *fruA* mutant, presumably because C-signaling activated FruA produced from $P_{van}$-*fruA*.

***Expressions of FruA regulated genes are dependent on CsgA induced activation of FruA***

In order to investigate this, we asked if the effect of CsgA dependent activation of FruA is specific for *dev* transcription? Four other genes (*fmgA, fmgB, fmgD* and *fmgE*), which were earlier suggested to be combinatorially regulated by MrpC and FruA. We compared expression levels of all four genes between *csgA* mutant, *csgA* $P_{van}$-*fruA* and *csgA* $P_{van}$-*fruA D59E.* The *csgA* mutant showed significantly low level of all four *fmg* genes compared to the wild type. Similar to *dev,* despite boosting the level of FruA, expressions of the *fmg* genes were not recovered to the wild type level in *csgA* $P_{van}$-*fruA* and *csgA* $P_{van}$-*fruA D59E.* Hence, CsgA dependent activation of FruA is critical for induction of genes combinatorially regulated by MrpC and FruA.

## Discussion

Our systematic, quantitative analysis of a key circuit in the GRN governing *M. xanthus* fruiting body formation implicates posttranslational regulation of FruA by C-signaling as primarily responsible for *dev* transcript accumulation during the period leading up to and including commitment to spore formation. Mathematical modeling of the *dev* transcript level allowed us to predict the magnitude of potential regulatory mechanisms. Experiments ruled out C-signal-dependent stabilization of *dev* mRNA or highly cooperative binding of FruA and MrpC to two sites in the *dev* promoter region as the explanation for the much higher *dev* transcript level in WT than in the *csgA* mutant. Although the FruA level was twofold lower in the *csgA* mutant than in WT (Fig. 3B and 8A), boosting the FruA level in the *csgA* mutant had no effect on the *dev* transcript level (Fig. 8B). Taken together, our experimental and computational analyses provide evidence that C-signaling activates FruA at least ninefold posttranslationally during *M. xanthus* development (Fig. 9). The activation of FruA may be considerably greater than ninefold if the *dev* promoter region approaches saturation (Fig. 5C and S10). Since efficient C-signaling requires cells to move into close proximity [33-35], we propose that activation of FruA by C-signaling acts as a checkpoint for mound formation during the developmental process (Fig. 9).

### *Regulation of FruA by C-signaling*

If activation of FruA by C-signaling acts as a checkpoint for mound formation, then active FruA should be present at 18 h PS since mound formation is well underway (Fig. 2). In agreement, mathematical modeling of our data using the assumptions of hypothesis 3 at each time point from 18 to 30 h PS yields a similar result (Fig. S10). This analysis implies that FruA has already

been activated by C-signaling at least ninefold by 18 h PS, if the assumptions of hypothesis 3 apply.

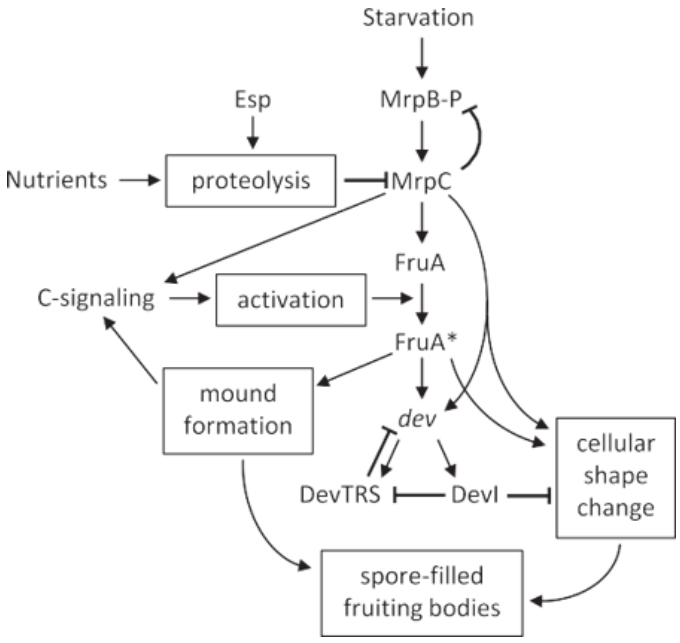


**Figure 2.9 Updated model of the gene regulatory network governing formation of fruiting bodies.** Relative to the simplified model shown in Fig. 1 (see legend), this model also includes phosphorylated MrpB (MrpB-P) which appears to activate transcription of *mrpC*, and negative autoregulation by MrpC which appears to involve competition with MrpB-P for binding to overlapping sites in the *mrpC* promoter region; proteolysis of MrpC, which is regulated by the Esp signal transduction system that normally slows the developmental process and is regulated by nutrient addition that can halt development; posttranslational activation of FruA to FruA* by C-signaling and promotion of mound formation by FruA*, thus enhancing short-range C-signaling by bringing cells into proximity; the possibility that DevI inhibits negative autoregulation by DevTRS; and speculation that the feed-forward loop involving MrpC and FruA* not only controls transcription of the *dev* operon, but that of genes involved in cellular shape change as well, committing cells to spore formation and resulting in spore- filled fruiting bodies. This model deletes activation of MrpC by C-signaling, which was included as a possibility in Fig. 1, but was not supported by our data. See the text for details and references.

The assumption that the distal site does not contribute to high cooperativity of MrpC and FruA binding to the *dev* promoter region applies since the *dev* transcript level did not differ significantly in the distal site mutant as compared with WT at 18 or 24 h PS (Fig. 7). We did not measure *dev* transcript stability at 18 to 27 h PS, but at 30 h PS there was no significant difference between WT and the *csgA* mutant (Fig. 6). Therefore, C-signaling may have already activated FruA at least ninefold by 18 h PS, and perhaps as much as 30-fold if the *dev* promoter region approaches saturation (90% saturation in the righthand panel of Fig. S10). We note that during the period from 18 to 30 h PS, the *dev* transcript level rises, but the rise is due to positive autoregulation by DevI (Fig. 4A). Hence, active FruA may not be the limiting factor for *dev* transcription during this period (i.e., the *dev* promoter region may indeed approach saturation binding of active FruA and MrpC). The proximal upstream site in the *dev* promoter region, which is crucial for transcriptional activation, exhibits a higher affinity for cooperative binding of FruA and MrpC than the distal upstream site [20] or several other sites [17, 24], perhaps conferring on *dev* transcription a relatively low threshold for active FruA.

The mechanism of FruA activation by C-signaling is unknown. Since FruA is similar to response regulators of two-component signal transduction systems, phosphorylation by a histidine protein kinase was initially proposed to control FruA activity [19, 31]. While this potential mechanism of posttranslational control cannot be ruled out, a kinase capable of phosphorylating FruA has not been identified despite considerable effort. Moreover, the atypical receiver domain of FruA and the inability of small-molecule phosphodonors to increase its DNA-binding activity suggest that FruA may not be phosphorylated [22].

Several atypical response regulators have been shown to be active without phosphorylation and a few are regulated by ligand binding [63, 64]. For example, the atypical receiver domain of *Streptomyces venezuelae* JadR1 is bound by jadomycin B, causing JadR1 to dissociate from DNA, and the acylated antibiotic undecylprodigiosin of *Streptomyces coelicolor* may use a similar mechanism to modulate DNA-binding activity of the atypical response regulator RedZ [65]. Conceivably, FruA activity could likewise be regulated by binding of *M. xanthus* diacylglycerols, which have been implicated in C-signaling [54]. Alternatively, FruA could be regulated by a posttranslational modification other than phosphorylation or by binding to another protein (i.e., sequestration).

In addition to regulating FruA activity posttranslationally, C-signaling appears to regulate the FruA level posttranscriptionally. The FruA level was reproducibly twofold lower in the *csgA* mutant than in WT (Fig. 3B and 8A), but the *fruA* transcript level was not significantly different (Fig. 4C and S11A). These results suggest that positive posttranscriptional regulation of the FruA level requires C-signaling. C-signaling may increase synthesis (i.e., increase *fruA* mRNA accumulation slightly and also increase translation of *fruA* mRNA) and/or decrease turnover of FruA. We did not investigate this further because the FruA deficit in the *csgA* mutant could be overcome with $P_{van}$-*fruA*, yet there was very little effect on the *dev* transcript level (Fig. 8). This demonstrates that the activity of FruA, rather than its level, primarily controls the level of *dev* transcript. Additionally, boosting the level of FruA with $P_{van}$-*fruA* failed to recover level of *fmg* transcripts in the *csgA* mutant, suggesting activity of FruA but the level is critical for regulating expressions of FruA dependent genes. Overexpressing the phosphomimetic form of FruA (FruA D59E), also failed to recover the level of *dev* and *fmg* transcripts. This finding contradicts the

previously proposed idea of phosphorylation to be the potential mechanism for CsgA induced activation of FruA.

***Regulation by Dev proteins***

DevI inhibits sporulation if overexpressed, as in the *devS* mutant [29] (Fig. 2 and S1). Deletion of *devI* or the entire *dev* operon allows spores to begin forming about 6 h earlier than normal, but does not increase the final number of spores [28] (Fig. S1). The level of MrpC was about twofold higher on average in the *devI* mutant than in WT at 15 h PS, perhaps accounting for the observed earlier sporulation, although the difference diminished at 18-24 h PS [28], as reported here (Fig. 3A). It was concluded that DevI may transiently and weakly inhibit translation of *mrpC* transcripts during the period leading up to commitment, delaying sporulation [28]. As noted above, DevI positively autoregulates, causing a small rise in the *dev* transcript level by 30 h PS (Fig. 4A, 7, and 8B). Although the mechanism of this feedback loop is unknown, one possibility is that DevI inhibits negative autoregulation by DevTRS (Fig. 9).

In previous studies, mutations in *devT*, *devR*, or *devS* relieved negative autoregulation, resulting in ~10-fold higher *dev* transcript accumulation at 24 h PS [28, 29]. In this study, a *devS* mutant likewise accumulated ~10-fold more *dev* transcript than WT at 24-30 h PS, and the difference was ~20-fold at 18 and 21 h PS (Fig. 4A), suggesting that negative autoregulation mediated by DevS has a stronger effect leading up to the commitment period than during commitment. Strong negative autoregulation may promote commitment to sporulation by lowering the level of DevI, which would raise the MrpC level by relieving inhibition of translation of *mrpC* transcripts [28]. Our data suggest that negative autoregulation by DevTRS weakens during the commitment period, perhaps accounting for the observed small rise in the

*dev* transcript level (Fig. 4A, 7, and 8B). If the elevated *dev* transcript level is accompanied by a small increase in the level of DevI, then DevI may inhibit translation of *mrpC* transcripts, causing the MrpC level to decrease slightly by 30 h PS in WT (Fig. 3A). DevI is predicted to be a 40-residue polypeptide [29] and currently no method has been devised to measure the DevI level. This is a worthwhile goal of future research, as is understanding how cells overcome DevI-mediated inhibition of sporulation (depicted in Fig. 9 as inhibition of cellular shape change).

In addition to regulating the timing of commitment to spore formation, Dev proteins appear to play a role in maturation of spores. Mutations in *dev* genes strongly impair expression of the *exo* operon [28, 66], which encodes proteins that help form the polysaccharide spore coat necessary to maintain cellular shape change and form mature spores [67, 68].

***The role of MrpC***

Our results add to a growing list of observations that indicate MrpC functions differently during *M. xanthus* development than originally proposed. We found that MrpC negatively autoregulates accumulation of *mrpC* mRNA about twofold at 18 and 24 h PS (Fig. S6A), and it does so at 18 h PS without significantly altering transcript stability (Fig. S7). This contradicts an earlier study that concluded MrpC positively autoregulates, based on finding that expression of an *mrpC-lacZ* fusion was abolished in an *mrpC* mutant [15]. Recently, and in agreement with our result, it was reported that MrpC is a negative autoregulator that competes with MrpB for binding to the *mrpC* promoter region [60]. MrpB, likely when phosphorylated, binds to two sites upstream of the *mrpC* promoter and activates transcription. MrpC binds to multiple sites upstream of the *mrpC* promoter [57, 60], including two that overlap the MrpB binding sites [60]. Purified MrpC competes with the MrpB DNA-binding domain for binding to the

overlapping sites, supporting a model in which MrpC negatively autoregulates by directly competing with phosphorylated MrpB for binding to overlapping sites [60] (Fig. 9).

The role of MrpC in cellular lysis during development appears to be less prominent than originally proposed. MrpC was reported to function as an antitoxin by binding to and inhibiting activity of the MazF toxin protein, an mRNA interferase shown to be important for developmental programmed cell death [58]. However, the effect of a null mutation in *mazF* on developmental lysis depends on the presence of a *pilQ1* mutation [13, 69]. In *pilQ*$^{+}$ backgrounds such as our WT strain DK1622, MazF is dispensable for lysis. Here, we found only a slight delay of the *mrpC* mutant relative to WT in terms of the declining number of sonication-sensitive cells at 18-48 h PS (Fig. S9A), comparable to other mutants (*csgA*, *fruA*, *devS*, *csgA* P$_{van}$-*fruA*) that were unable to form spores (Fig. S1 and S13; data not shown). Under our conditions, MrpC appears to play no special role in modulating the cell number during development.

Both the synthesis and the degradation of MrpC are regulated. Synthesis is regulated by phosphorylated MrpB and MrpC acting positively and negatively, respectively, at the level of transcription initiation as described above [60] (Fig. 9). Degradation is regulated by the complex Esp signal transduction system [59, 70, 71], which presumably senses a signal and controls the activity of an unidentified protease involved in MrpC turnover, thus ensuring that development proceeds at the appropriate pace (Fig. 9). Interestingly, preliminary results suggest that the Esp system does not govern the proteolysis of MrpC observed when nutrients are added at 18 h PS [14] (Y. Hoang, R. Rajagopalan, and L. Kroos; unpublished data). This implies that another system senses nutrients and degrades MrpC to halt development (Fig. 9).

***Combinatorial control by MrpC and FruA***

Nutrient-regulated proteolysis of MrpC provides a checkpoint for starvation during the period leading up to and including commitment to sporulation [14] (Fig. 9). If activation of FruA by C-signaling acts as a checkpoint for mound formation as we propose (Fig. 9), then combinatorial control by MrpC and activated FruA could ensure that only starving cells in mounds express genes that commit them to spore formation.

MrpC and FruA bind cooperatively to the promoter regions of five C-signal-dependent genes [20-24]. In each case, cooperative binding to a site located just upstream of the promoter appears to activate transcription. Hence, MrpC and FruA form a type 1 coherent feed-forward loop with AND logic [72]. This type of loop is abundant in GRNs and can serve as a sign-sensitive delay element [72, 73]. The sign sensitivity refers to a difference in the network response to stimuli in the "OFF to ON" direction versus the "ON to OFF" direction. What this means for the feed-forward loop created by MrpC, FruA, and their target genes is that target gene expression is delayed as MrpC accumulates, awaiting FruA activated by C-signaling (i.e., the "OFF to ON" direction) (Fig. 9). As cells move into mounds and engage in short-range C-signaling, activated FruA would bind cooperatively with MrpC, stimulating transcription of target genes that eventually commit cells to spore formation (depicted in Fig. 9 as cellular shape change). However, if nutrients reappear prior to commitment, MrpC is degraded and transcription of target genes rapidly ceases, halting commitment to sporulation (i.e., the "ON to OFF" direction). The number of target genes may be large since MrpC binds to the promoter regions of hundreds of developmental genes based on ChIP-seq analysis, and in 13 of 15 cases cooperative binding of MrpC and FruA was observed [17].

In addition to the feed-forward loop involving cooperative binding of MrpC and FruA to a site located just upstream of the promoter, the promoter regions of some genes have more complex architectures that confer greater dependence on C-signaling for transcriptional activation. For example, in the *fmgD* promoter region, binding of MrpC to an additional site that overlaps the promoter and the FruA binding site appears to repress transcription, and it has been proposed that a high level of active FruA produced by C-signaling is necessary to outcompete MrpC for binding and result in transcriptional activation [21] (Fig. S16A). In the *fmgE* promoter region, a distal upstream site with higher affinity for cooperative binding of MrpC and FruA appears to act negatively by competing for binding with the lower affinity site just upstream of the promoter [24] (Fig. S16B). In addition to *fmgD* and *fmgE*, other genes depend more strongly on C-signaling and are expressed later during development than *dev* [30]. We infer that such genes require a higher level of active FruA than *dev* in order to be transcribed. In contrast to the *dev* promoter region, which may have a relatively low threshold for active FruA and therefore approach saturation binding of active FruA and MrpC at 18 h PS (Fig. S10), we predict that the promoter regions of genes essential for commitment to sporulation have more complex architectures and a higher threshold for active FruA. According to this model, C-signal-dependent activation of FruA continues after 18 h PS and the rising level of active FruA triggers commitment beginning at 24 h PS. We speculate that genes governing cellular shape change are under combinatorial control of MrpC and FruA (Fig. 9), and have a high threshold for active FruA.

## Materials and methods

### *Bacterial strains, plasmids and primers*

The strains, plasmids, and primers used in this study are listed in Table S1. *Escherichia coli* strain DH5 was used for cloning. To construct pSS10, primers FruA-F-NdeI-Gibson and FruA-R-EcoRI-Gibson were used to generate PCR products using chromosomal DNA from *M. xanthus* strain DK1622 as template. The products were combined with NdeI-EcoRI-digested pMR3691 in a Gibson assembly reaction to enzymatically join the overlapping DNA fragments [74]. The cloned PCR product was verified by DNA sequencing. *M. xanthus* strains with $P_{van}$-*fruA* integrated ectopically were constructed by electroporation [75] of pSS10, selection of transformants on CTT agar containing 15 μg/ml of tetracycline [76], and verification by colony PCR using primers pMR3691 MCS G-F and pMR3691 MCS G-R. To express *fruA (D59E)* from the vanillate inducible promoter $P_{van}$-*fruA* was subjected to site directed mutagenesis using primers D59E F and D59E R, followed verification by PCR and sequencing using pMR3691 MCS G-F and pMR3691 MCS G-R. *M. xanthus* strains with $P_{van}$-*fruA(D59E)* integrated ectopically were constructed by electroporation [75], followed by selection of transformants on CTT agar containing 15 μg/ml of tetracycline [76], and further verification by colony PCR using primers pMR3691 MCS G-F and pMR3691 MCS G-R.

### *Growth and development of M. xanthus*

Strains of *M. xanthus* were grown at 32°C in CTTYE liquid medium (1% Casitone, 0.2% yeast extract, 10 mMTris-HCl [pH 8.0], 1 mM $KH_2PO_4$-$K_2HPO_4$, 8 mM $MgSO_4$ [final pH 7.6]) with shaking at 350 rpm. CTT agar (CTTYE lacking yeast extract and solidified with 1.5% agar) was used for growth on solid medium and was supplemented with 40 μg/ml of kanamycin sulfate or

15 μg/ml of tetracycline as required. Fruiting body development under submerged culture conditions was performed using MC7 (10 mM morpholinepropanesulfonic acid [MOPS; pH 7.0], 1 mM $CaCl_2$) as the starvation buffer as described previously [14]. Briefly, log-phase CTTYE cultures were centrifuged and cells were resuspended in MC7 at a density of approximately 1,000 Klett units. A 100 □l sample (designated $T_0$) was removed, glutaraldehyde (2% final concentration) was added to fix cells, and the sample was stored at 4°C at least 24 h before total cells were quantified as described below. For each developmental sample, 1.5 ml of the cell suspension plus 10.5 ml of MC7 was added to an 8.5-cm-diameter plastic petri plate. Upon incubation at 32°C, cells adhere to the bottom of the plate and undergo development. At the indicated times developing populations were photographed through a microscope and collected as described below.

***Microscopy***

Images of fruiting bodies were obtained using a Leica Wild M8 microscope equipped with an Olympus E-620 digital camera. In order to quantify cells in samples collected and dispersed as described below, high resolution images were obtained with an Olympus BX51 microscope using a differential interference contrast filter and a 40× objective lens, and equipped with an Olympus DP30BW digital camera.

***Sample collection***

At the indicated times the submerged culture supernatant was replaced with 5 ml of fresh MC7 starvation buffer with or without inhibitors as required. Developing cells were scraped from the plate bottom using a sterile cell scraper and the entire contents were collected in a 15-ml centrifuge tube. Samples were mixed thoroughly by repeatedly (three times total) vortexing for

15 s followed by pipetting up and down 15 times. For quantification of total cells, 100 □l of the mixture was removed, glutaraldehyde (2% final concentration) was added to fix cells, and the sample was stored at 4°C for at least 24 h before counting as described below. For measurement of sonication-resistant spores, 400 μl of the mixture was removed and stored at -20°C. For immunoblot analysis, 100 μl of the mixture was added to an equal volume of 2× sample buffer (0.125 M Tris-HCl [pH 6.8], 20% glycerol, 4% sodium dodecyl sulfate [SDS], 0.2% bromophenol blue, 0.2 M dithiothreitol), boiled for 5 min, and stored at -20°C. Immediately after collecting the three samples just described, the remaining 4.4 ml of the developing population was mixed with 0.5 ml of RNase stop solution (5% phenol [pH < 7] in ethanol), followed by rapid cooling in liquid nitrogen until almost frozen, centrifugation at 8,700 × *g* for 10 min at 4°C, removal of the supernatant, freezing of the cell pellet in liquid nitrogen, and storage at -80°C until RNA extraction. Control experiments with a sample collected at 30 h PS indicated that the majority of spores remain intact after boiling in 2× sample buffer or RNA extraction as described below (data not shown), so the proteins and RNAs analyzed are from developing cells that have not yet formed spores.

***Quantification of total cells and sonication-resistant spores***

During development a small percentage of the rod-shaped cells transition to ovoid spores that become sonication-resistant. The number of sonication-resistant spores in developmental samples was quantified as described previously [14]. Briefly, each 400- μl sample collected as described above was thawed and sonicated using a model 450 sonifier (Branson) at output setting 2 for 10-s intervals three times with cooling on ice in between. A 60 μl sample was removed and ovoid spores were counted microscopically using a Neubauer counting chamber.

A remaining portion of the sample was used to determine total protein concentration as described below. The total cell number, including rod-shaped cells, ovoid spores, and cells in transition between the two, was determined using the glutaraldehyde-fixed samples collected as described above. Each sample was thawed and mixed by vortexing and pipetting, then 10 or 20 μl was diluted with MC7 to 400 μl, sonicated once for 10 s, and all cells were counted microscopically. The total cell number minus the number of sonication-resistant cells was designated the number of sonication-sensitive cells (consisting primarily of rod-shaped cells) and was expressed as a percentage of the total cell number in the corresponding $T_0$ sample (consisting only of rod-shaped cells).

***RNA extraction and analysis***

RNA was extracted using the hot-phenol method and the RNA was digested with DNase I (Roche) as described previously [71]. One □g of total RNA was subjected to cDNA synthesis using Superscript III reverse transcriptase (InVitrogen) and random primers (Promega), according to the instructions provided by the manufacturers. Control reactions were not subjected to cDNA synthesis. One □l of cDNA at the appropriate dilution (as determined empirically) and 20 pmol of each primer were subjected to qPCR in a 25 □l reaction using 2× reaction buffer (20 mM Tris-HCl [pH 8.3], 13 mM $MgCl_2$, 100 mM KCl, 400 □M dNTPs, 4% DMSO, 2× SYBR Green I [Molecular Probes], 0.01% Tween 20, 0.01% NP40, and 0.01 □g/□l of Taq polymerase) as described previously [77]. qPCR was done in quadruplicate for each cDNA using a LightCycler® 480 System (Roche). A standard curve was generated for each set of qPCRs using *M. xanthus* wild-type strain DK1622 genomic DNA and gene expression was quantified using the relative standard curve method (user bulletin 2; Applied Biosystems). 16S rRNA was used

as the internal standard for each sample. Relative transcript levels for mutants are the average of three biological replicates after each replicate was normalized to the transcript level observed for one replicate of WT at 18 h PS in the same experiment. Transcript levels for WT at other times PS were likewise normalized to that observed for WT at 18 h PS in the same experiment. For WT at 18 h PS, the transcript levels of at least three biological replicates from different experiments were normalized to their average, which was set as 1.

***Immunoblot analysis***

A semi-quantitative method of immunoblot analysis was devised to measure the relative levels of MrpC and FruA in many samples collected in different experiments. Equal volumes (10 μl for measurement of MrpC and 15 μl for measurement of FruA) of samples prepared for immunoblot analysis as described above were subjected to SDS-PAGE and immunoblotting as described previously [14, 78]. On each immunoblot, a sample of the wild-type strain DK1622 at 18 h PS served as an internal control for normalization of signal intensities across immunoblots. Signals were detected using a ChemiDoc MP imaging system (Bio-Rad), with exposure times short enough to ensure signals were not saturated, and signal intensities were quantified using Image Lab 5.1 (Bio-Rad) software. After normalization to the internal control, each signal intensity was divided by the total protein concentration of a corresponding sample that had been sonicated for 10-s intervals three times as described above. After removal of a sample for spore quantification, the remaining portion was centrifuged at 10,000 × *g* for 1 min and the total protein concentration of the supernatant was determined using a Bradford [79] assay kit (Bio-Rad). The resulting values of normalized signal intensity/total protein concentration were

further normalized to the average value for all biological replicates of WT at 18 h PS, which was set as 1.

***Mathematical modeling***

*Activation of dev transcription by FruA and MrpC*

FruA and MrpC bind cooperatively to the *dev* promoter region and activate transcription [20]. In agreement, no *dev* mRNA was detected in either the *fruA* mutant (Fig. 4A) or the *mrpC* mutant (Fig. 7). We represent the activation of *dev* transcript by FruA and MrpC using a phenomenological Hill's function,

$$\Pi_{\mathrm{FM}} = \alpha_{\mathrm{FM}} \left[ \frac{\left( \frac{[\mathrm{FruA}][\mathrm{MrpC}]}{\mathrm{K_{FM}}} \right)^{a}}{1 + \left( \frac{[\mathrm{FruA}][\mathrm{MrpC}]}{\mathrm{K_{FM}}} \right)^{a}} \right]$$

where $\alpha_{\mathrm{FM}}$ denotes the maximal *dev* transcription rate, $\mathrm{K_{FM}}$ is the half-saturation constant, and $a$ denotes the cooperativity of binding. Note that this expression will give $\Pi_{\mathrm{FM}} = 0$ when $[\mathrm{FruA}] = 0$ or $[\mathrm{MrpC}] = 0$ (i.e., we have neglected any basal transcription rate as we did not detect *dev* mRNA in the *fruA* or *mrpC* mutant. The expression in brackets can be thought as the promoter occupancy probability ($P$ in the equation below), a dimensional parameter telling what fraction of the promoters will be occupied by the transcription factors for a given value of $\mathrm{K_{FM}}$.

$$P = \frac{\left( \frac{[\mathrm{FruA}][\mathrm{MrpC}]}{\mathrm{K_{FM}}} \right)^{a}}{1 + \left( \frac{[\mathrm{FruA}][\mathrm{MrpC}]}{\mathrm{K_{FM}}} \right)^{a}}$$

Note that the sensitivity of this expression to changes in the concentrations of FruA and MrpC are maximal when $P \sim 0$ and minimal near saturation when $P \sim 1$. In Figure 5 we assess how

different hypotheses about the role of C-signaling in *dev* regulation play out at different levels of $\mathrm{K_{FM}}$. To facilitate the biological interpretation of the findings, we plot these as a function of *dev* promoter saturation.

*Feedback regulation by Dev proteins*

The *dev* mRNA level is further regulated by Dev proteins DevI and DevS. Our finding that the *dev* transcript level is lower in the *devI* mutant than in WT (Fig. 4A) indicates that DevI is a positive regulator of *dev* mRNA accumulation. In contrast, the *dev* transcript level in the *devS* mutant is significantly higher than in WT (Fig. 4A), indicating that DevS is a negative regulator of *dev* mRNA accumulation. Since the exact mechanisms of regulation by DevI and DevS are unclear, we assume for simplicity that these proteins regulate the *dev* transcript level through independent mechanisms. We model these regulation functions as follows:

$$\Pi_{\mathrm{I}} = \left( 1 + \alpha_{\mathrm{I}} \frac{\left(\frac{[\mathrm{DevI}]}{\mathrm{K_I}}\right)^{b}}{1 + \left(\frac{[\mathrm{DevI}]}{\mathrm{K_I}}\right)^{b}} \right), \qquad \Pi_{\mathrm{S}} = \left( \frac{1}{1 + \left(\frac{[\mathrm{DevS}]}{\mathrm{K_S}}\right)^{c}} \right)$$

Here, $\alpha_{\mathrm{I}}$ is a dimensionless parameter characterizing the feedback strength (i.e., the fold-increase in transcription of the *dev* operon due to DevI), $\mathrm{K_I}$ is the half-saturation constant, and *b* denotes cooperativity of DevI binding. Likewise, $\mathrm{K_S}$ is the half-saturation constant and *c* denotes the cooperativity of DevS binding. Note that these functions are normalized so that $\Pi_{\mathrm{I}} = 1$ for the *devI* mutant and $\Pi_{\mathrm{S}} = 1$ for the *devS* mutant (i.e., when $[\mathrm{DevI}] = 0$ or $[\mathrm{DevS}] = 0$).

We assume that regulation by the Dev proteins is independent of that by FruA and MrpC, and the effects will be multiplicative:

$$[\mathrm{mRNA}_{dev}] = \frac{\alpha_{\mathrm{FM}}}{\delta_{dev}} \underbrace{\left( \frac{\left(\frac{[\mathrm{FruA}][\mathrm{MrpC}]}{\mathrm{K_{FM}}}\right)^{a}}{1+\left(\frac{[\mathrm{FruA}][\mathrm{MrpC}]}{\mathrm{K_{FM}}}\right)^{a}} \right)}_{\Pi_{\mathrm{FM}}} \underbrace{\left( 1+\alpha_{\mathrm{I}} \frac{\left(\frac{[\mathrm{DevI}]}{\mathrm{K_I}}\right)^{b}}{1+\left(\frac{[\mathrm{DevI}]}{\mathrm{K_I}}\right)^{b}} \right)}_{\Pi_{\mathrm{I}}} \underbrace{\left( \frac{1}{1+\left(\frac{[\mathrm{DevS}]}{\mathrm{K_S}}\right)^{c}} \right)}_{\Pi_{\mathrm{S}}}$$

where, $K_{FM}$, $K_I$, and $K_S$ are the saturation constants for regulation by [FruA][MrpC], [DevI], and [DevS], respectively.

*Numerical procedure to estimate unknown regulation parameters*

To explain the difference in the *dev* mRNA level in the *csgA* mutant as compared with WT, in terms of perturbation of potential regulatory mechanisms, we use a mathematical approach where we constrain the FruA ratio ($[\mathrm{FruA}]_{\mathrm{WT}}/[\mathrm{FruA}]_{csgA} \cong 2$) and find the regulation parameters that can result in the observed 22-fold difference in $[\mathrm{mRNA}_{\mathrm{dev}}]$. Specifically, we use the expression of *dev* transcript ratio between WT and the *csgA* mutant below:

$$\frac{[\mathrm{mRNA}_{dev}]_{\mathrm{WT}}}{[\mathrm{mRNA}_{dev}]_{csgA}}$$

$$= \frac{\delta_{dev,csgA}}{\delta_{dev,\mathrm{WT}}} \frac{1+\left(\frac{[\mathrm{FruA}]_{csgA}[\mathrm{MrpC}]_{csgA}}{\mathrm{K_{FM}}}\right)^{a}}{1+\left(\frac{[\mathrm{FruA}]_{\mathrm{WT}}[\mathrm{MrpC}]_{\mathrm{WT}}}{\mathrm{K_{FM}}}\right)^{a}} \left(\frac{[\mathrm{FruA}]_{\mathrm{WT}}[\mathrm{MrpC}]_{\mathrm{WT}}}{[\mathrm{FruA}]_{csgA}[\mathrm{MrpC}]_{csgA}}\right)^{a} \left(\frac{\Pi_{\mathrm{I,WT}}\,\Pi_{\mathrm{S,WT}}}{\Pi_{\mathrm{I},csgA}\Pi_{\mathrm{S},csgA}}\right)$$

$$\frac{[\mathrm{mRNA}_{dev}]_{\mathrm{WT}}}{[\mathrm{mRNA}_{dev}]_{csgA}} = \frac{1}{\delta_R} \left( \frac{R^{a}+\left(\frac{P_{\mathrm{WT}}}{1-P_{\mathrm{WT}}}\right)}{1+\left(\frac{P_{\mathrm{WT}}}{1-P_{\mathrm{WT}}}\right)} \right) \left(\frac{\Pi_{\mathrm{I,WT}}\,\Pi_{\mathrm{S,WT}}}{\Pi_{\mathrm{I},csgA}\Pi_{\mathrm{S},csgA}}\right)$$

where,

$$R = \frac{[\mathrm{FruA}]_{\mathrm{WT}}}{[\mathrm{FruA}]_{csgA}} \frac{[\mathrm{MrpC}]_{\mathrm{WT}}}{[\mathrm{MrpC}]_{csgA}}, \delta_R = \frac{\delta_{dev,\mathrm{WT}}}{\delta_{dev,csgA}} \text{ and } P_{\mathrm{WT}} = \frac{\left(\frac{[\mathrm{FruA}]_{\mathrm{WT}}[\mathrm{MrpC}]_{\mathrm{WT}}}{\mathrm{K_{FM}}}\right)^{a}}{1+\left(\frac{[\mathrm{FruA}]_{\mathrm{WT}}[\mathrm{MrpC}]_{\mathrm{WT}}}{\mathrm{K_{FM}}}\right)^{a}}.$$

First, we estimate the contribution from Dev protein regulation terms ($\Pi_{\mathrm{I}}, \Pi_{\mathrm{S}}$) in determining the *dev* transcript level in WT and the *csgA* mutant. Since we did not measure the Dev proteins

explicitly in our experiments, we estimate their contribution in regulating *dev* transcription in WT by comparing the changes in transcript level in their absence (i.e., in the *devI* and *devS* mutants). Based on our transcript data for WT, and the *devI* and *devS* mutants (Fig. 4A), we have the following relations between the regulation functions; $[\mathrm{mRNA}_{dev}]_{\mathrm{WT}} = \delta_{dev,\mathrm{WT}}^{-1}\Pi_{\mathrm{FM,WT}}\Pi_{\mathrm{I,WT}}\Pi_{\mathrm{S,WT}} = 2.9$, $\delta_{dev,\mathrm{WT}}^{-1}\Pi_{\mathrm{FM,WT}}\Pi_{\mathrm{S,WT}} = 1$ and $\delta_{dev,\mathrm{WT}}^{-1}\Pi_{\mathrm{FM,WT}}\Pi_{\mathrm{I,WT}} = 32$. Using these relations, we obtain $\Pi_{\mathrm{I,WT}} = 2.9$, $\Pi_{\mathrm{S,WT}} = 0.091$. For the *csgA* mutant, assuming regulation by Dev proteins is absent due to the low *dev* transcript level, we have $\Pi_{\mathrm{I},csgA} \approx 1$ and $\Pi_{\mathrm{S},csgA} \approx 1$. With these estimates, the above expression for *dev* transcript ratio has three unknown parameters $\delta_R, a, P_{\mathrm{WT}}$.

Next, we determine the required fold change in degradation rate $\delta_R$ for different promoter saturation probability $P_{\mathrm{WT}}$ values that explains the observed 22-fold difference in *dev* transcript. To estimate this, we set the cooperativity constant $(a)$ to 2 and take the fold change in FruA from the experiments, while assuming MrpC is unchanged between WT and the *csgA* mutant. The result is plotted in Fig. 5A. Then, we determine the required cooperativity $a$ for different $P_{\mathrm{WT}}$ values with the FruA fold change from the experiments and assuming no change in the degradation rate ($\delta_R = 1$). The result is plotted in Fig. 5B. Finally, we compute the fold change in FruA with $\delta_R = 1$ and $a = 2$ for different $P_{\mathrm{WT}}$ values. The result is shown in Fig. 5C.

***RNA stability***

At the indicated time the submerged culture supernatant was replaced with fresh MC7 starvation buffer supplemented with 50 □g/ml of rifampicin to inhibit RNA synthesis. Samples were collected immediately (designated $t_0$) and 8 and 16 min later for RNA extraction and analysis as described above, except for each biological replicate the transcript levels after 8 and

16 min were normalized to the transcript level at $t_0$, which was set as 1, and the natural log of the resulting values was plotted versus minutes after rifampicin treatment and the slope of a linear fit of the data was used to compute the mRNA half-life.

***Induction of $P_{van}$-fruA***

To induce expression of *fruA* and *fruA (D59E)* fused to a vanillate-inducible promoter in *M. xanthus*, the CTTYE growth medium was supplemented with 0.5 mM vanillate when the culture reached 50 Klett units. Growth was continued until the culture reached 100 Klett units, then the culture was centrifuged and cells were resuspended at a density of approximately 1,000 Klett units in MC7 supplemented with 0.5 mM vanillate, followed by submerged culture development as described previously [14].

**Acknowledgements**

We thank Monique Floer for advice about high-throughput qPCR and for use of the LightCycler® 480 System. We thank Montserrat Elias-Arnanz and Penelope Higgs for sharing strains. This work was supported by the National Science Foundation (award MCB-1411272) and by salary support for L.K. from Michigan State University AgBioResearch.

**Author contributions**

Conception or design of the study: LK, OI, SS, PP

Acquisition of the data: SS, PP

Analysis or interpretation of the data: SS, PP, LK, OI

Writing of the manuscript: LK, SS, PP, OI

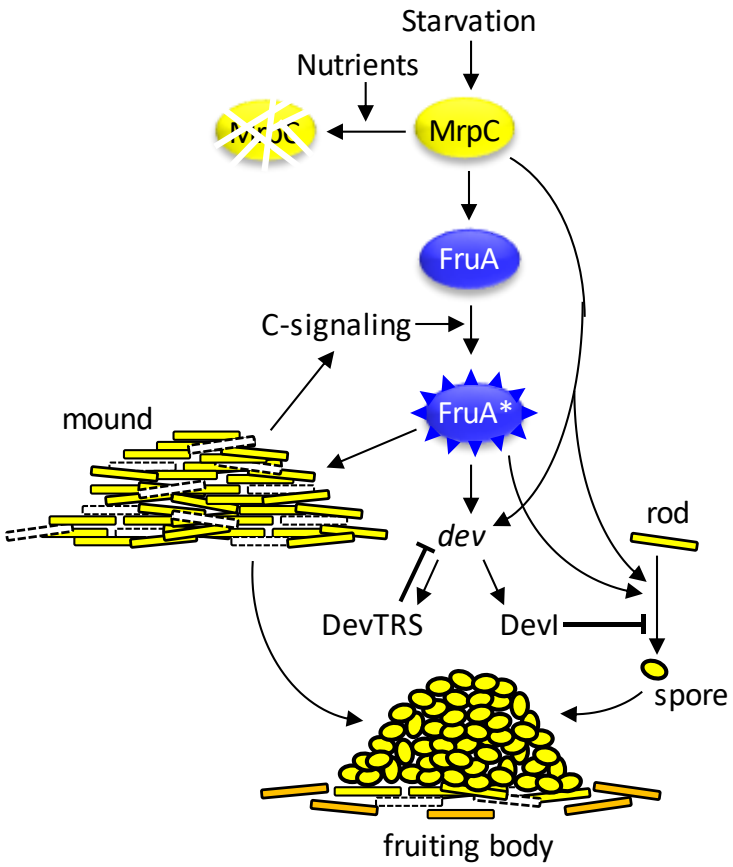


**Figure 2.10 Abbreviated summary.** Starvation promotes MrpC accumulation, whereas nutrients favor proteolysis. MrpC activates transcription of *fruA*, but FruA protein appears to be activated by short-range C-signaling in a cycle leading to mound formation and lysis of some cells. Activated FruA* and MrpC are proposed to cooperatively stimulate transcription of the *dev* operon and genes that commit starving rod-shaped cells to form spores, while Dev proteins slow commitment, resulting in a spore-filled fruiting body surrounded by peripheral rods.

**APPENDIX**

**Table S2.1 Cell and spore numbers counted in chapter 2.**

| Strain | Sonication-sensitive cells at T0 ($10^7$/mL) | Sonication-resistant spores at T48 ($10^7$/mL) |
|---|---|---|
| wild type | 140 ± 16 | 1.5 ± 0.3 |
| *csgA* | 150 ± 30 | < 0.05 |
| *fruA* | 150 ± 25 | < 0.05 |
| *devI* | 150 ± 27 | 2 ± 0.4 |
| *devS* | 140 ± 17 | < 0.05 |
| *ladA* | 150 ± 5 | 0.7 ± 0.3 |
| distal site | 150 ± 6 | 1.4 ± 0.2 |
| *mrpC* | 130 ± 16 | < 0.05 |
| *csgA* P*van-fruA* | 150 ± 7 | < 0.05 |
| *csgA* P*van-fruA D59E* | 140 ± 8 | < 0.05 |

Wild-type DK1622 and its indicated mutant derivatives were subjected to starvation under submerged culture conditions. The number of rod-shaped sonication-sensitive cells at T0 and the number of sonication-resistant spores at 48 h poststarvation were counted microscopically using a Neubauer chamber. Values indicate the average of at least 3 biological replicates and one standard deviation.

**Table S2.2 Strains, plasmids and primers used in chapter 2.**

| Bacterial strain | Description | Source |
|---|---|---|
| *E. coli* | | |
| DH5a | $l^-$ f80dlacZDM15 D(*lacZYA-argF*)*U169 recA1 endA1 hsdR17*($r_K^-$ $m_K^-$) *supE44 thi-1 gyrA relA1* | [80] |
| *M. xanthus* | | |
| DK1622 | Laboratory strain | [81] |
| SW2808 | Δ*mrpC* | [15] |
| DK5285 | *fruA*::Tn*5 lac* Ω4491 ($Km^r$) | [30] |
| DK11209 | Δ*devS* | [27] |
| MRR7 | Δ*devI* | [29] |
| DK5208 | *csgA*::Tn*5-132* W205 ($Tc^r$) | [82] |
| MRR33 | *csgA*::pRR028 ($Km^r$) | [28] |
| MSS1 | A deletion of chromosomal DNA between positions -254 and -228 relative to the *dev* transcriptional start site | [20] |
| MSS3 | *csgA*::pRR028 ($Km^r$) MXAN_0018-MXAN_0019::pSS10 ($Tc^r$) | This study |
| MSS5 | *csgA*::pRR028 ($Km^r$) MXAN_0018-MXAN_0019::pSS9 ($Tc^r$) | This study |
| MSS6 | *fruA*::Tn*5 lac* Ω4491 ($Km^r$) MXAN_0018-MXAN_0019::pSS10 ($Tc^r$) | This study |
| MSS7 | *fruA*::Tn*5 lac* Ω4491 ($Km^r$) MXAN_0018-MXAN_0019::pSS9 ($Tc^r$) | This study |
| MRR027 | DK1622::*ladA* | This study |
| **Plasmids** | **Description** | **Source** |
| pSS10 | $Tc^r$; pMR3691 with *fruA* inserted at MCS_G | This study |
| pSS9 | $Tc^r$; pMR3691 with *fruA (D59E)* inserted at MCS_G | This study |
| pMR3691 | $Tc^r$; *M. xanthus* MXAN_0018-MXAN_0019-$P_{R3-4}$::*vanR*-$P_{van}$-MCS_G | [76] |
| **Primers** | **Description** | **Source** |
| FruA-F-NdeI-Gibson | GATGCGAGGAAACGCATATGGCAACCAATCAAGCAG CGATTCGTG | This study |
| FruA-R-EcoRI-Gibson | GTACGCGTAACGTTCGAATTCCTAGAGGTCCGGCGGC GGCCGGA | This study |
| pMR3691 MCS G-F | CACGATGCGAGGAAACGCA | This study |
| pMR3691 MCS G-R | CACCGGTACGCGTAACGTTC | This study |

**Table S2.2 (cont'd)**

| Primers | Description | Source |
|---|---|---|
| 16S rRNA fwd | CAAGGGAACTGAGAGACAGG | [83] |
| 16S rRNA rev | CTCTAGAGATCCACTACTTGCG | [83] |
| fruA oPH252 | CGTCACGGAAGGCATCAATC | [28] |
| fruA oPH253 | CGAGATGATTTCCGGTGTGC | [28] |
| mrpC qPCR F | GGAGGCCATCGACTTCAAGG | [14] |
| mrpC qPCR R | GGCCGGACTTCAGCAGGTAG | [14] |
| cas6-F | TGGGGAAATCTAATGGTGTTTG | This study |
| cas6-R | GAGAACAGCAGATAGGCATGGT | This study |
| D59E F | CCGCAGGTCGCGGTGATGGAGGTGGAGGGCGACAGCGAG | This study |
| D59E R | CTCGCTGTCGCCCTCCACCTCCATCACCGCGACCTGCGG | This study |
| FmgA-F9 | AAGACGCGCATCAAGGACG | This study |
| FmgA-R9 | CCAGACTTCGAAGCCATCCGAG | This study |
| FmgB-F3 | TGCGCTGCTGTACGACTCC | This study |
| FmgB-R3 | GATGGCCTGGACGGGGCA | This study |
| FmgD-F3N | TTACGGTGGCACCGCATTC | This study |
| FmgD-R3N | CTGGGCTTCCGTCATCTTG | This study |
| FmgE-F3N | CTCATCTGTCGCGGCCAA | This study |
| FmgE-R3N | ACAGCGGTCAGTTCTGAATG | This study |
| LadA-F2 | TTCACCTCGCCCTGCGCC | This study |
| LadA-R2 | GATGGACAACGTGGAGAC | This study |

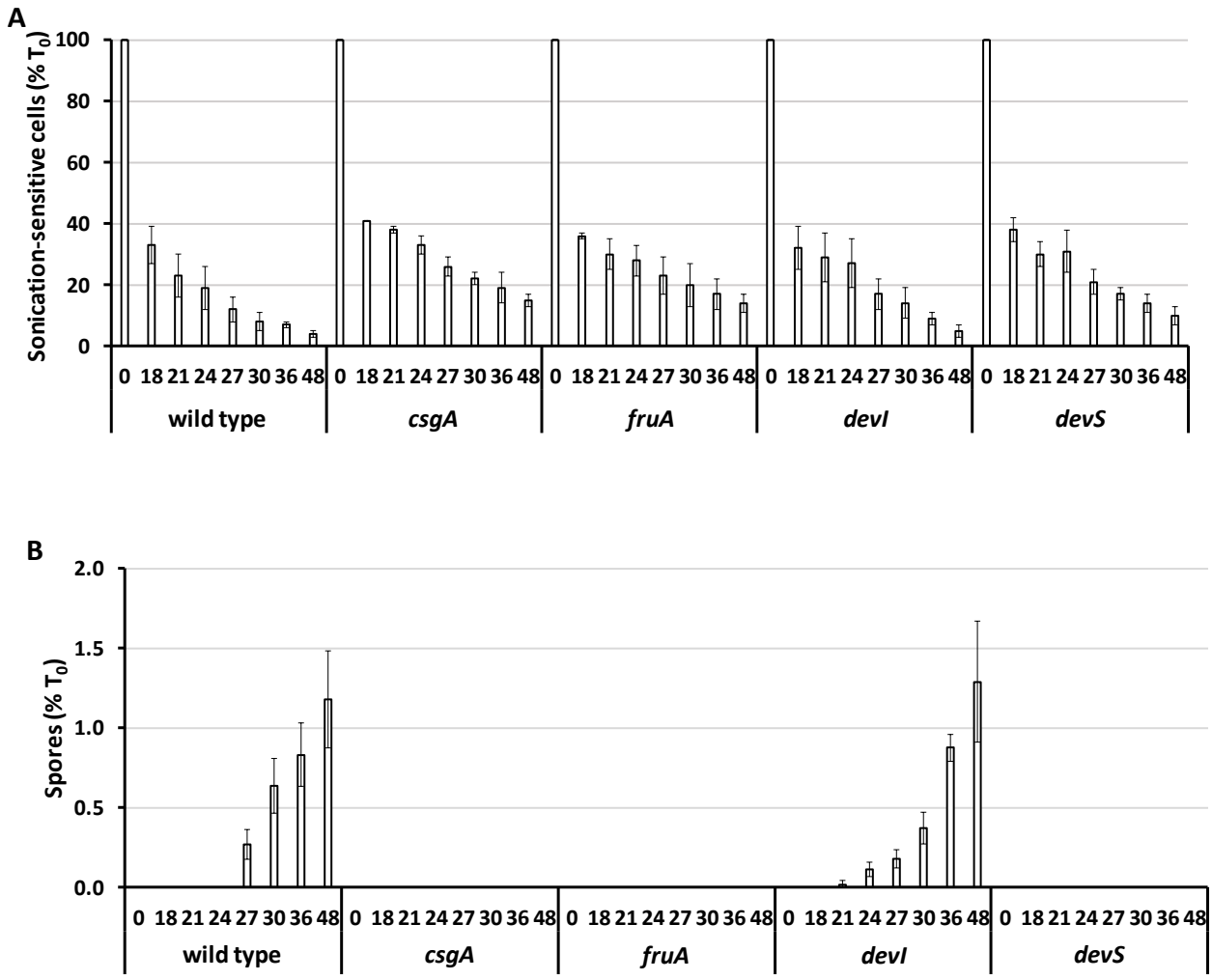


**Figure S2.1 Cellular changes during *M. xanthus* development.** Wild-type DK1622 and its indicated mutant derivatives were subjected to starvation under submerged culture conditions and samples were collected at the indicated number of hours poststarvation for quantification of (A) sonication-sensitive cells and (B) sonication-resistant spores. Values are expressed as a percentage of the number of rod-shaped cells present at the time starvation initiated development ($T_0$). Bars show the average of three biological replicates and error bars show one standard deviation.

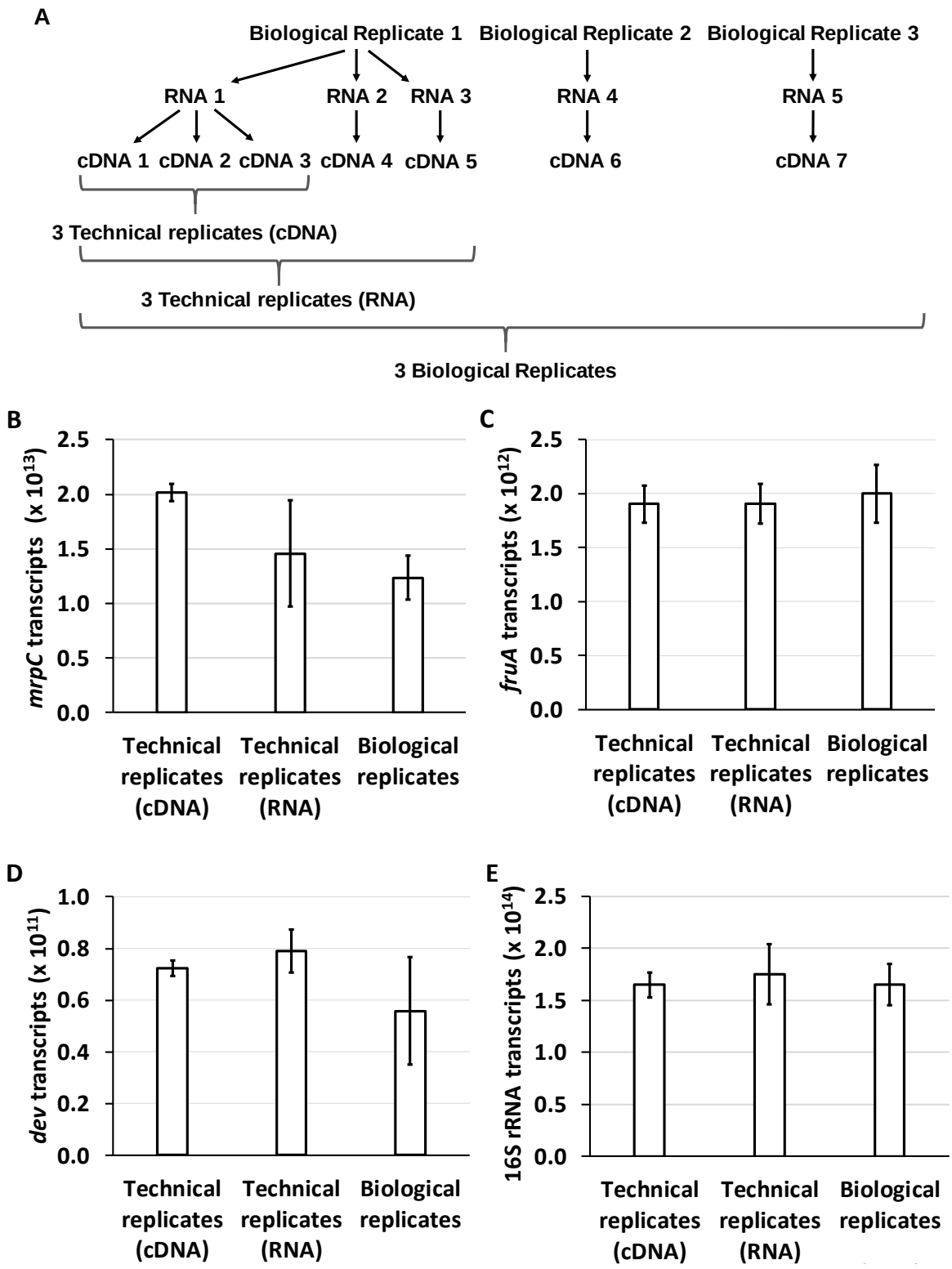


**Figure S2.2 Reproducibility of RNA measurements.**

**Figure S2.2 (cont'd)**

(A) Experimental scheme. Three biological replicates of wild-type DK1622 were subjected to starvation under submerged culture conditions and samples were collected at 24 h poststarvation. One biological replicate sample was used to prepare RNA in triplicate and one of these RNA samples was used to prepare cDNA in triplicate. (B-E) Variation in transcript numbers among cDNA technical replicates, RNA technical replicates (the average of cDNA technical replicates was used as one of the values), and biological replicates. Transcript numbers are per mg total RNA. Bars show the average and error bars show one standard deviation.

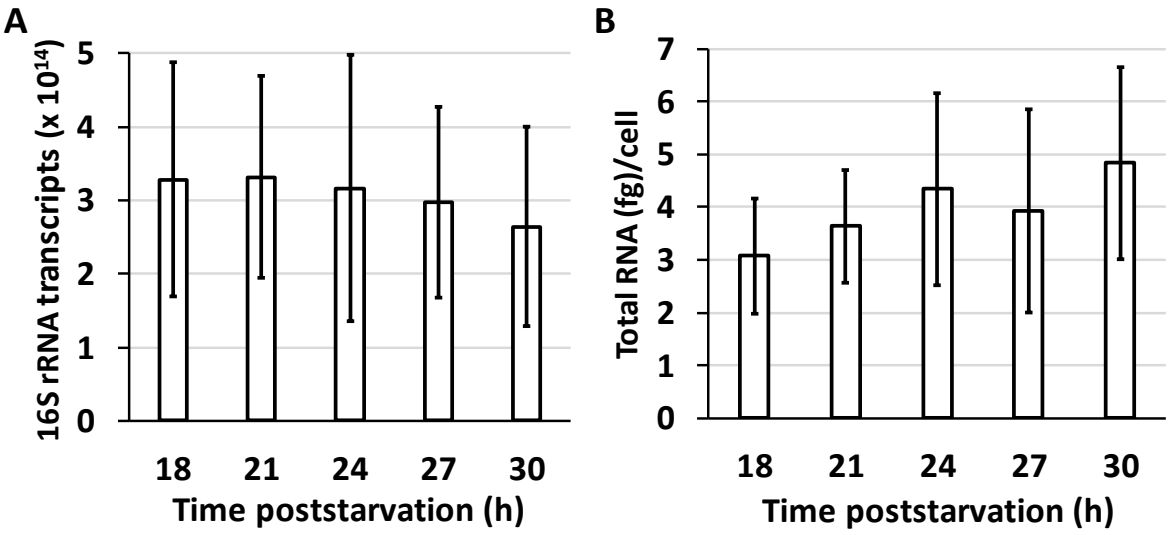


**Figure S2.3 Validation of 16S rRNA as an internal standard for RT-qPCR analysis during *M. xanthus* development**. Four biological replicates of wild-type DK1622 were subjected to starvation under submerged culture conditions and RNA was prepared from samples collected at the indicated times poststarvation. (A) Transcript numbers per mg total RNA. (B) Total RNA yield per cell. The RNA yield in femtograms (fg) was divided by the number of rod-shaped cells in the sample prior to RNA preparation. Bars show the average and error bars show one standard deviation.

.

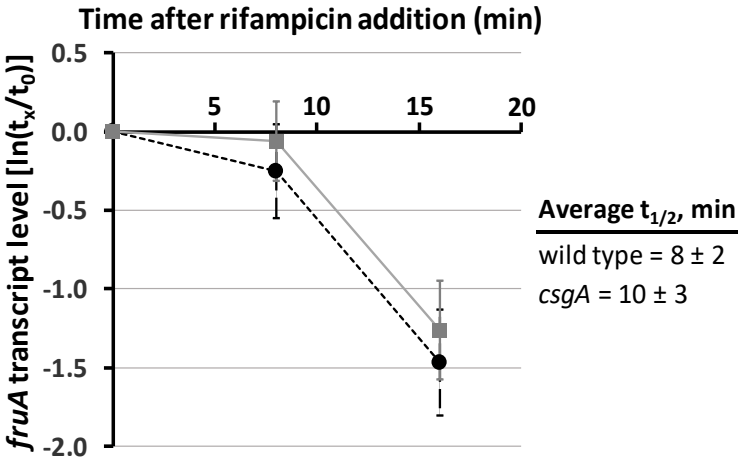


**Figure S2.4 *fruA* transcript stability in wild type and *csgA* mutant**. Wild-type DK1622 and the *csgA* mutant were subjected to starvation under submerged culture conditions for 30 h. The overlay was replaced with fresh starvation buffer containing rifampicin (50 mg/ml) and samples were collected immediately ($t_0$) and at the times indicated ($t_x$) for measurement of the *fruA* transcript level by RT-qPCR. Transcript levels at $t_x$ were normalized to that at $t_0$ for each of three biological replicates and used to determine the transcript half-life for each replicate. The average half-life (Average $t_{1/2}$) and one standard deviation are shown, and the difference is not statistically significant ($p$ = 0.42 in a Student's two-tailed $t$-test). The graph shows the average $\ln(t_x/ t_0)$ and one standard deviation for the three biological replicates of wild type (black dashed line) and the *csgA* mutant (gray solid line).

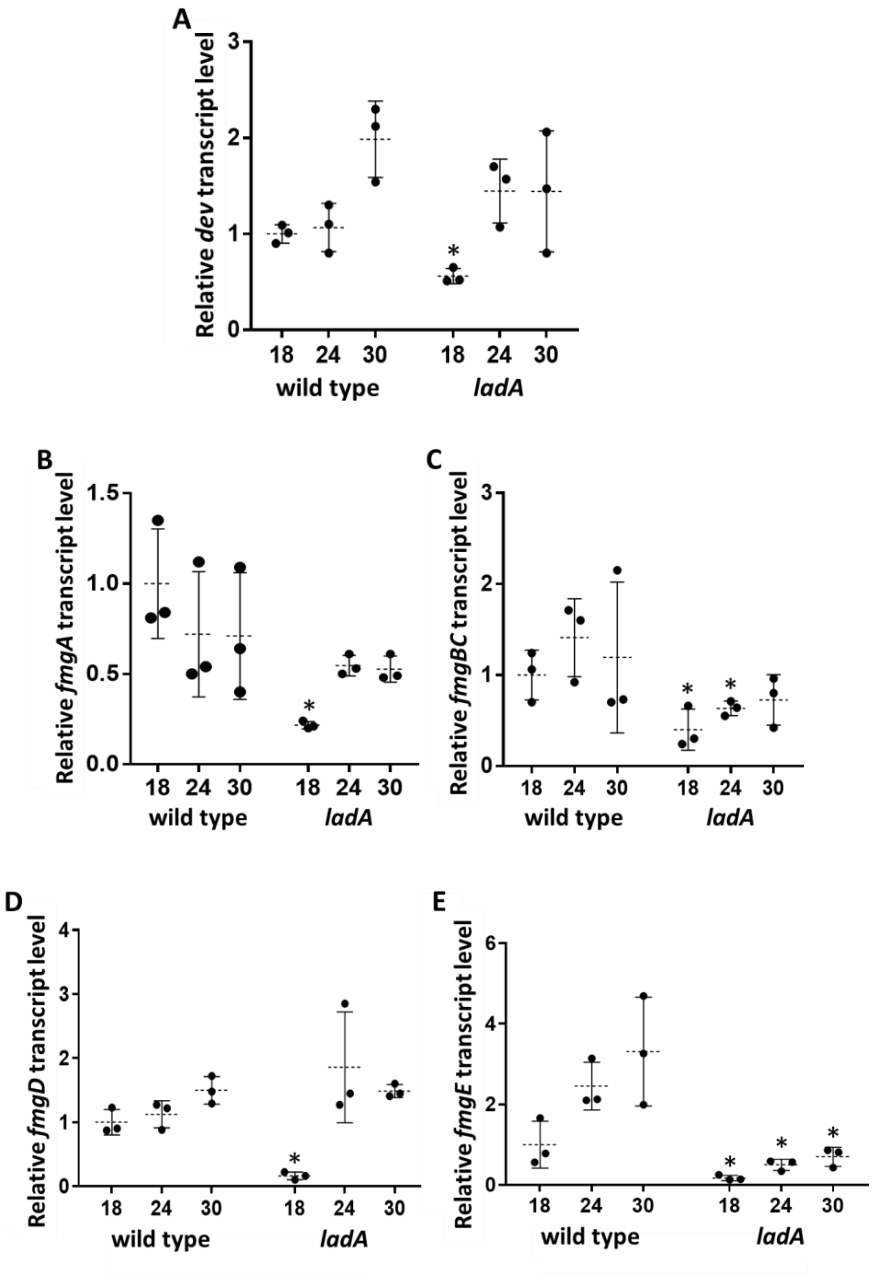


**Figure S2.5 Levels of *dev* and *fmg* transcripts in a *ladA* mutant.** Wild type DK1622 and its *ladA* mutant derivative were subjected to starvation under submerged culture conditions and samples were collected at the indicated number of hours poststarvation (PS) for measurement of (A) *dev*, (B) *fmgA*, (C) *fmgBC*, (D) *fmgD*, and (E) *fmgE* transcript levels by RT-qPCR. Graphs show the data points and average of three biological replicates, relative to wild-type DK1622 at 18 h PS, and error bars show one standard deviation. Asterisks indicate a significant difference ($p < 0.05$ in Student's two-tailed *t*-tests) from wild type at the corresponding time PS.

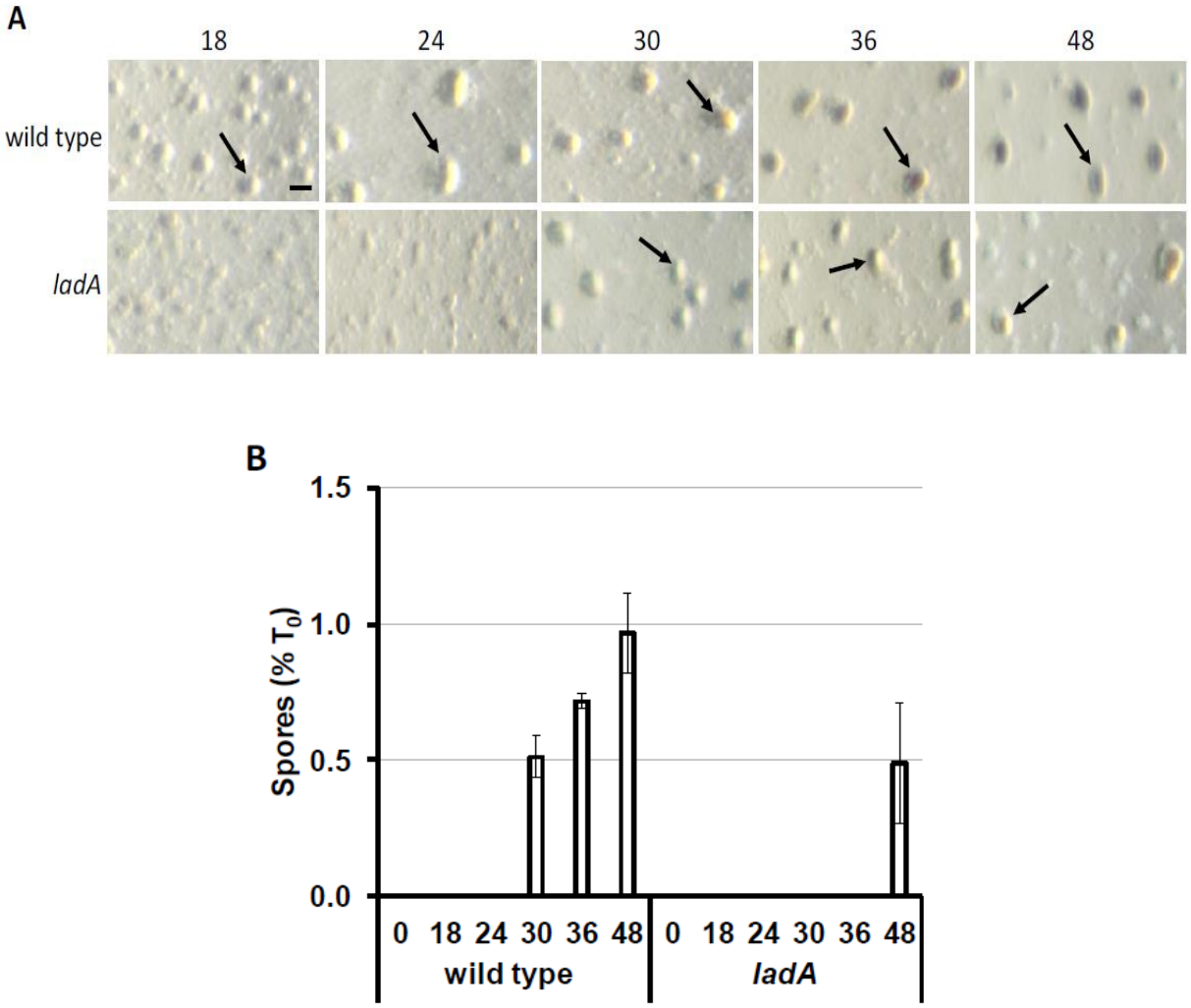


**Figure S2.6 Developmental phenotype and quantification of sonication resistant spores of the *ladA* mutant.** Wild-type DK1622 and its *ladA* mutant derivative were subjected to starvation under submerged culture conditions. (A) Microscopy. Images were obtained at the indicated number of hours poststarvation (PS). DK1622 formed mounds by 18 h PS (an arrow points to one) and the mounds darkened at 36 to 48 h. The *ladA* mutant formed mounds at 30 h, and the mounds did not darken until 48 h. Bar, 100 mm. Similar results were observed in at least three biological replicates. (B) Quantification of sonication-resistant spores. Values are expressed as a percentage of the number of rod-shaped cells present at the time starvation initiated development ($T_0$) (Table S1). Bars show the average of three biological replicates and error bars show one standard deviation.

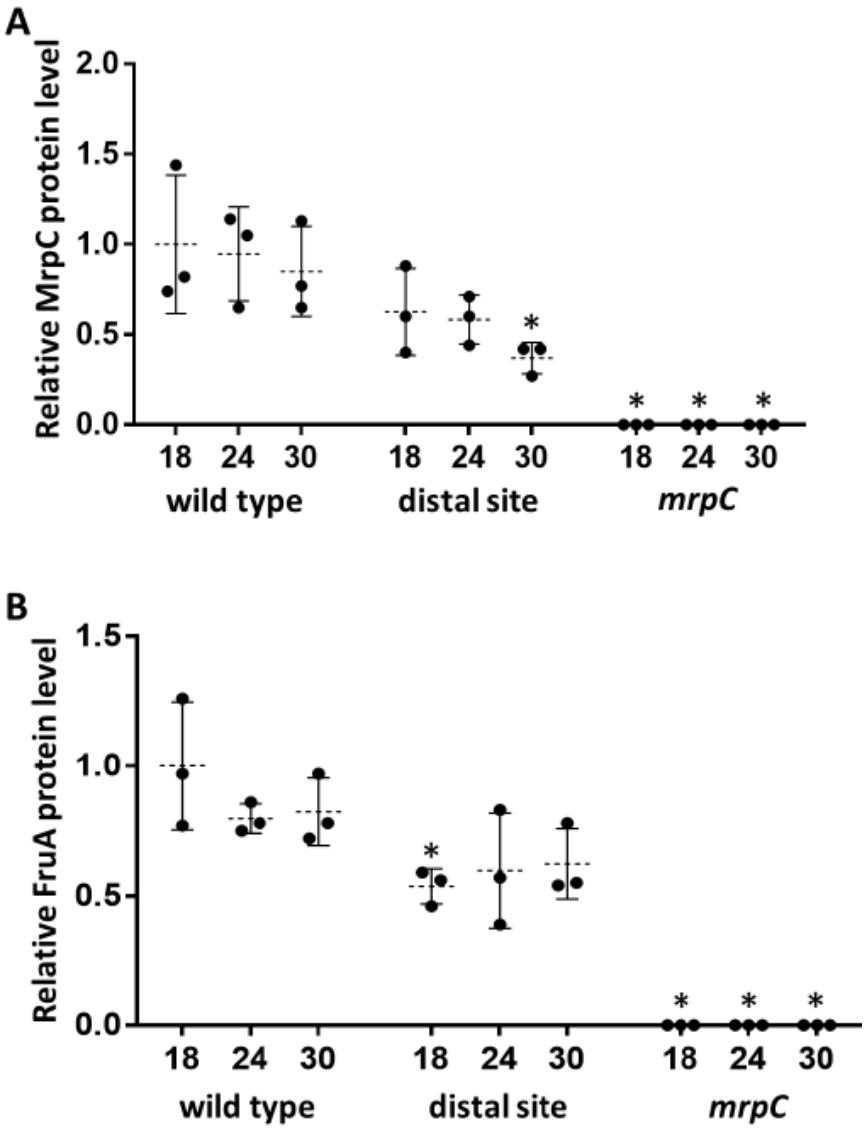


**Figure S2.7 Levels of MrpC and FruA in wild type, *distal site* mutant and *mrpC* mutant during *M. xanthus* development.** Wild-type DK1622 and its indicated mutant derivatives were subjected to starvation under submerged culture conditions and samples were collected at the indicated number of hours poststarvation (PS) for measurement of (A) MrpC and (B) FruA levels by immunoblot. Graphs show the data points and average of at least three biological replicates, relative to wild-type DK1622 at 18 h PS, and error bars show one standard deviation. Asterisks indicate a significant difference ($p < 0.05$ in Student's two-tailed *t*-tests) from wild type at the corresponding time PS.

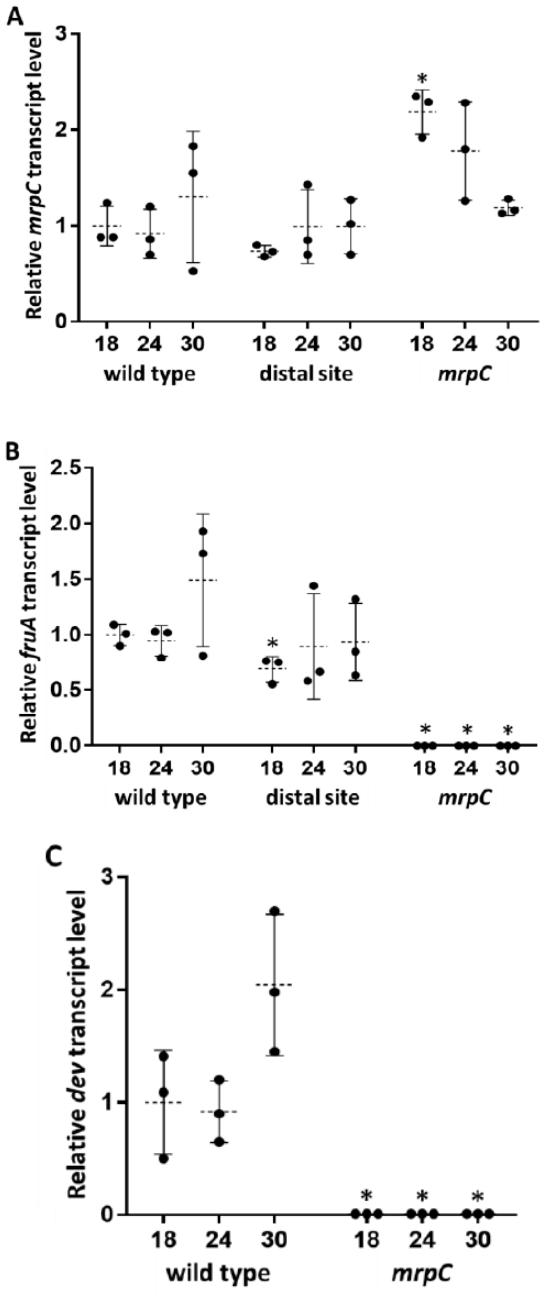


**Figure S2.8 *mrpC, fruA* and *dev* transcript levels in wild type, *distal site* mutant and *mrpC* mutant during *M. xanthus* development.** Wild-type DK1622 and its indicated mutant derivatives were subjected to starvation under submerged culture conditions and samples were collected at the indicated number of hours poststarvation (PS) for measurement of (A) *mrpC*, (B) *fruA*, and (C) *dev* transcript levels by RT-qPCR. Graphs show the data points and average of at least three biological replicates, relative to wild-type DK1622 at 18 h PS, and error bars show one standard deviation. Asterisks indicate a significant difference ($p < 0.05$ in Student's two-tailed *t*-tests) from wild type at the corresponding time PS.

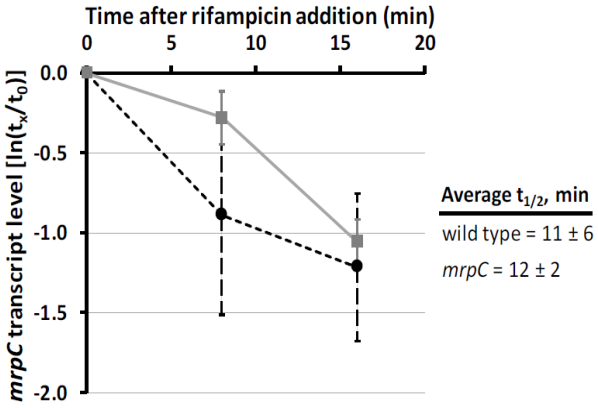


**Figure S2.9 *mrpC* transcript stability in wild type and *mrpC* mutant at 18 h poststarvation.** Wild-type DK1622 and the *mrpC* mutant were subjected to starvation under submerged culture conditions for 18 h. The overlay was replaced with fresh starvation buffer containing rifampicin (50 mg/ml) and samples were collected immediately ($t_0$) and at the times indicated ($t_x$) for measurement of the *mrpC* transcript level by RT-qPCR. Transcript levels at $t_x$ were normalized to that at $t_0$ for each of three biological replicates and used to determine the transcript half-life for each replicate. The average half-life (Average $t_{1/2}$) and one standard deviation are shown, and the difference is not statistically significant ($p$ = 0.85 in a Student's two-tailed *t*-test). The graph shows the average ln($t_x$/ $t_0$) and one standard deviation for the three biological replicates of wild type (black dashed line) and the *mrpC* mutant (gray solid line).

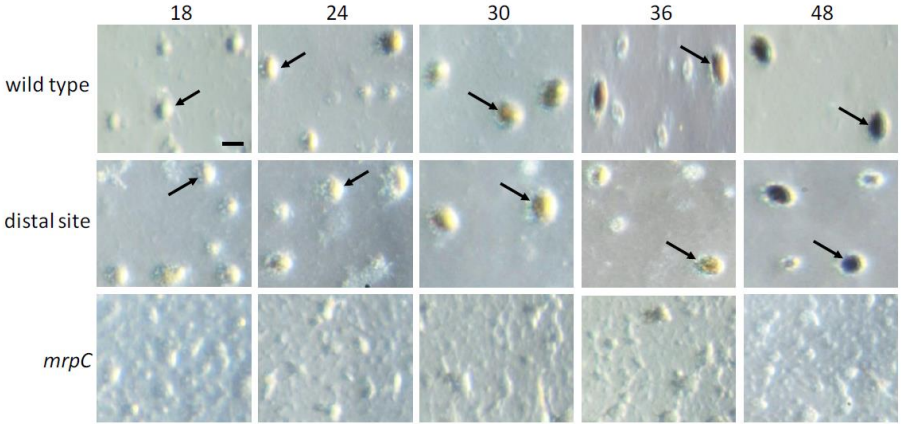


**Figure S2.10 Developmental phenotype of wild type, *distal site* mutant and *mrpC* mutant.** Wild-type DK1622 and its indicated mutant derivatives were subjected to starvation under submerged culture conditions and images were obtained at the indicated number of hours poststarvation (PS). The wild type and the distal site mutant formed mounds by 18 h PS (an arrow points to one) and the mounds darkened at 36 to 48 h. The *mrpC* mutant failed to form mounds. Bar, 100 µm. Similar results were observed in at least three biological replicates.

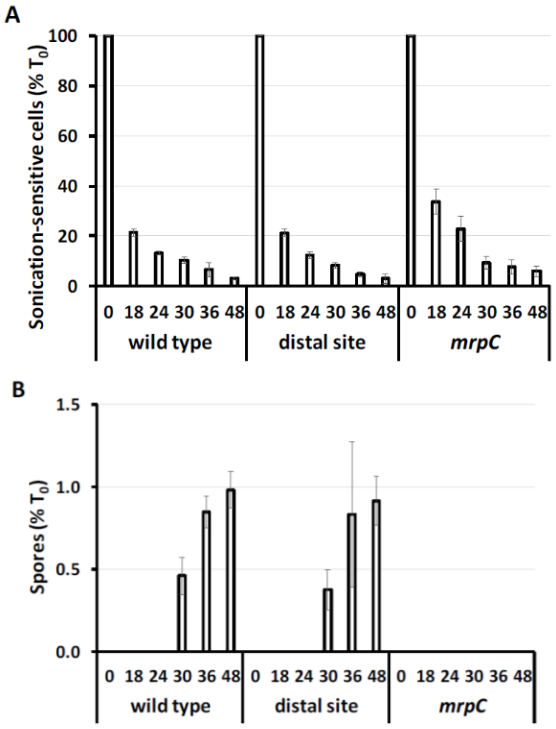


**Figure S2.11 Cellular changes in wild type, *distal site* mutant and *mrpC* mutant**. Wild-type DK1622 and its indicated mutant derivatives were subjected to starvation under submerged culture conditions and samples were collected at the indicated number of hours poststarvation for quantification of (A) sonication-sensitive cells and (B) sonication-resistant spores. Values are expressed as a percentage of the number of rod-shaped cells present at the time starvation initiated development (T0) (Table S1). Bars show the average of three biological replicates and error bars show one standard deviation

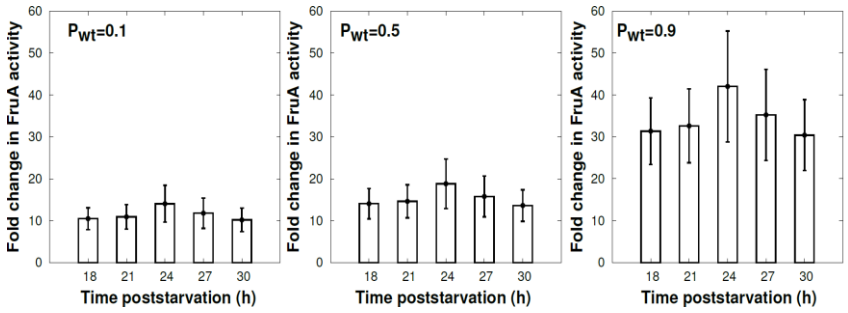


**Figure S2.12 Mathematical modeling prediction of the required reduction in FruA activity in the *csgA* mutant in comparison to wild type, to explain the experimental data.** Bars show the average of 108 datasets representing all possible combinations of four biological replicates of wild type and three biological replicates of each mutant (*csgA, devI, devS*), and error bars show one standard deviation.

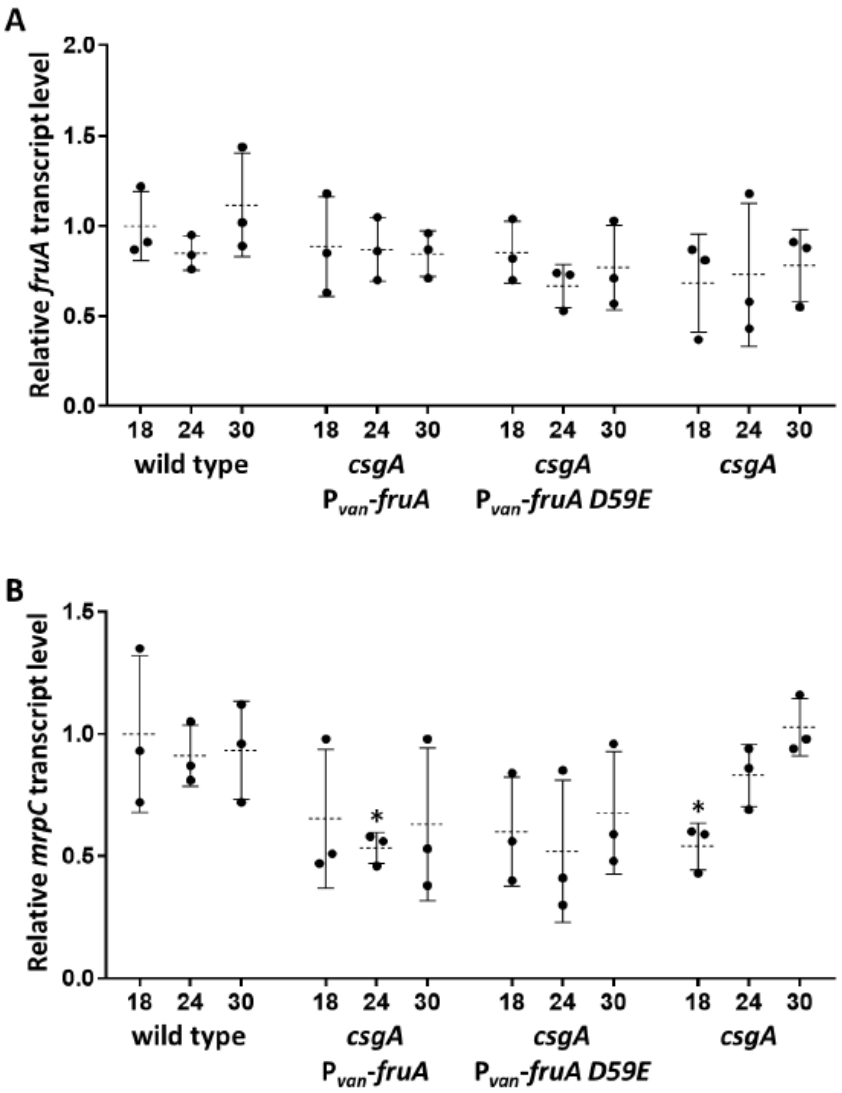


**Figure S2.13 *mrpC* and *fruA* transcript levels in wild type, *csgA* mutant and *csgA* ($P_{van}$-*fruA*) mutant.** Wild-type DK1622 and its indicated mutant derivatives were subjected to starvation under submerged culture conditions and samples were collected at the indicated number of hours poststarvation (PS) for measurement of (A) *fruA* and (B) *mrpC* transcript levels by RT-qPCR. Bars show the average of at least three biological replicates, relative to wild-type DK1622 at 18 h PS, and error bars show one standard deviation. Asterisks indicate a significant difference ($p < 0.05$ in Student's two-tailed *t*-tests) from wild type at the corresponding time PS.

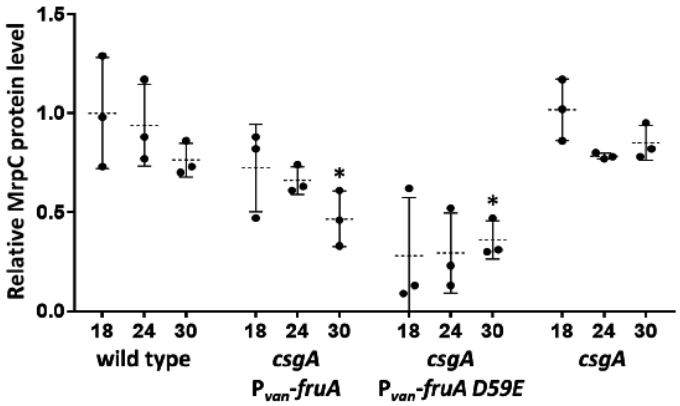


**Figure S2.14 MrpC protein level in wild type, *csgA* mutant and *csgA* ($P_{van}$-*fruA*) mutant.** Wild-type DK1622 and its indicated mutant derivatives were subjected to starvation under submerged culture conditions and samples were collected at the indicated number of hours poststarvation (PS) for measurement of MrpC levels by immunoblot. Bars show the average of at least three biological replicates, relative to wild-type DK1622 at 18 h PS, and error bars show one standard deviation. Asterisks indicate a significant difference ($p < 0.05$ in Student's two-tailed *t*-tests) from wild type at the corresponding time PS.

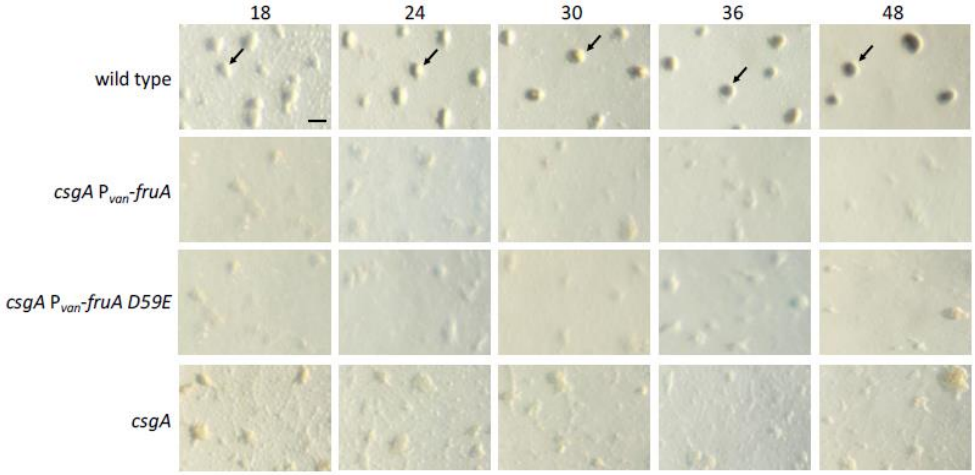


**Figure S2.15 Developmental phenotype of wild type, *csgA* mutant and *fruA* ($P_{van}$-*fruA*) mutant.** Wild-type DK1622 and its indicated mutant derivatives were subjected to starvation under submerged culture conditions and images were obtained at the indicated number of hours poststarvation (PS). The wild type formed mounds by 18 h PS (an arrow points to one) and the mounds darkened at 36 to 48 h. The *csgA* P*van-fruA*, *csgA* P*van-fruA D59E*, and *csgA* mutants failed to form mounds. Bar, 100 mm. Similar results were observed in at least three biological replicates.

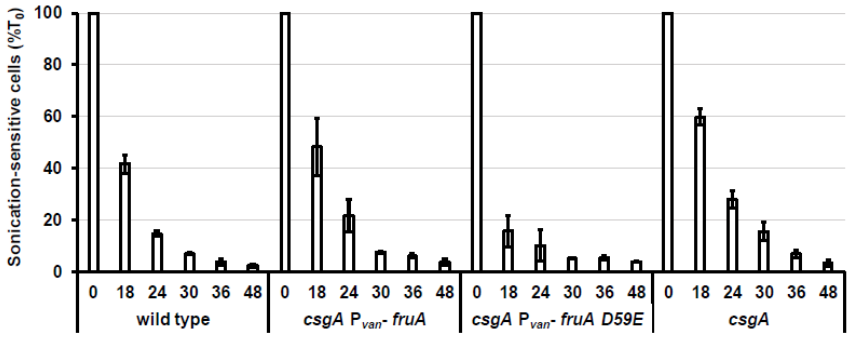


**Figure S2.16 Cellular changes of wild type, *csgA* mutant and *fruA* (P$_{van}$-*fruA*) mutant.** Wild-type DK1622 and its indicated mutant derivatives were subjected to starvation under submerged culture conditions and samples were collected at the indicated number of hours poststarvation for quantification of sonication-sensitive cells. Values are expressed as a percentage of the number of rod- shaped cells present at the time starvation initiated development (T0) (Table S1). Bars show the average of three biological replicates and error bars show one standard deviation.

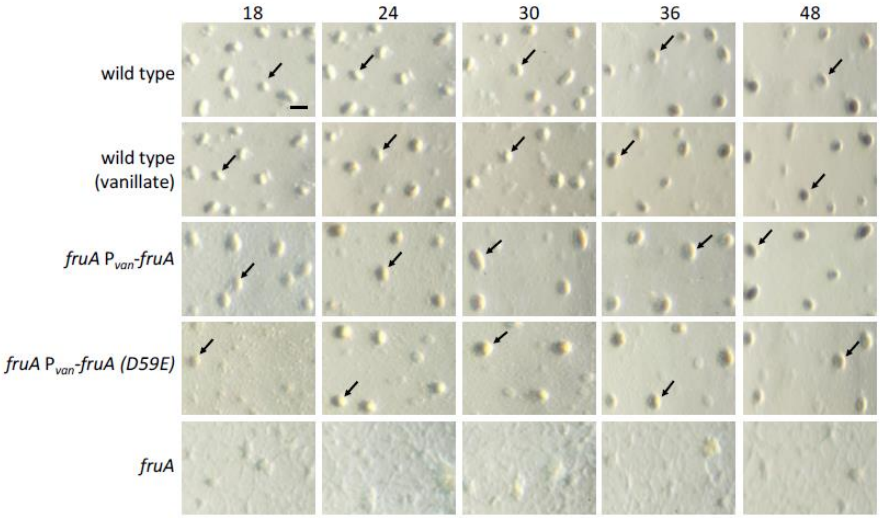


**Figure S2.17 Developmental phenotype of *fruA* (P$_{van}$-*fruA*) mutant and *fruA* (P$_{van}$-*fruAD59E*) mutant**. Wild-type DK1622 without or with vanillate induction and its indicated mutant derivatives with vanillate induction were subjected to starvation under submerged culture conditions and images were obtained at the indicated number of hours poststarvation (PS). The wild type without or with vanillate, and the *fruA* P*van- fruA* and *fruA* P*van-fruA D59E* strains, formed mounds by 18 h PS (arrows point to mounds) and the mounds darkened at 36 to 48 h. The *fruA* mutant failed to form mounds. Bar, 100 mm. Similar results were observed in at least three biological replicates.

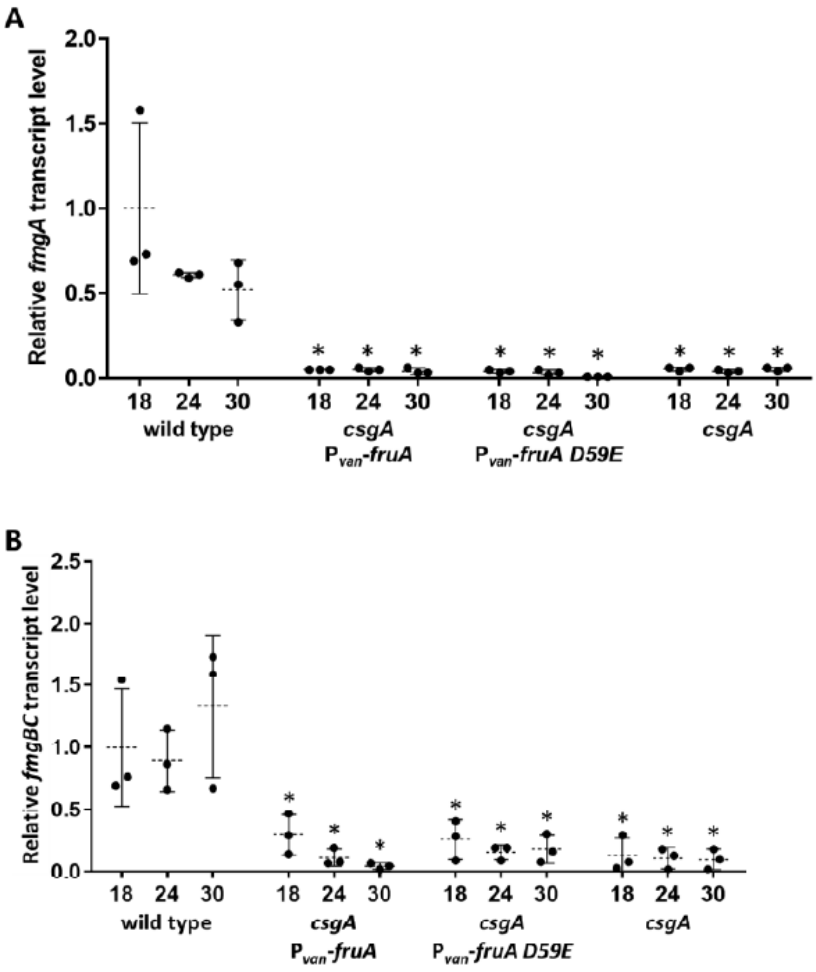


**Figure S2.18 Levels of *fmg* transcripts in *csgA* mutant and *csgA* ($P_{van}$-*fruA*) mutant, *csgA* mutant and *csgA* ($P_{van}$-*fruAD59E*) mutant.**

**Figure S2.18 (cont'd)**

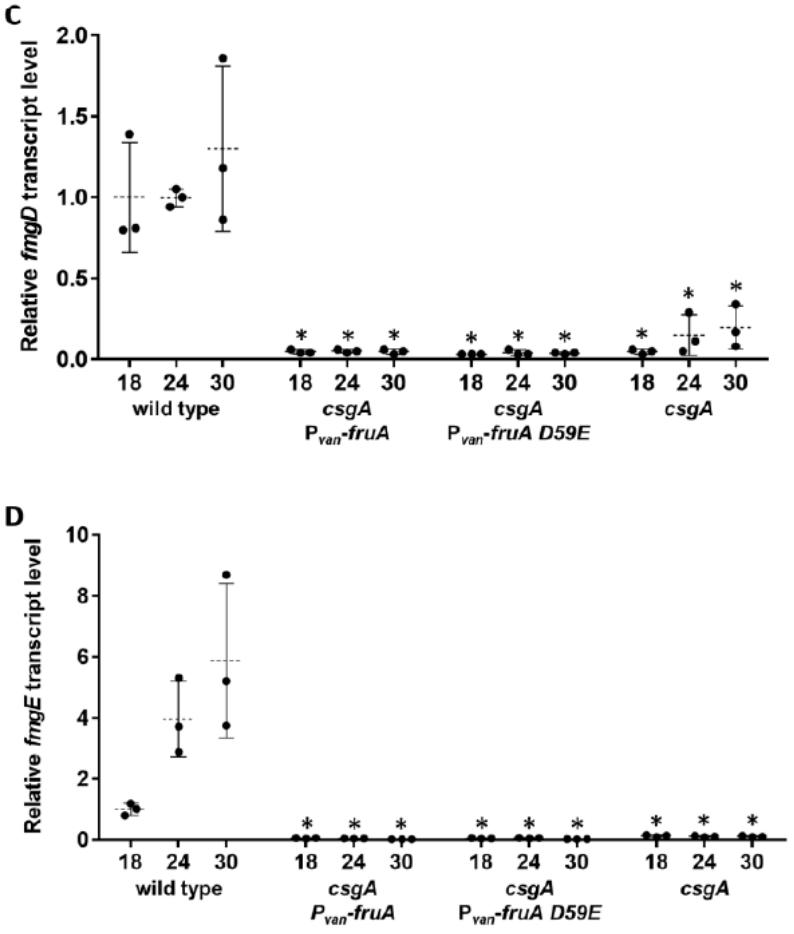


Wild-type DK1622 and its indicated mutant derivatives were subjected to starvation under submerged culture conditions and samples were collected at the indicated number of hours poststarvation (PS) for measurement of (A) *fmgA*, (B) *fmgBC*, (C) *fmgD*, and (D) *fmgE* transcript levels by RT-qPCR. Bars show the average of at least three biological replicates, relative to wild-type DK1622 at 18 h PS, and error bars show one standard deviation. Asterisks indicate a significant difference ($p < 0.05$ in Student's two-tailed *t*-tests) from wild type at the corresponding time PS.

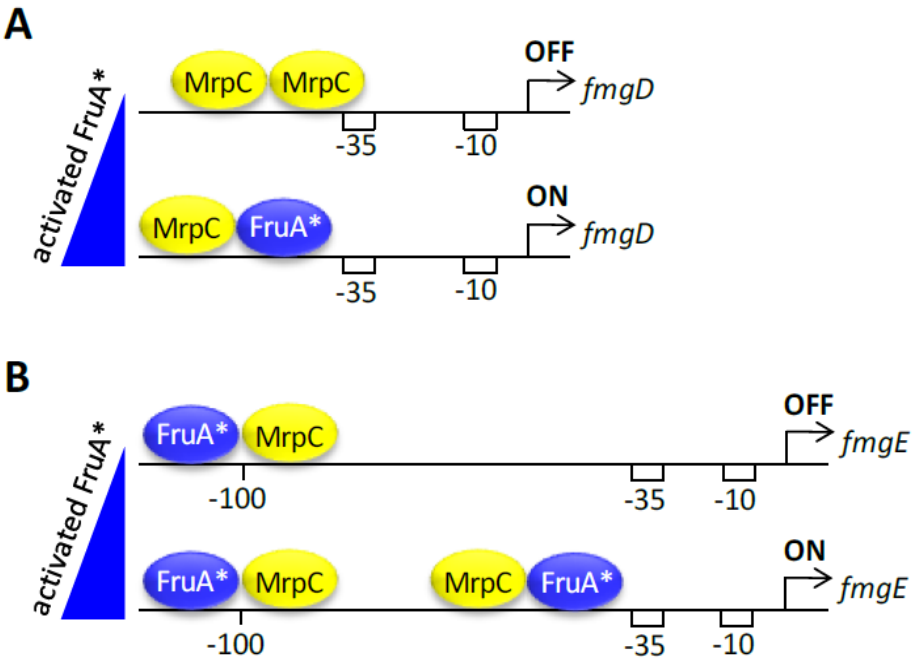


**Figure S2.19 Models for regulation of *fmgD* and *fmgE*.** C-signaling causes the level of activated FruA* to rise as development proceeds (triangles). (A) Cooperative binding of two MrpC initially represses *fmgD* transcription, but eventually FruA* outcompetes the downstream MrpC for binding to the upstream MrpC, activating transcription. (B) MrpC and activated FruA* bind cooperatively first to a higher affinity centered at -100 bp relative to the *fmgE* transcriptional start site. As FruA* rises, the lower affinity site just upstream of the promoter is also cooperatively bound by FruA* and MrpC, activating transcription. In both panels, boxes indicate the promoter -35 and -10 regions.

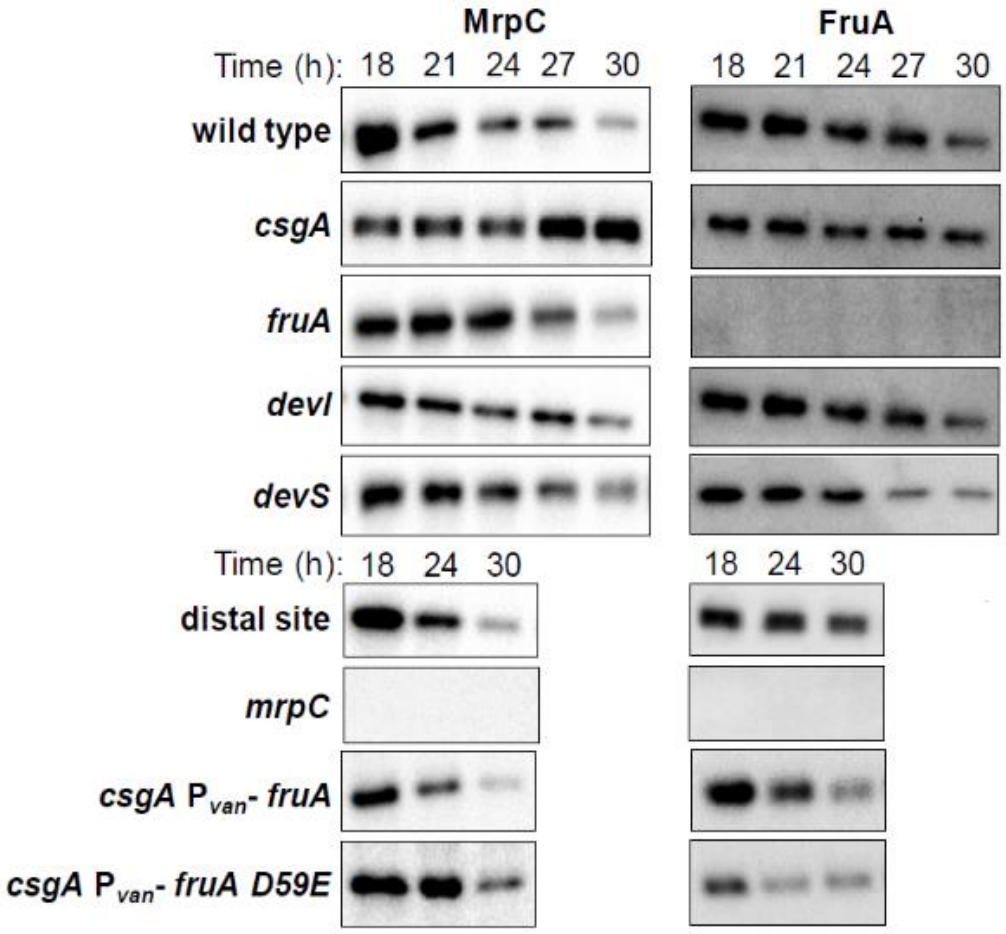


**Figure S2.20 Representative MrpC and FruA immunoblots for wild type and mutants.** Wild-type DK1622 and its indicated mutant derivatives were subjected to starvation under submerged culture conditions and samples were collected at the indicated number of hours poststarvation (PS) for measurement of MrpC and FruA levels by immunoblot. Equal volumes (10 µl for measurement of MrpC and 15 µl for measurement of FruA) of whole-cell extract samples were subjected to semi-quantitative immunoblot analysis as described in the Experimental Procedures.

**REFERENCES**

## REFERENCES


1. Davidson EH, Levine MS: Properties of developmental gene regulatory networks. *Proc Natl Acad Sci USA* 2008, 105(51):20063-20066.

2. Frum T, Ralston A: Cell signaling and transcription factors regulating cell fate during formation of the mouse blastocyst. *Trends Genet* 2015, 31(7):402-410.

3. Drapek C, Sparks EE, Benfey PN: Uncovering gene regulatory networks controlling plant cell differentiation. *Trends Genet* 2017, 33(8):529-539.

4. van Gestel J, Vlamakis H, Kolter R: Division of labor in biofilms: the ecology of cell differentiation. *Microbiol Spectr* 2015, 3(2):MB-0002-2014.

5. Norman TM, Lord ND, Paulsson J, Losick R: Stochastic switching of cell fate in microbes. *Annu Rev Microbiol* 2015, 69:381-403.

6. Bush MJ, Tschowri N, Schlimpert S, Flardh K, Buttner MJ: c-di-GMP signalling and the regulation of developmental transitions in streptomycetes. *Nat Rev Microbiol* 2015, 13(12):749-760.

7. Kroos L: Highly signal-responsive gene regulatory network governing *Myxococcus* development. *Trends Genet* 2017, 33:3-15.

8. Barratt MJ, Lebrilla C, Shapiro HY, Gordon JI: The gut microbiota, food science, and human nutrition: a timely marriage. *Cell Host Microbe* 2017, 22(2):134-141.

9. Jansson JK, Hofmockel KS: The soil microbiome-from metagenomics to metaphenomics. *Curr Opin Microbiol* 2018, 43:162-168.

10. Yang Z, Higgs P (eds.): Myxobacteria: genomics, cellular and molecular biology. Norfolk, UK: Caister Academic Press; 2014.

11. Bretl DJ, Kirby JR: Molecular mechanisms of signaling in *Myxococcus xanthus* development. *J Mol Biol* 2016, 428:3805-3830.

12. O'Connor KA, Zusman DR: Development in *Myxococcus xanthus* involves differentiation into two cell types, peripheral rods and spores. *J Bacteriol* 1991, 173(11):3318-3333.

13. Lee B, Holkenbrink C, Treuner-Lange A, Higgs PI: *Myxococcus xanthus* developmental cell fate production: heterogeneous accumulation of developmental regulatory proteins and reexamination of the role of MazF in developmental lysis. *J Bacteriol* 2012, 194(12):3058-3068.

14. Rajagopalan R, Kroos L: Nutrient-regulated proteolysis of MrpC halts expression of genes important for commitment to sporulation during *Myxococcus xanthus* development. *J Bacteriol* 2014, 196:2736-2747.

15. Sun H, Shi W: Genetic studies of *mrp*, a locus essential for cellular aggregation and sporulation of *Myxococcus xanthus*. *J Bacteriol* 2001, 183(16):4786-4795.

16. Sun H, Shi W: Analyses of *mrp* genes during *Myxococcus xanthus* development. *J Bacteriol* 2001, 183(23):6733-6739.

17. Robinson M, Son B, Kroos L: Transcription factor MrpC binds to promoter regions of many developmentally-regulated genes in *Myxococcus xanthus*. *BMC Genomics* 2014, 15:1123.

18. Ueki T, Inouye S: Identification of an activator protein required for the induction of *fruA*, a gene essential for fruiting body development in *Myxococcus xanthus*. *Proc Natl Acad Sci USA* 2003, 100(15):8782-8787.

19. Ogawa M, Fujitani S, Mao X, Inouye S, Komano T: FruA, a putative transcription factor essential for the development of *Myxococcus xanthus*. *Mol Microbiol* 1996, 22(4):757-767.

20. Campbell A, Viswanathan P, Barrett T, Son B, Saha S, Kroos L: Combinatorial regulation of the *dev* operon by MrpC2 and FruA during *Myxococcus xanthus* development. *J Bacteriol* 2015, 197:240-251.

21. Lee J, Son B, Viswanathan P, Luethy P, Kroos L: Combinatorial regulation of *fmgD* by MrpC2 and FruA during *Myxococcus xanthus* development. *J Bacteriol* 2011, 193:1681-1689.

22. Mittal S, Kroos L: A combination of unusual transcription factors binds cooperatively to control *Myxococcus xanthus* developmental gene expression. *Proc Natl Acad Sci USA* 2009, 106:1965-1970.

23. Mittal S, Kroos L: Combinatorial regulation by a novel arrangement of FruA and MrpC2 transcription factors during *Myxococcus xanthus* development. *J Bacteriol* 2009, 191:2753-2763.

24. Son B, Liu Y, Kroos L: Combinatorial regulation by MrpC2 and FruA involves three sites in the *fmgE* promoter region during *Myxococcus xanthus* development. *J Bacteriol* 2011, 193:2756-2766.

25. Boysen A, Ellehauge E, Julien B, Sogaard-Andersen L: The DevT protein stimulates synthesis of FruA, a signal transduction protein required for fruiting body morphogenesis in *Myxococcus xanthus*. *J Bacteriol* 2002, 184(6):1540-1546.

26. Thony-Meyer L, Kaiser D: *devRS*, an autoregulated and essential genetic locus for fruiting body development in *Myxococcus xanthus*. *J Bacteriol* 1993, 175:7450-7462.

27. Viswanathan P, Murphy K, Julien B, Garza AG, Kroos L: Regulation of *dev*, an operon that includes genes essential for *Myxococcus xanthus* development and CRISPR-associated genes and repeats. *J Bacteriol* 2007, 189:3738-3750.

28. Rajagopalan R, Kroos L: The *dev* operon regulates the timing of sporulation during *Myxococcus xanthus* development. *J Bacteriol* 2017, 199(10):e00788-00716.

29. Rajagopalan R, Wielgoss S, Lippert G, Velicer GJ, Kroos L: *devI* is an evolutionarily young negative regulator of *Myxococcus xanthus* development. *J Bacteriol* 2015, 197(7):1249-1262.

30. Kroos L, Kaiser D: Expression of many developmentally regulated genes in *Myxococcus* depends on a sequence of cell interactions. *Genes Dev* 1987, 1:840-854.

31. Ellehauge E, Norregaard-Madsen M, Sogaard-Andersen L: The FruA signal transduction protein provides a checkpoint for the temporal co-ordination of intercellular signals in *Myxococcus xanthus* development. *Mol Microbiol* 1998, 30:807-817.

32. Shimkets LJ, Gill RE, Kaiser D: Developmental cell interactions in *Myxococcus xanthus* and the *spoC* locus. *Proc Natl Acad Sci USA* 1983, 80:1406-1410.

33. Kim SK, Kaiser D: Cell motility is required for the transmission of C-factor, an intercellular signal that coordinates fruiting body morphogenesis of *Myxococcus xanthus*. *Genes Dev* 1990, 4:896-905.

34. Kim SK, Kaiser D: Cell alignment required in differentiation of *Myxococcus xanthus*. *Science* 1990, 249:926-928.

35. Kroos L, Hartzell P, Stephens K, Kaiser D: A link between cell movement and gene expression argues that motility is required for cell-cell signaling during fruiting body development. *Genes Dev* 1988, 2:1677-1685.

36. Sager B, Kaiser D: Two cell-density domains within the *Myxococcus xanthus* fruiting body. *Proc Natl Acad Sci USA* 1993, 90:3690-3694.

37. Kim SK, Kaiser D: C-factor: a cell-cell signaling protein required for fruiting body morphogenesis of *M. xanthus*. *Cell* 1990, 61:19-26.

38. Lobedanz S, Sogaard-Andersen L: Identification of the C-signal, a contact-dependent morphogen coordinating multiple developmental responses in *Myxococcus xanthus*. *Genes Dev* 2003, 17(17):2151-2161.

39. Rolbetzki A, Ammon M, Jakovljevic V, Konovalova A, Sogaard-Andersen L: Regulated secretion of a protease activates intercellular signaling during fruiting body formation in *M. xanthus*. *Dev Cell* 2008, 15(4):627-634.

40. Sun H, Shi, W.: Genetic studies of mrp, a locus essential for cellular aggregation and sporulation of Myxococcus xanthus. *Journal of bacteriology* 2001, 183(16):4786-4795.

41. Sun H, Shi, W.: Analyses of mrp genes during Myxococcus xanthus development. *Journal of bacteriology* 2001, 183(23):6733-6739.

42. Nariya H, Inouye, S.: Identification of a protein Ser/Thr kinase cascade that regulates essential transcriptional activators in Myxococcus xanthus development. *Molecular microbiology* 2005, 58(2):367-379.

43. Hagen TJ, Shimkets, L. J.: Nucleotide sequence and transcriptional products of the csg locus of Myxococcus xanthus. *Journal of bacteriology* 1990, 172(1):15-23.

44. Kim SK, Kaiser, D.: C-factor: a cell-cell signaling protein required for fruiting body morphogenesis of M. xanthus. *Cell* 1990, 61(1):19-26.

45. Ueki T, Inouye, S.: Identification of an activator protein required for the induction of fruA, a gene essential for fruiting body development in Myxococcus xanthus. *Proceedings of the National Academy of Sciences of the United States of America* 2003, 100(15):8782-8787.

46. Ellehauge E, Norregaard-Madsen, M, Sogaard-Andersen, L.: The FruA signal transduction protein provides a checkpoint for the temporal co-ordination of intercellular signals in Myxococcus xanthus development. *Molecular microbiology* 1998, 30(4):807-817.

47. Mittal S, Kroos, L.: A combination of unusual transcription factors binds cooperatively to control Myxococcus xanthus developmental gene expression. *Proceedings of the National Academy of Sciences of the United States of America* 2009, 106(6):1965-1970.

48. Campbell A, Viswanathan, P, Barrett, T, Son, B, Saha, S, Kroos, L.: Combinatorial regulation of the dev operon by MrpC2 and FruA during Myxococcus xanthus development. *Journal of bacteriology* 2015, 197(2):240-251.

49. Thony-Meyer L, Kaiser, D.: devRS, an autoregulated and essential genetic locus for fruiting body development in Myxococcus xanthus. *Journal of bacteriology* 1993, 175(22):7450-7462.

50. Viswanathan P, Murphy, K, Julien, B, Garza, A. G, Kroos, L.: Regulation of dev, an operon that includes genes essential for Myxococcus xanthus development and CRISPR-associated genes and repeats. *Journal of bacteriology* 2007, 189(10):3738-3750.

51. Rajagopalan R, Wielgoss, S, Lippert, G, Velicer, G. J, Kroos, L.: devI is an evolutionarily young negative regulator of Myxococcus xanthus development. *Journal of bacteriology* 2015, 197(7):1249-1262.

52. Rajagopalan R, Kroos L: The dev Operon Regulates the Timing of Sporulation during Myxococcus xanthus Development. *Journal of bacteriology* 2017, 199(10).

53. Ogawa M, Fujitani, S, Mao, X, Inouye, S, Komano, T.: FruA, a putative transcription factor essential for the development of Myxococcus xanthus. *Molecular microbiology* 1996, 22(4):757-767.

54. Boynton TO, Shimkets LJ: *Myxococcus* CsgA, *Drosophila* Sniffer and human HSD17B10 are cardiolipin phospholipases. *Genes Dev* 2015, 29:1903-1914.

55. Stock AM, Robinson VL, Goudreau PN: Two-component signal transduction. *Annu Rev Biochem* 2000, 69:183-215.

56. Nariya H, Inouye S: Identification of a protein Ser/Thr kinase cascade that regulates essential transcriptional activators in *Myxococcus xanthus* development. *Mol Microbiol* 2005, 58(2):367-379.

57. Nariya H, Inouye S: A protein Ser/Thr kinase cascade negatively regulates the DNA-binding activity of MrpC, a smaller form of which may be necessary for the *Myxococcus xanthus* development. *Mol Microbiol* 2006, 60(5):1205-1217.

58. Nariya H, Inouye M: MazF, an mRNA interferase, mediates programmed cell death during multicellular *Myxococcus* development. *Cell* 2008, 132(1):55-66.

59. Schramm A, Lee B, Higgs PI: Intra- and inter-protein phosphorylation between two hybrid histidine kinases controls *Myxococcus xanthus* developmental progression. *J Biol Chem* 2012, 287:25060–25072.

60. McLaughlin PT, Bhardwaj V, Feeley BE, Higgs PI: MrpC, a CRP/Fnr homolog, functions as a negative autoregulator during the *Myxococcus xanthus* multicellular developmental program. *Mol Microbiol* 2018, Epub ahead of print.

61. Srinivasan D, Kroos L: Mutational analysis of the *fruA* promoter region demonstrates that C-box and 5-base-pair elements are important for expression of an essential developmental gene of *Myxococcus xanthus*. *J Bacteriol* 2004, 186(17):5961-5967.

62. Viswanathan P, Ueki T, Inouye S, Kroos L: Combinatorial regulation of genes essential for *Myxococcus xanthus* development involves a response regulator and a LysR-type regulator. *Proc Natl Acad Sci USA* 2007, 104:7969-7974.

63. Bourret RB: Receiver domain structure and function in response regulator proteins. *Curr Opin Microbiol* 2010, 13(2):142-149.

64. Desai SK, Winardhi RS, Periasamy S, Dykas MM, Jie Y, Kenney LJ: The horizontally-acquired response regulator SsrB drives a *Salmonella* lifestyle switch by relieving biofilm silencing. *eLife* 2016, 5:e10747.

65. Wang L, Tian X, Wang J, Yang H, Fan K, Xu G, Yang K, Tan H: Autoregulation of antibiotic biosynthesis by binding of the end product to an atypical response regulator. *Proc Natl Acad Sci U S A* 2009, 106(21):8617-8622.

66. Licking E, Gorski L, Kaiser D: A common step for changing cell shape in fruiting body and starvation-independent sporulation of *Myxococcus xanthus*. *J Bacteriol* 2000, 182(12):3553-3558.

67. Muller FD, Schink CW, Hoiczyk E, Cserti E, Higgs PI: Spore formation in *Myxococcus xanthus* is tied to cytoskeleton functions and polysaccharide spore coat deposition. *Mol Microbiol* 2012, 83(3):486-505.

68. Ueki T, Inouye S: Identification of a gene involved in polysaccharide export as a transcription target of FruA, an essential factor for *Myxococcus xanthus* development. *J Biol Chem* 2005, 280(37):32279-32284.

69. Boynton TO, McMurry JL, Shimkets LJ: Characterization of *Myxococcus xanthus* MazF and implications for a new point of regulation. *Mol Microbiol* 2013, 87(6):1267-1276.

70. Cho K, Zusman DR: Sporulation timing in *Myxococcus xanthus* is contolled by the *espAB* locus. *Mol Microbiol* 1999, 34:714-725.

71. Higgs PI, Jagadeesan S, Mann P, Zusman DR: EspA, an orphan hybrid histidine protein kinase, regulates the timing of expression of key developmental proteins of *Myxococcus xanthus*. *J Bacteriol* 2008, 190:4416-4426.

72. Mangan S, Alon U: Structure and function of the feed-forward loop network motif. *Proc Natl Acad Sci USA* 2003, 100(21):11980-11985.

73. Mangan S, Zaslaver A, Alon U: The coherent feedforward loop serves as a sign-sensitive delay element in transcription networks. *J Mol Biol* 2003, 334(2):197-204.

74. Gibson DG, Young L, Chuang RY, Venter JC, Hutchison CA, 3rd, Smith HO: Enzymatic assembly of DNA molecules up to several hundred kilobases. *Nat Methods* 2009, 6(5):343-345.

75. Kashefi K, Hartzell PL: Genetic suppression and phenotypic masking of a Myxococcus xanthus frzF- defect. *Molecular microbiology* 1995, 15(3):483-494.

76. Iniesta AA, Garcia-Heras F, Abellon-Ruiz J, Gallego-Garcia A, Elias-Arnanz M: Two systems for conditional gene expression in *Myxococcus xanthus* inducible by isopropyl-β-D-thiogalactopyranoside or vanillate. *J Bacteriol* 2012, 194(21):5875-5885.

77. Bryant GO, Prabhu V, Floer M, Wang X, Spagna D, Schreiber D, Ptashne M: Activator control of nucleosome occupancy in activation and repression of transcription. *PLoS Biol* 2008, 6(12):2928-2939.

78. Yoder-Himes D, Kroos L: Regulation of the *Myxococcus xanthus* C-signal-dependent Ω4400 promoter by the essential developmental protein FruA. *J Bacteriol* 2006, 188:5167-5176.

79. Bradford M: A rapid and sensitive method for the quantitation of microgram quantities of protein utilizing the principle of protein-dye binding. *Anal Biochem* 1976, 72:248-254.

80. Hanahan D: Studies on transformation of *Escherichia coli* with plasmids. *J Mol Biol* 1983, 166:557-580.

81. Kaiser D: Social gliding is correlated with the presence of pili in *Myxococcus xanthus*. *Proc Natl Acad Sci USA* 1979, 76:5952-5956.

82. Shimkets LJ, Asher SJ: Use of recombination techniques to examine the structure of the *csg* locus of *Myxococcus xanthus*. *Mol Gen Genet* 1988, 211:63-71.

83. Ossa F, Diodati ME, Caberoy NB, Giglio KM, Edmonds M, Singer M, Garza AG: The *Myxococcus xanthus* Nla4 protein is important for expression of stringent response-associated genes, ppGpp accumulation, and fruiting body development. *J Bacteriol* 2007, 189(23):8474-8483.

**CHAPTER 3: Differential regulation of late-acting operons by FruA and MrpC during *Myxococcus xanthus* development**


## Abstract

Upon nutrient depletion *Myxococcus xanthus* undergoes multicellular development. Rod-shaped cells coordinate their movements to build mounds. Within mounds, rods differentiate into round stress-resistant spores. Short-range C-signaling is proposed to activate FruA, which binds DNA cooperatively with MrpC to increase transcription of many genes. This mechanism likely regulates transcription of the late-acting *fadIJ* operon involved in spore metabolism, based on comparisons of transcript levels and degradation rates in wild-type cells and mutants. Regulation of late-acting operons implicated in spore coat biogenesis (*exoA-I*, *nfsA-H*, *MXAN_3259-MXAN_3263*) was found to be more complex. These operons are negatively regulated by unactivated FruA during mound formation, then positively regulated by C-signal-activated FruA during sporulation. MrpC also negatively regulated *exo* and *MXAN_3259* during mound formation, but positively regulated *nfs*. During sporulation, MrpC continued to positively regulate *nfs*, switched to positive regulation of *MXAN_3259*, and continued to negatively regulate *exo*. DNA-binding studies suggest that FruA exerts its effects by binding to promoter regions, whereas the effects of MrpC may be indirect. A third transcription factor, Nla6, was shown previously to bind to the *exo* and *MXAN_3259* promoter regions. Here, transcript measurements indicated that Nla6 is a positive regulator of all four late-acting operons during mound formation, whereas the small protein DevI is a negative regulator during sporulation. We conclude that multiple regulators control expression of late-acting operons and we propose that differential regulation by FruA in response to C-signaling and by MrpC ensures that spore resistance and surface characteristics meet environmental demands.

## Introduction

The gram-negative soil bacterium *Myxococcus xanthus* provides an attractive model system to study signal-induced gene regulation and bacterial community behavior. Under starvation conditions, cells move on solid surfaces and form mounds, within which some of the rod-shaped cells differentiate into round spores [3]. During this multicellular developmental process of fruiting body formation, a majority of the population undergoes lysis, while some cells remain outside of fruiting bodies as peripheral rods [4]. The period between 24 and 30 h poststarvation (PS) is critical for commitment to sporulation, since during this period cells commit to forming spores despite perturbation of the starvation signal by addition of nutrient medium [5].

The developmental process of *M. xanthus* is governed by a signal-responsive gene regulatory network [6]. Starvation triggers production of the intracellular secondary messenger molecule (p)ppGpp, which leads to production of the extracellular A- and C-signals [7, 8]. The short-range C-signal is suggested to be a proteolytic fragment of the CsgA protein [9], or diacylglycerols produced by enzymatic activity of full-length CsgA [10]. C-signal appears to posttranslationally activate a transcription factor, FruA [1, 11], by an unknown mechanism. FruA is similar to response regulators of two-component signal-transduction systems [12]. Response regulators are typically activated by phosphorylation by a histidine kinase [11]. However, recent studies suggest that phosphorylation is unlikely to be the mechanism by which FruA is activated in response to C-signaling [1, 13].

Transcription of *fruA* is regulated by a cascade of starvation-responsive transcription factors. Among these transcription factors, MrpC binds upstream of the *fruA* promoter and

activates transcription [14, 15]. MrpC undergoes proteolysis if nutrient medium is added to developing cells [5]. This response is ultrasensitive to the concentration of nutrient medium added [16]. However, by 24 PS, cells begin to commit to sporulation, resisting the effects of adding nutrient medium [5].

MrpC and FruA combinatorially regulate transcription of the *dev* operon [17], which includes eight genes comprising a CRISPR-Cas system that may protect developing *M. xanthus* against phage infection [18]. The first gene in the dev operon, *devI*, codes for a 40-residue protein that inhibits sporulation when overproduced [19], delays sporulation of wild-type strain DK1622 by about 6 h [1, 20], and exerts weak positive autoregulation on *dev* transcript accumulation [1]. In contrast, in-frame deletions in three genes of the *dev* operon (*devTRS*) increase accumulation of the *dev* transcript tenfold during development [1, 20], indicating that DevTRS proteins exert strong negative autoregulation. Systematic experimental analysis in combination with mathematical modeling of the *dev* transcript level suggested that C-signal-dependent posttranslational activation of FruA is critical for expression of the *dev* operon and for commitment to spore formation [1] (see Fig. 3 in Chapter 1).

While transcription of the *dev* operon is critical for the timing of spore formation [20], the products of other operons (*exoA-I, nfsA-H, MXAN_3259-3263*, *fadIJ*) act late during the developmental process, but regulation of these operons is not well-understood [21-25] [26]. Here, we report systematic investigation of the regulation of these late-acting operons, as well as the phenotypes of mutants.

Previous work on the regulation and function of the late-acting operons has provided some insights. Transcription of the *exoA-I* operon depends on FruA binding to the promoter region

[27]. Additionally, the enhancer-binding protein [28], Nla6, binds to the *exo* promoter region [25]. The protein products of the *exo* operon are involved in the export of polysaccharide chains that form the spore coat, which is necessary to generate compact and rigid stress-bearing spores [29]. A transposon insertion mutation in *exoC* causes a defect in spore morphogenesis upon chemical induction of sporulation [30]. Additionally, a plasmid insertion *exoC* mutant failed to complete the rod to spore transition during chemically-induced sporulation [22]. In this study we investigated the impact of an *exoC* insertion mutation on sporulation induced by starvation. We also systematically analyzed the effects of mutations in regulatory genes on the *exo* transcript level during development.

The previously identified *nfsA-H* locus [31] was found to be an operon critical for spore morphogenesis upon chemical induction of sporulation [22]. The Nfs proteins appear to arrange the polysaccharide of the spore coat after secretion by Exo proteins [21]. Studies with a reporter fusion to *nfsA* suggested that C-signaling positively regulates *nfs* transcription and, unusually, that FruA negatively regulates *nfs* transcription [31]. We examined these effects, as well as others, by measuring the *nfs* transcript level in mutants.

An insertion mutation in the predicted polysaccharide deacetylase encoding gene *MXAN_3259* was shown to phenocopy an *exo* mutant by forming mounds but not mature spores [25]. Nla6 binds to the *MXAN_3259* upstream region and positively regulates transcription early in development, then negatively regulates later, based on comparison of *MXAN_3259* transcript levels in an *nla6* mutant with a WT strain [25]. We further explored the regulation and function of the putative *MXAN_3259-MXAN_3263* operon.

The putative *fadIJ* operon (*MXAN_5372-MXAN_5371*) is induced twofold during development [32], specifically in sporulating cells [24], and appears to code for a fatty acid β-oxidation pathway that impacts spore structure and resistance properties [24]. A reporter fusion to *fadI* failed to be induced in the absence of C-signaling, FruA, or MrpC during development [24]. We report systematic investigation of the *fadI* insertion mutant phenotype and of *fadI* transcriptional regulation.

## Results

### *Mutations in certain "late" genes impair development*

In previous work, we established methods to systematically analyze *M. xanthus* development under submerged culture conditions [1]. We used those methods to investigate the effects of mutations in so-called "late" genes [16], which lie in operons induced later during development than *mrpC* and *fruA*. Specifically, we examined the effects of an insertion in *exoC* of the *exoA-I* operon [22], a deletion of the entire *nfsA-H* operon [23], an insertion in *MXAN_3259* of the putative *MXAN_3259-MXAN_3263* operon [25], and an insertion in *fadI* of the *fadIJ* operon (*MXAN5372-MXAN5371*) [24]. Figure 1 shows images of wild-type [33] strain DK1622 and each mutant from 18-48 h poststarvation (PS). As expected, the WT strain formed distinct mounds by 18 h PS and the mounds began to darken by 30 h [1]. Darkening typically correlates with spore formation. The *fadI* mutant was indistinguishable from the WT strain. The *exoC* and *MXAN_3259* mutants formed normal-looking mounds by 18 h, but the mounds did not darken as much at the WT strain, suggesting a sporulation defect. The *nfsA-H* mutant was delayed by about 3 h in mound formation and darkening of the mounds appeared to be delayed and reduced.

To quantify changes at the cellular level, samples harvested from submerged culture were treated with glutaraldehyde to fix cells or were left untreated [1]. The untreated samples were used to quantify sonication-resistant spores and mature spores that are heat- and sonication-resistant and capable of germination. The fixed samples were used to quantify "sonication-sensitive cells" (i.e. the total number of cells observed in the fixed sample minus the number of sonication-resistant spores observed in the corresponding untreated sample). The majority of sonication-sensitive cells are rod-shaped cells, but cells in transition from rods to sonication-resistant spores may also be observed.

In agreement with our published data [34], sonication-resistant spores were first observed for the WT strain at 27 h PS, and as a percentage of the rod-shaped cells present at the time starvation initiated development ($T_0$), rose from 0.2% to nearly 2% by 48 h (Fig. 2). The *fadI* mutant formed about two-fold more spores than the WT strain. Consistent with the mound darkening defects we observed (Fig. 1), the *nfsA-H* mutant formed about two-fold less spores than the WT strain, and the *exoC* and *MXAN_3259* mutants failed to make a detectable number of spores (at a detection limit of 0.04% of the $T_0$ number) (Fig. 2).

The *exoC* and *MXAN_3259* mutants also failed to make a detectable number of mature spores by 72 h PS, while the *nfsA-H* mutant made about ten-fold less mature spores than the WT strain, and the *fadI* mutant made a similar number of mature spores as the WT strain (Table S1).

The WT strain exhibited a similar decline of sonication-sensitive cells during development as reported previously [1], with only 31% of the cells present at $T_0$ remaining by 18 h PS and only 6% remaining by 48 h (Fig. S1A). The decrease in cell number correlates with a decrease in the

total protein concentration of developing cultures, which was suggested to reflect lysis of the majority of cells early during development under submerged culture conditions [35]. The mutants showed similar decreases in cell number as the WT strain (Fig. S1A).

Interestingly, we observed a small percentage of cells in the fixed samples of the *exoC* and *MXAN_3259* mutants that were not rod-shaped. These cells could be premature spores that do not achieve sonication resistance. Previously, *exo* and *nfs* mutants have been reported to fail to complete morphogenesis from rods to spores, instead transiently exhibiting deformed cell morphology before reverting into rods [22]. Those observations were made upon chemical induction of sporulation, rather than starvation-induced development, as used in our experiments. We counted the number of cells that were not rod-shaped in the fixed samples. For the WT strain and the *fadI* and *nfsA-H* mutants, the number of sonication-resistant spores observed in the corresponding untreated sample (Fig. 2) was subtracted. Using this approach, about 3% of the WT cells present at $T_0$ were neither rods nor sonication-resistant spores at 24 h (Fig. S1B). The percentage decreased at later times, presumably as cells in transition from rods to spores became sonication-resistant (Fig. 2). The *fadI* mutant showed about half as many cells in transition as the WT strain at 24 h, and the number declined to a greater extent in the *fadI* mutant than in the WT strain by 48 h (Fig. S1B), consistent with the *fadI* mutant forming a larger number of sonication-resistant spores (Fig. 2). The other mutants exhibited less cells in transition at 24 h (0.4-0.7%), but in each case the percentage rose to at least 1% later (Fig. S1B). These results suggest that the *exoC* and *MXAN_3259* mutants, which fail to form a detectable

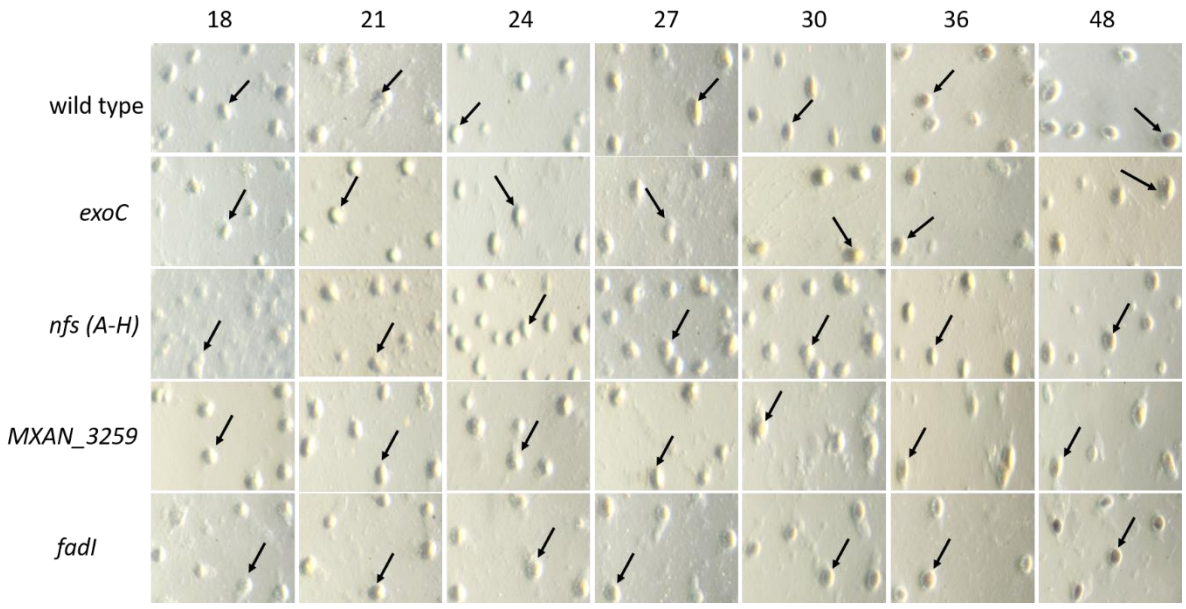


**Figure 3.1 Development of *M. xanthus* strains.** Wild-type strain DK1622 and its indicated mutant derivates were subjected to starvation under submerged culture condition and images were obtained at the indicated number of hours poststarvation. The wild-type strain and all the mutants except *nfsA-H* formed compact mounds by 18 h (an arrow points to one in each panel). The *nfsA-H* mutant formed compact mounds by 21 h. Mounds of the wild-type strain began to darken by 30 h. Mounds of the *exoC*, *nfsA-H*, and *MXAN_3259* mutants darkened by 30 h but remained slightly less dark than mounds of the wild-type strain and the fadI mutant by 48 h. Bar, 100 mm. Similar results were observed in at least three biological replicates.

number of sonication-resistant spores, as well as the *nfsA-H* mutant, which forms about half as many sonication-resistant spores as the WT strain (Fig. 2), begin to change shape during starvation-induced development, but are impaired in their ability to make spores, as reported previously for *exo* and *nfs* mutants upon chemical induction of sporulation [22]. In agreement, WT cells in transition from rods to spores have been visualized in mounds using a fluorescent membrane stain and confocal laser scanning microscopy, and all the mutants examined in this

study exhibit transitioning cells in mounds, which are distinguishable from cells undergoing lysis (Y Hoang and Lee Kroos, unpublished data).

We conclude that genes in the *exoA-I* and *nfsA-H* operons, and in the putative *MXAN3259-MXAN3263* operon, are important for normal spore formation.

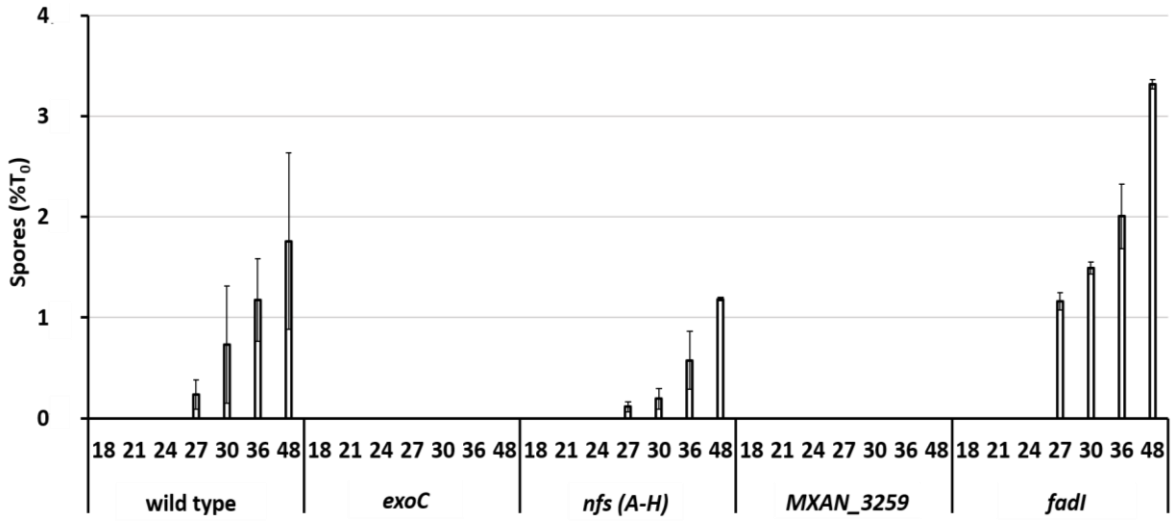


**Figure 3.2 Cellular changes during *M. xanthus* development.** Wild-type strain DK1622 and its mutant derivatives were subjected to starvation under submerged culture conditions. Samples were collected at the indicated hours post-starvation for quantification of sonication-resistant spores. Values are expressed as a percentage of the number of rod-shaped cells present at the time when starvation initiated development ($T_0$) (Table S1). Bars show the average of three biological replicates and error bars indicate one standard deviation.

***Late gene transcript levels are very low in the absence of C-signaling***

In our previous work, we also established methods to systematically analyze transcript levels during *M. xanthus* development [34]. Those methods were used to investigate the effect of nutrient medium addition to developing cells, and it was found that transcript levels of late genes decrease within 1 h after nutrient medium addition at 18 h PS [16]. Here, we report using

the same methods to determine the effects of mutations on late gene transcript levels. We measured transcript levels of the WT strain and mutants at 18-30 h PS, the period leading up to and including the time that many cells commit to spore formation [35] and sonication-resistant spores begin to be observed (Fig. 2). In agreement with a prior study [16], in the WT strain late gene transcript levels rose between 18 and 30 h PS (Fig. 3). As noted previously [20], the fold-increase of the *exo* transcript level varied greatly between biological replicates (Fig. 3A), which we do not understand. The *MXAN_3259* transcript level is likewise greatly variable (Fig. 3C). The *nfs* (Fig. 3B) and *fadI* (Fig. 3D) transcript levels varied less between biological replicates and on average both increased fourfold between 18 and 30 h, much less than the *exo* (24-fold) and *MXAN_3259* (70-fold) transcript levels.

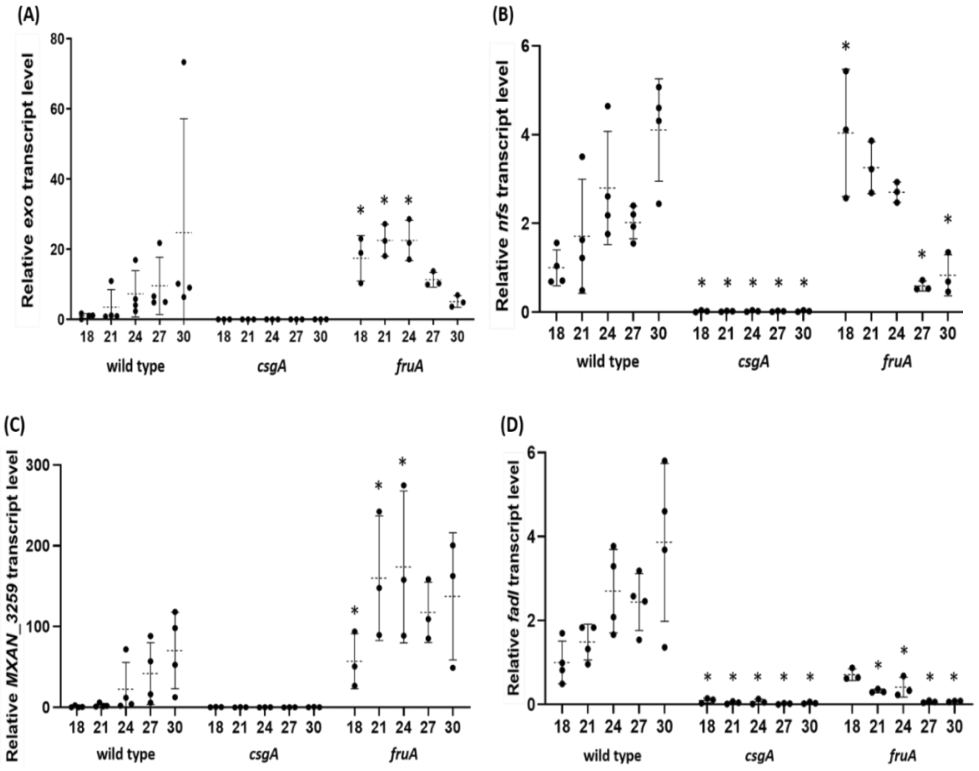


**Figure 3.3 Transcript levels in wild type, *csgA* mutant and *fruA* mutant.**

**Figure 3.3 (cont'd)**

Wild-type strain DK1622 and its indicated mutant derivatives were subjected to starvation under submerged culture conditions and samples were collected at the indicated number of hours poststarvation for measurement of (A) *exo*, (B) *nfs*, (C) *MXAN_3259* and (D) *fadI* transcript levels by RT-qPCR. Graphs show the data points and average of at least three biological replicates, relative to wild-type strain at 18 h, and error bars indicate one standard deviation. Asterisks indicate a significant difference ($p < 0.05$ in Student's two-tailed t-tests) from the wild-type at the corresponding time poststarvation.

In a *csgA* null mutant unable to produce C-signal, the late gene transcript levels do not increase during development as in the WT strain (Fig. 3, asterisks indicate $p < 0.05$ in Student's two-tailed *t*-tests comparing the mutant to the WT strain at each time point). Asterisks are absent above the *exo* and *nfs* transcript levels in the *csgA* mutant because the statistical test yielded $p > 0.05$, but this is due to the large variation between biological replicates in the WT strain. In the *csgA* mutant, the *exo* and *nfs* transcript levels were low in all biological replicates at each time point. We conclude that late gene transcript levels are very low in the absence of C-signaling. In agreement, reporter activity from fusions to *exo* [30], *nfs* [23], and *fadI* [24] was very low in *csgA* mutants relative to WT strains during development.

The low transcript levels could be due to decreased synthesis and/or increased degradation in the *csgA* mutant compared with the WT strain. To measure the transcript degradation rates, we added rifampicin to block transcription at 30 h PS and determined the transcript levels at intervals thereafter. The degradation rates of the late gene transcripts did not differ significantly between the *csgA* mutant and the WT strain (Fig. 4). These results suggest that decreased synthesis of late gene transcripts primarily accounts for the low transcript levels in the absence of C-signaling.

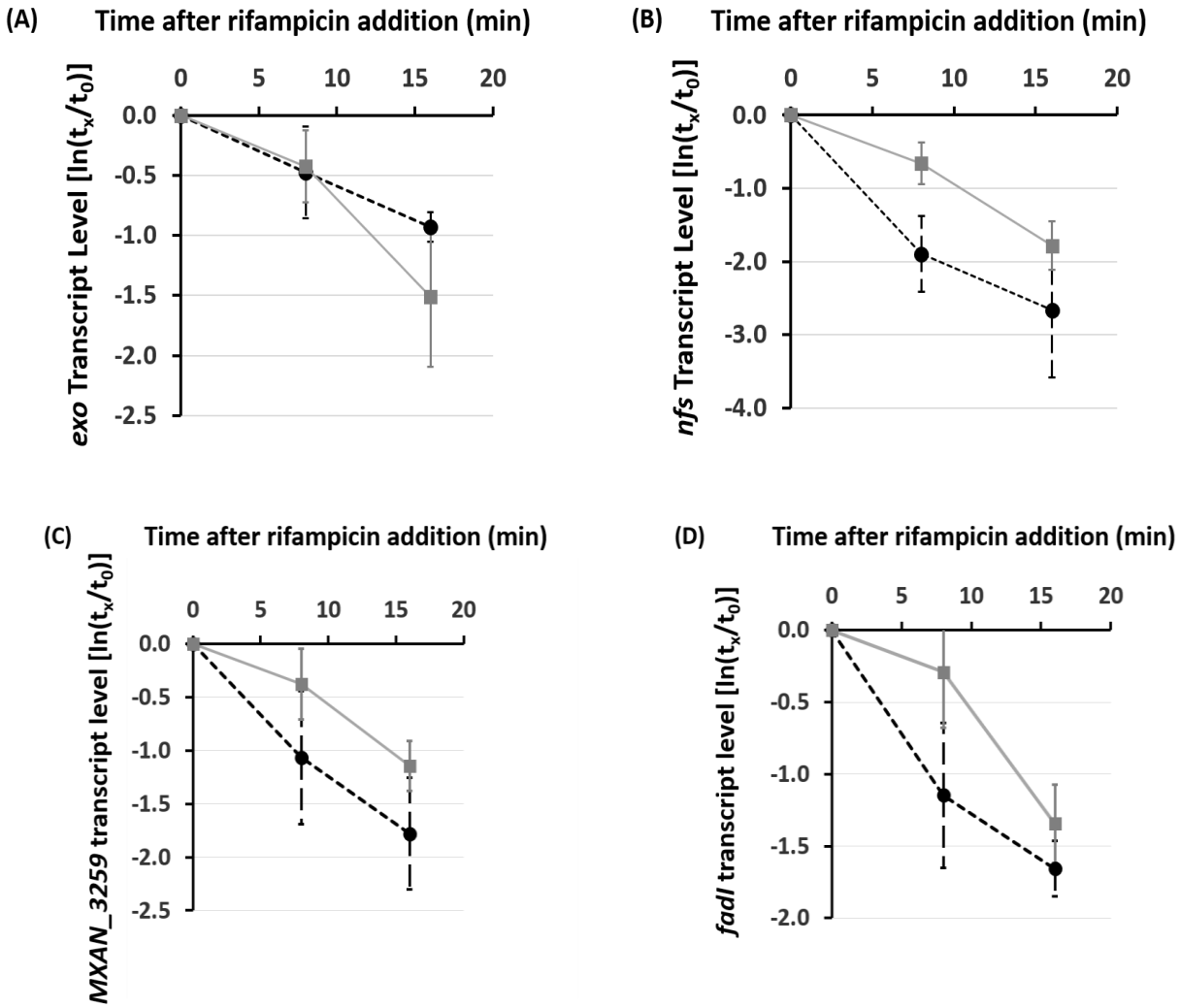


(E)

| Transcript | Half-life in the wild-type strain (min) | Half-life in the *csgA* mutant (min) | *p* value comparing the wild-type strain to the *csgA* mutant |
|---|---|---|---|
| *exo* | $12 \pm 2$ | $8 \pm 3$ | $p = 0.13$ |
| *nfs* | $5 \pm 2$ | $7 \pm 1$ | $p = 0.26$ |
| *MXAN_3259* | $7 \pm 3$ | $10 \pm 2$ | $p = 0.20$ |
| *fadI* | $7 \pm 1$ | $9 \pm 2$ | $p = 0.26$ |

**Figure 3.4 Transcript stability in wild type and *csgA* mutant.**

**Figure 3.4 (cont'd)**

Wild-type DK1622 and a *csgA* mutant were subjected to starvation under submerged culture conditions for 30 h. The overlay was replaced with fresh starvation buffer containing rifampicin (50 mg/ml) and samples were collected immediately ($t_0$) and at the times indicated ($t_x$) for measurement of the *exo* (A), *nfs* (B), *MXAN_3259* (C) and *fadI* (D) transcript level by RT-qPCR. Transcript levels at $t_x$ were normalized to that at $t_0$ for each of three biological replicates and used to determine the transcript half-life for each replicate. The graph shows the average $\ln(t_x/ t_0)$ and one standard deviation for the three biological replicates of wild type (black dashed line) and the *csgA* mutant (gray dashed line). The average half-life and one standard deviation are reported in (E). Natural log of the transcript levels was plotted vs minutes of rifampicin treatment for each biological replicate and the slope of the linear fit of the graph were used to calculate the half-life of the transcripts. No significant difference in transcript stability between the wild type and respective mutants were found by student's two tailed *t*-tests as indicated by the respective *P* values on the table ($P > 0.05$).

Considerable evidence supports a model in which C-signaling activates FruA posttranslationally in order to increase transcription of genes during *M. xanthus* development [11] [1]. We showed previously that the FruA level is about two-fold lower in the *csgA* mutant than in the WT strain at 18-30 h PS [1]. Boosting the FruA level in the *csgA* mutant to the WT level using a vanillate-inducible promoter ($P_{van}$) fused to *fruA* did not increase the transcript levels of five genes or operons (*fmgA*, *fmgBC*, *fmgD*, *fmgE*, *dev*) [1] known to be under combinatorial control of FruA and MrpC [36] [37-39]. Neither did boosting the level FruA D59E (with a phosphomimetic substitution in its receiver domain) using a $P_{van}$-*fruA D59E* fusion, increase the transcript levels [1]. To test whether boosting the level of native FruA or its D59E variant in the *csgA* mutant increases the late gene transcript levels at 18-30 h, we used the same approach. The late gene transcript levels remained low in all cases (Fig. S2), suggesting that neither the two-fold lower level of FruA nor a lack of D59 phosphorylation causes late gene transcript levels to remain low in the *csgA* mutant. Rather, we propose that C-signaling

regulates FruA by a mechanism other than phosphorylation of its receiver domain, allowing increased transcription of the late genes as well as the *fmg* and *dev* genes known to be under combinatorial control of FruA and MrpC.

***The exo, nfs, and MXAN_3259 transcript levels are elevated in a fruA mutant***

To determine whether C-signal-dependent activation of FruA might explain the failure of late gene transcript levels to rise in the *csgA* mutant between 18 and 30 h PS (Fig. 3), we measured transcript levels in a *fruA* null mutant. We expected the late gene transcript levels to remain low, as observed previously for the *dev* transcript level in the *fruA* mutant [1]. Instead, we observed that *exo*, *nfs*, and *MXAN_3259* transcript levels were elevated in the *fruA* mutant relative to the WT strain at 18 h (Fig. 3). The *exo* and *MXAN_3259* transcript levels were also elevated at 21 and 24 h. In contrast, the *fadI* transcript level, like the *dev* transcript level [1], remained low in the *fruA* mutant (Fig. 3D), consistent with a model in which C-signaling activates FruA and activated FruA increases *fadI* and *dev* transcription. Activated FruA may also increase *nfs* transcription at 27 and 30 h, since the *nfs* transcript level is lower in the *fruA* mutant than in the WT strain at those times (Fig. 3B). On average, the *exo* transcript level is lower in the *fruA* mutant than in the WT strain at 30 h, but this difference is due to one biological replicate of the WT strain with a much greater transcript level than the other three replicates (Fig. 3A), so the evidence that activated FruA increases *exo* transcription at 30 h is weak. The *MXAN_3259* transcript level stays elevated in the *fruA* mutant through 30 h (Fig. 3C), providing no evidence that activated FruA is necessary to increase *MXAN_3259* transcription.

Comparison of the *fruA* and *csgA* mutants suggests that FruA which has not been activated by C-signaling negatively regulates late gene transcript levels. The average levels of all four late

gene transcripts were elevated in the *fruA* mutant compared with the *csgA* mutant at 18-30 h (Fig. 3), with the exception of the *fadI* transcript level at 27 and 30 h (Fig. 3B). Since FruA is present but cannot be activated by C-signaling in the *csgA* mutant, unactivated FruA appears to be responsible for the observed negative regulation. As noted above, the FruA level is about two-fold lower in the *csgA* mutant than in the WT strain at 18-30 h [1]. In the WT strain, unactivated FruA may account for the lower *exo* (Fig. 3A) and *MXAN_3259* (Fig. 3C) transcript levels at 18-24 h, and the lower *nfs* transcript level at 18 h (Fig. 3B), than in the *fruA* mutant. The *fadI* transcript level in the WT strain exceeded that in the *fruA* mutant (Fig. 3D), suggesting that positive regulation by activated FruA overcomes negative regulation by unactivated FruA in this case.

Taken together, the effects of mutations in *fruA* and *csgA* on late gene transcript levels suggest that regulation of these genes during the period leading up to and including commitment to spore formation depends at least in part on a C-signal-dependent switch from negative regulation by unactivated FruA to positive regulation by activated FruA.

***The exo, nfs, and MXAN_3259 transcript levels differ in mrpC and fruA mutants***

MrpC appears to directly activate transcription from the *fruA* promoter [40]. In agreement, FruA was undetectable in an *mrpC* null mutant at 18-30 h PS [34]. Hence, the *mrpC* mutant lacks both MrpC and FruA. To compare the effects of losing both transcription factors with the effects of losing only FruA, we measured late gene transcript levels of the *mrpC* mutant in parallel with the *fruA* mutant and the WT strain at 18, 24, and 30 h.

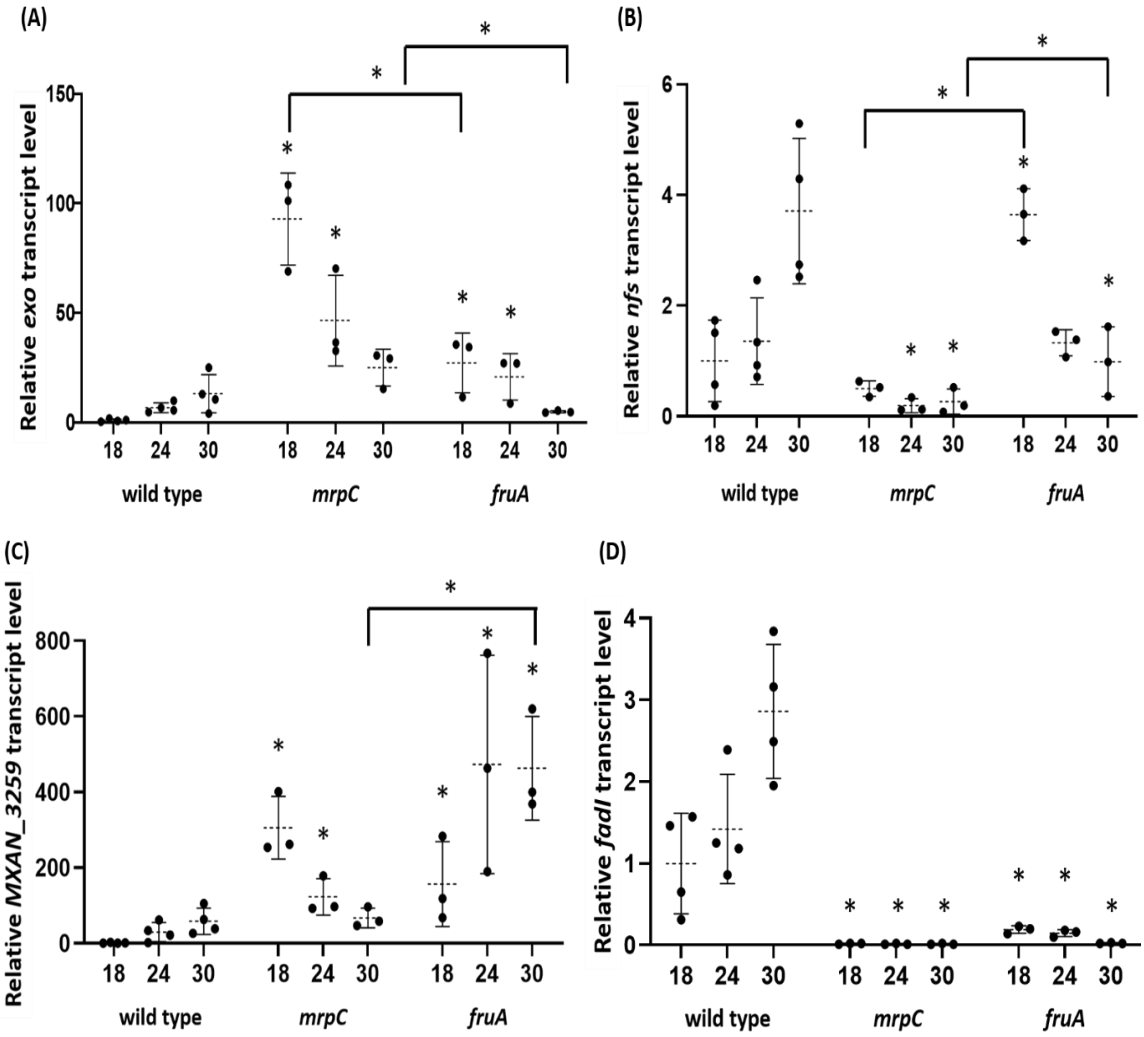


**Figure 3.5 Transcript levels in wild type, *mrpC* mutant and *fruA* mutant during *M. xanthus* development.** Wild-type strain DK1622 and its indicated mutant derivatives were subjected to starvation under submerged culture conditions and samples were collected at the indicated number of hours poststarvation for measurement of (A) *exo*, (B) *nfs*, (C) *MXAN_3259* and (D) *fadI* transcript levels by RT-qPCR. Graphs show the data points and the average of at least three biological replicates, relative to the wild-type strain at 18 h, and error bars indicate one standard deviation. Asterisks indicate a significant difference ($p < 0.05$ in Student's two-tailed t-tests) from the wild-type strain at the corresponding time poststarvation, or a significant difference between the mutants.

Strikingly, for each late gene, the pattern of effects on transcript levels differed (Fig. 5). The *exo* transcript level was on average elevated in the *mrpC* mutant compared with both the WT strain and the *fruA* mutant at all times (Fig. 5A, instances of $p < 0.05$ indicated by asterisks). The *nfs* transcript level remained low in the *mrpC* mutant, unlike either the WT strain or the *fruA* mutant (Fig. 5B). The *MXAN_3259* transcript level was elevated in the *mrpC* mutant relative to the WT strain at 18 and 24 h (Fig. 5C). Relative to the *fruA* mutant, the *MXAN_3259* transcript level was on average elevated in the *mrpC* mutant at 18 h, but lower in the *mrpC* mutant at 24 and 30 h. The *fadI* transcript level remained low in the *mrpC* mutant, unlike the WT strain, but similar to the *fruA* mutant (Fig. 5D). Among the late genes, only the *fadI* transcript level did not differ between the *mrpC* and *fruA* mutants.

To determine whether the absence of MrpC and FruA affects the degradation rates of the late gene transcripts, we added rifampicin to block transcription at 18 h PS and determined the transcript levels at intervals thereafter. We chose 18 h for this analysis since the *exo* (Fig. 5A) and *MXAN_3259* (Fig. 5C) transcript levels were elevated in the *mrpC* mutant relative to the WT strain at that time. The degradation rates did not differ significantly between the *mrpC* mutant and the WT strain (Fig. S3). These results suggest that increased synthesis of the *exo* and *MXAN_3259* transcripts primarily accounts for the elevated transcript levels in the absence of MrpC and FruA.

Our results suggest that MrpC negatively regulates transcription of *exo* and *MXAN_3259* independently of unactivated FruA at 18 h PS, because the average transcript levels were elevated in the *mrpC* mutant compared with the *fruA* mutant at that time (Fig. 5A and 5C). At later times, MrpC appears to continue to negatively regulate *exo* transcription independently of

FruA, but MrpC appears to positively regulate *MXAN_3259* transcription. MrpC also appears to positively regulate transcription of *nfs* and *fadI* (Fig. 5B and 5D).

The DNA-binding domain of FruA has been shown to bind *in vitro* to two sites in the *exo* upstream region, which appears to contain three promoters [41]. Deletion of a site spanning from -89 to -64 bp upstream of the apparent start site of transcription from $P_{D1}$ reduced β-galactosidase activity from a *lacZ* fusion about threefold at 20 h PS, suggesting that FruA binding to the site activates transcription. Binding of MrpC to the *exo* upstream region was not tested. Conversely, binding of FruA to the *nfs* upstream region has not been tested, but ChIP-seq analysis suggested that MrpC is bound at 18 h PS to a site located at -137 bp relative to the predicted *nfsA* translation start codon [42]. Since our results suggest that both FruA and MrpC regulate transcription of both *exo* and *nfs* (Fig. 3 and 5), we tested the binding of purified proteins to upstream DNA fragments using electrophoretic mobility shift assays (EMSAs).

As a control, we performed EMSAs with a *dev* upstream DNA fragment (Fig. S9). As expected, the fragment was bound separately by $His_6$-MrpC (lane 1) and FruA-$His_6$ (lane 3), and cooperatively by the two proteins, producing a complex that migrated more slowly and was more abundant (lane 6) [37]. The FruA DNA-binding domain (FruA-DBD-$His_8$) bound separately (lane 2), but there was little or no indication of cooperative binding with MrpC (lane 5), suggesting that the FruA N-terminal region is important for cooperative binding with MrpC to the *dev* promoter region**,** as observed previously for the *fmgA* promoter region [36]. The *exo* upstream DNA fragment was bound by FruA-DBD-$His_8$ (lane 8), as expected [41], and by FruA-$His_6$ (lane 9), but there was no detectable binding by $His_6$-MrpC separately (lane 7) or cooperatively (lanes 11 and 12). The *nfs* upstream DNA fragment was bound separately by $His_6$-

MrpC very weakly (lane 13), in qualitative agreement with a suggestion based on ChIP-seq analysis [42]. The fragment was also bound separately by FruA-DBD-$His_8$ (lane 14) and FruA-$His_6$ (lane 15), but there was no indication of cooperative binding with MrpC (lanes 17 and 18).

Altogether, the EMSA results suggest that FruA may directly regulate transcription of *exo*, but regulation of *exo* by MrpC is likely indirect, whereas both proteins may directly regulate *nfs* transcription, with MrpC acting positively and FruA acting negatively (see Discussion).

***FruA can positively regulate exo and MXAN_3259 transcript levels in the absence of MrpC***

To examine the effects of FruA on late gene transcript levels in the absence of MrpC, we used the $P_{van}$-*fruA* fusion mentioned earlier to produce FruA in the *mrpC* mutant. The inducer (vanillate) was added during growth and at 0 h PS. By 6 h, the FruA level was about three-fold greater than in the WT strain, but FruA reached that level at 12 and 18 h in the WT strain, while the level did not change in the *mrpC* mutant containing the $P_{van}$-*fruA* fusion (Fig. S4A). To our surprise, the *exo* transcript level was greatly elevated in the *mrpC* $P_{van}$-*fruA* strain relative to the WT strain at 6-18 h (Fig. 6A). The result was unexpected since unactivated FruA appeared to negatively regulate the *exo* transcript level based on comparison of the *fruA* and *csgA* mutants at 18-30 h (Fig. 3A). However, MrpC appeared to negatively regulate *exo* transcription independently of unactivated FruA at 18 h (Fig. 5A and S3A), so relief of negative regulation by MrpC likely explains in part the elevated *exo* transcript level in the *mrpC* $P_{van}$-*fruA* strain. In addition, positive regulation by FruA activated in response to C-signaling may also explain in part the elevated *exo* transcript level in the *mrpC* $P_{van}$-*fruA* strain, since the level was elevated relative to the *mrpC* mutant at 6 h and on average at 12 and 18 h (Fig. 6A) (see Discussion). The *MXAN_3259* transcript level was also elevated in the *mrpC* $P_{van}$-*fruA* strain relative to the WT

strain at 6-18 h and relative to the *mrpC* mutant on average at 6 and 12 h (Fig. 6C), so similar explanations may apply (see Discussion).

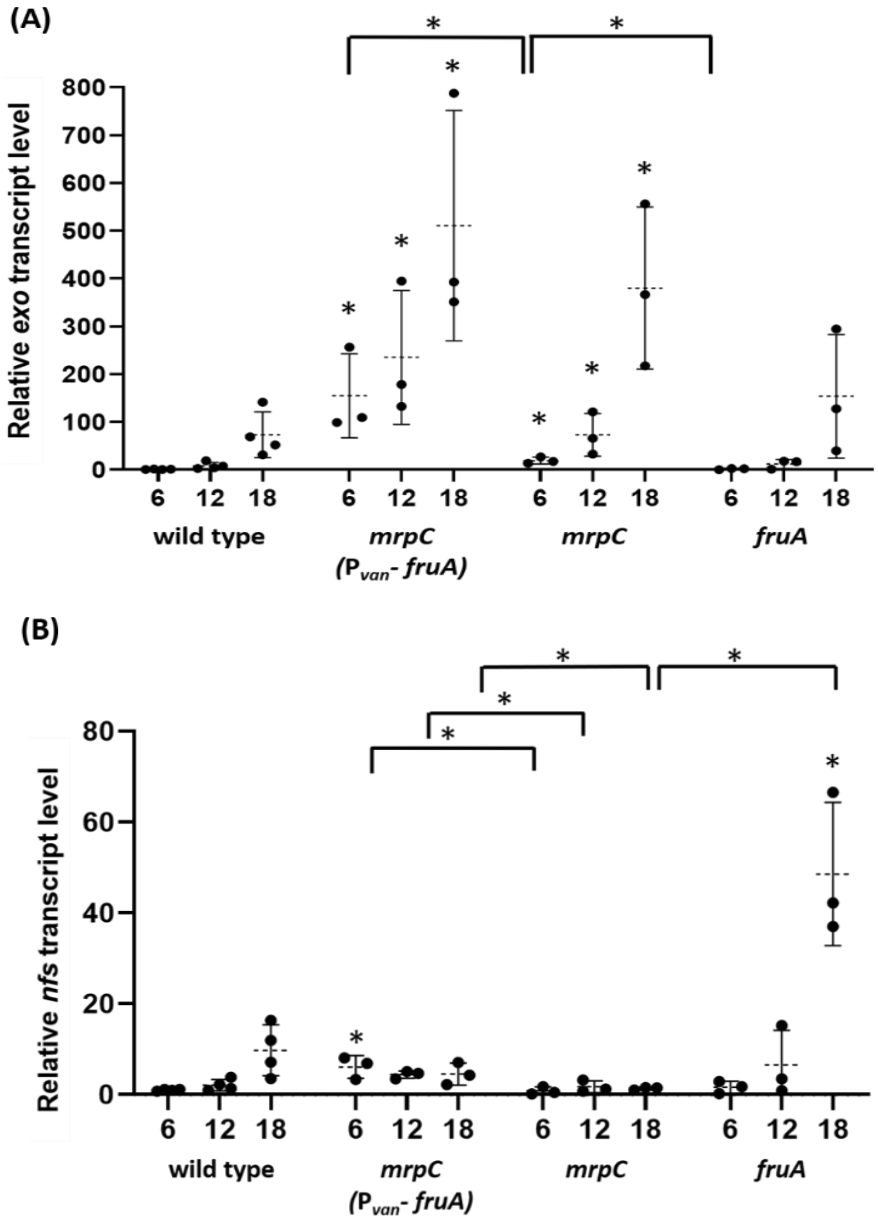


**Figure 3.6 Transcript levels in wild type, *mrpC* ($P_{van}$-*fruA*) mutant, *mrpC* mutant and *fruA* mutant during early time points.**

**Figure 3.6 (cont'd)**

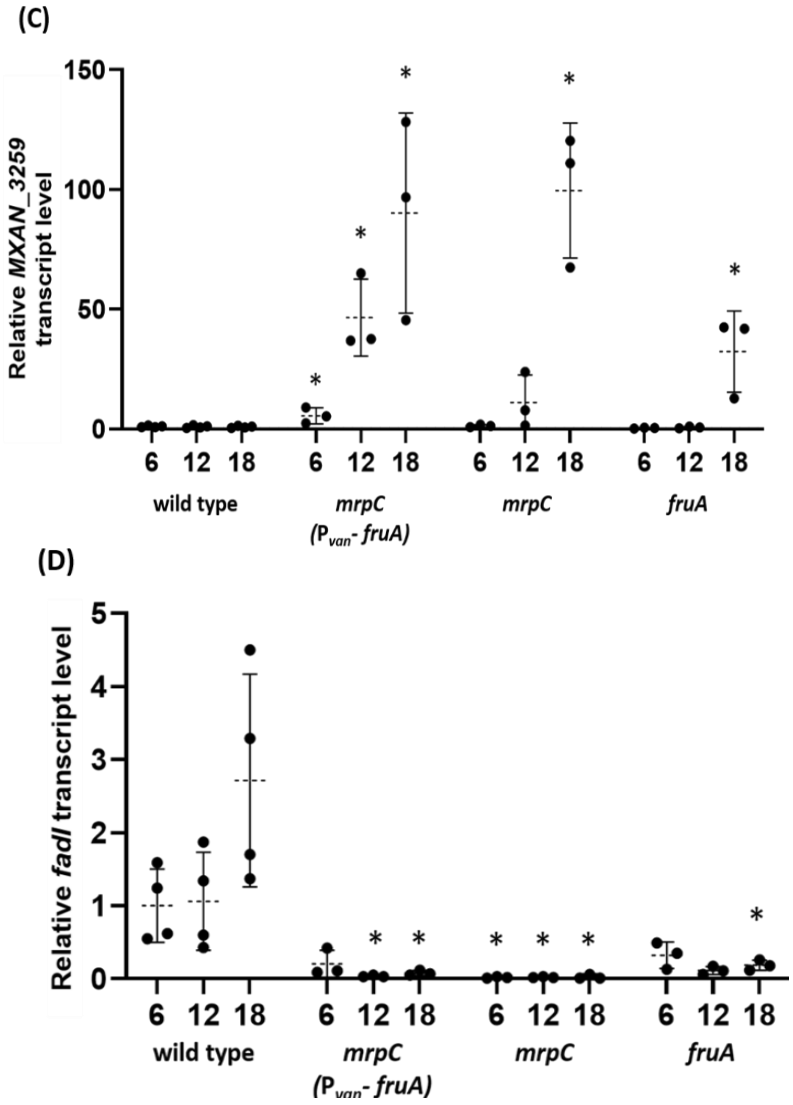


Wild-type strain DK1622 and its indicated mutant derivatives were subjected to starvation under submerged culture conditions and samples were collected at the indicated number of hours poststarvation for measurement of (A) *exo*, (B) *nfs,* (C) *MXAN_3259* and (D) *fadI* transcript levels by RT-qPCR. Graphs show the data points and the average of at least three biological replicates, relative to the wild-type strain at 6 h, and error bars indicate one standard. Asterisks indicate a significant difference ($p < 0.05$ in Student's two-tailed t-tests) from wild type at the corresponding time poststarvation, or a significant difference between the mutants.

The *nfs* (Fig. 6B) and *fadI* (Fig. 6D) transcript levels were not elevated in the *mrpC* $P_{van}$-*fruA* strain compared to the WT strain at 18 h PS, suggesting that FruA was unable to overcome the apparent need for MrpC to positively regulate transcription of these genes (Fig. 5B, 5D, S3B, and S3D). The *nfs* transcript level was slightly elevated in the *mrpC* $P_{van}$-*fruA* strain relative to the WT strain at 6 h and relative to the *mrpC* mutant at 6-18 h (Fig. 6B), perhaps due to positive regulation by FruA activated in response to C-signaling.

***Late gene transcript levels are low in the absence of Nla6***

The Nla6 transcription factor appears to be a direct regulator of *exo* and *MXAN_3259*. The Nla6 DNA-binding domain binds to the *exo* and *MXAN_3259* promoter regions *in vitro*, and the transcript levels suggest positive regulation by Nla6 during the first 8 h PS, and negative regulation by Nla6 at 24 h [25]. Since our results showed that FruA and MrpC impact late gene transcript levels at 18 h (Fig. 3 and 5) and in some cases earlier during development (Fig. 6), we examined the effects of null mutations in *nla6* on the FruA and MrpC protein levels and late gene transcript levels at 6, 12, and 18 h. We constructed a new *nla6* mutant and compared it with one described previously [43]. The new mutant is tetracycline-resistant ($Tc^r$) and the one described previously is kanamycin-resistant ($Km^r$). Both mutants formed immature mounds by 12 h, but failed to progress to more mature mounds with distinct, round edges by 18 h (Fig. S5). Later during development, the $Km^r$ *nla6* mutant mounds matured somewhat at 24-30 h, but failed to darken by 36-48 h (Fig. S6). The $Tc^r$ *nla6* mutant mounds did not mature until 36 h and also failed to darken by 48 h.

The two *nla6* mutants were indistinguishable in terms of the molecular markers we tested. The FruA and MrpC protein levels were similar to the WT strain at 6-18 h PS (Fig. S4). The late

gene transcript levels remained low in both *nla6* mutants (Fig. S7). These results suggest that Nla6 positively regulates the *exo*, *nfs*, and *fadI* transcript levels by 18 h in the WT strain (note that the *MXAN_3259* transcript level had not increased by 18 h). Because the *exo*, *nfs*, and *MXAN_3259* transcript levels were elevated in the *mrpC* and/or *fruA* mutants at 18 h (Fig. 3 and 5) and in some cases earlier during development (Fig. 6), we tried to construct *mrpC nla6* and *fruA nla6* double mutants, but our efforts were unsuccessful (see Discussion). Therefore, we were unable to determine whether positive regulation by Nla6 could account for the elevated *exo* and *MXAN_3259* transcript levels observed in both the *mrpC* and *fruA* mutants, and the elevated *nfs* transcript level in the *fruA* mutant (Fig. 3, 5, and 6).

***Late gene transcript levels are low in the absence of DevS***

Using reporter fusions, transcription of *exo* [30] and *nfs* [44] appeared to be very low in a *devRS* mutant compared with a WT strain during development. The *exo* transcript level was also very low in a *devS* null mutant compared with WT strain DK1622 at 30 h PS [20]. Here, we report late gene transcript levels at 18-30 h in *devI* and *devS* null mutants. We chose these mutants because sporulation occurs about 6 h earlier than normal in the *devI* mutant [20] and sporulation is severely impaired in the *devS* mutant [18]. DevI appears to delay sporulation of the WT strain, and overproduction of DevI in the absence of DevS (or DevR or DevT), due to loss of negative autoregulation of *dev* transcription, appears to strongly inhibit sporulation [19] [20].

We found that late gene transcript levels remain low in the *devS* mutant at 18-30 h PS (Fig. S8). These results suggest that in the absence of DevS, overproduction of DevI inhibits expression of several late genes that are important for sporulation (Fig. S8). We acknowledge that comparing transcript levels in the *devS* mutant with the WT strain at each time point rarely

yielded $p < 0.05$ in a Student's two-tailed *t*-test (indicated by an asterisk in Fig. S8), but this is due to the large variation between biological replicates in the WT strain. We emphasize that transcript levels were low in all biological replicates of the *devS* mutant at all times.

On average, late gene transcript levels were elevated in the *devI* mutant compared with the WT strain at most times from 18-30 h PS (Fig. S8), consistent with the notion that in the absence of DevI, late genes important for sporulation may be expressed earlier than normal. However, our evidence is weak on this point owing to large variation between biological replicates of both the *devI* mutant and the WT strain, yielding $p > 0.05$ in Student's two-tailed *t*-tests at most time points.

**Discussion**

Our systematic cellular and molecular analysis of the function and regulation of late genes during *M. xanthus* development provides several new insights. First, we found that mutations in late genes do not prevent the initial cellular shape change associated with sporulation, but mutations in *exoC* and *MXAN_3259* prevent formation of sonication-resistant spores and mature spores, while a mutation in *nfsA-H* reduces sonication-resistant spore formation about twofold and reduces mature spore formation about tenfold. Second, our analysis of late gene transcript levels in a *csgA* mutant and a derivative engineered to produce a phosphomimetic form of FruA is consistent with a model in which posttranslational regulation of FruA by C-signaling allows increased transcription of the late genes and may involve a mechanism other than phosphorylation of the FruA receiver domain. Third, we discovered that FruA which has not yet been activated by C-signaling negatively regulates the transcript levels of three late genes (*exo, nfs*, *MXAN_3259*) during the period leading up to spore formation. Fourth, our

results suggest that MrpC also negatively regulates transcription of *exo* and *MXAN_3259* prior to sporulation, independently of unactivated FruA, but the effects of MrpC differ for the two genes later during development, and MrpC appears to positively regulate *nfs* and *fadI* transcription both leading up to and including the period of spore formation. Fifth, purified FruA bound *in vitro* to *exo* and *nfs* upstream DNA fragments, consistent with direct regulation, whereas binding of MrpC was very weak or undetectable, suggesting indirect regulation. Sixth, although production of FruA normally requires MrpC, ectopic production of FruA in an *mrpC* mutant prematurely elevated the *exo* and *MXAN_3259* transcript levels, but the levels of *nfs* and *fadI* transcripts remained low, further supporting differential regulation of late gene transcription by FruA and MrpC. Seventh, our results also implicate Nla6 as a positive regulator and DevI as a negative regulator of late gene transcript levels. We incorporate these new insights into a model of the regulatory network governing mound and spore formation (Fig. 7). We propose that multiple regulators act in concert to differentially control late genes and thus ensure proper formation of mature spores.

***New insights into late gene function***

Our results show that mutations in *exoC*, *nfsA-H*, and *MXAN_3259* do not prevent the initial cellular shape change associated with sporulation (Fig. S1B) but do impact the formation of sonication-resistant spores beginning at 27 h PS (Fig. 2). Previously, mutants were examined for starvation-induced spore formation at 120 h [23, 25]. Our findings indicate a much earlier role of Exo, Nfs, and MXAN_3259 proteins during starvation-induced sporulation than established previously. Glutaraldehyde fixation of cells followed by brief sonication allowed us to visualize and enumerate cells that were not rod-shaped in samples of the *exoC* and *MXAN_3259*

mutants. These cells appear to be changing shape from rods to spores (Fig. S1B) and likely resemble cells of *exoC* and *nfsA-H* mutants that fail to complete morphogenesis upon chemical induction of sporulation in liquid culture [22]. Under such conditions, neither glutaraldehyde nor sonication are necessary to observe individual cells. In contrast, starvation-induced submerged culture results in mounds of developing cells (Fig. 1) that are difficult to disperse. For the WT strain and the *nfsA-H* and *fadI* mutants, we estimated the number of cells in transition from rods to spores (Fig. S1B) by subtracting the number of sonication-resistant spores in a sample taken at the same time, but not fixed with glutaraldehyde, and sonicated longer (Fig. 2).

The WT strain may exhibit a higher percentage of cells changing shape than the *fadI* mutant (Fig. S1B) because the mutant makes more sonication-resistant spores (Fig. 2). The *fadI* insertion mutant presumably has a reduced rate of fatty acid β-oxidation, as appeared to be the case for a *fadIJ* (*MXAN5372-MXAN5371*) deletion mutant [24], so perhaps altered metabolism enhanced formation of sonication-resistant spores by the *fadI* mutant at 27-48 h (Fig. 2), albeit not mature spores at 72 h (Table S1).

The *nfsA-H* mutant made about two-fold less sonication-resistant spores than the WT strain, and the *exoC* and *MXAN_3259* mutants made less than the detection limit (Fig. 2). For these three mutants, the lower percentage of cells changing shape as compared with the WT strain at 24 and 27 h (Fig. S1B) may reflect reduced ability to initiate and/or maintain the cellular shape change associated with sporulation. Upon chemical induction of sporulation, *exo* and *nfs* mutants appeared to initiate the transition from rods to spores, but then revert into rods [22]. Given the evidence that Exo and Nfs proteins function in spore coat polysaccharide export [21,

22] and deposition [21, 22], respectively, our results suggest that defective spore coat biogenesis of the *exoC* and *nfsA-H* mutants reduces their ability to maintain cellular shape change as early as 24 h (Fig. S1B) and blocks or reduces their ability to form sonication-resistant spores by 27 h (Fig. 2) and mature spores by 72 h (Table S1). The *MXAN_3259* mutant was indistinguishable from the *exoC* mutant in our cellular assays. As noted previously, MXAN_3259 (renamed MXAN_RS15785 in NCBI) is predicted to be a polysaccharide deacetylase [25]. The downstream genes of the predicted *MXAN_3259-MXAN_3263* operon are predicted to code for an oligosaccharide flippase (MXAN_RS15790), a serine acetyltransferase (MXAN_RS15795), and glycosyltransferases (MXAN_RS15800 and MXAN_RS15805). Since all these proteins may function in polysaccharide export and modification, defective spore coat biogenesis of the *MXAN_3259* mutant likely explains its behavior in our cellular assays.

***MrpC and unactivated FruA negatively regulate certain late genes***

Our systematic analysis of late gene transcript levels revealed differential regulation by MrpC and by FruA in response to activation by C-signaling (Fig. 7). The *fadI* transcript levels in *csgA*, *fruA*, and *mrpC* mutants (Fig. 3 and 5) were consistent with a model in which C-signaling activates FruA posttranslationally in order to increase transcription cooperatively with MrpC. This model is based on analysis of *dev* [1, 11, 37] and *fmg* [1, 36, 38, 39, 45] genes. An early study of β-galactosidase activity from *lacZ* fusions indicated positive regulation of many genes after about 6 h PS by C-signaling [46]. Subsequent analysis of *dev* [11, 47] and *fmg* [38, 39, 48, 49] fusions in *fruA* mutants, and similarity of FruA to response regulators [50], suggested that phosphorylation of FruA in response to C-signaling might increase transcription during development. However, several observations suggest that FruA may not be phosphorylated

[36], but is activated by C-signaling *via* a different posttranslational mechanism [1]. Although the mechanism of FruA activation remains a mystery, our results suggest that *fadIJ* transcription may be increased by cooperative binding of MrpC and activated FruA, like transcription of *dev* and *fmg* genes appears to be. This model is also in agreement with measurements of fluorescence intensity from a *fadI-tdTomato* fusion in a WT strain and *csgA*, *fruA*, and *mrpC* mutants during development [24]. On the other hand, ChIP-seq analysis did not detect MrpC binding upstream of *fadI* [42], so positive regulation of *fadIJ* transcription by MrpC could be indirect, perhaps relying on activated FruA.

Differential regulation by MrpC and by FruA in response to C-signaling, of the late genes implicated in spore coat biogenesis (*exoA-I*, *nfsA-H*, *MXAN_3259-MXAN_3263*) (Fig. 7), is more complex than described above for *fadIJ*, whose products appeared to have little impact on sporulation in our assays. Strikingly, comparison of transcript levels in the WT strain with those in the *csgA*, *fruA*, and *mrpC* mutants (Fig. 3, 5, and 6) and comparison of transcript degradation rates (Fig. 4 and S3) suggests that FruA which has not been activated by C-signaling negatively regulates *exo, nfs*, and *MXAN_3259* transcription at 18 h PS and that MrpC negatively regulates *exo* and *MXAN_3259* transcription independently of unactivated FruA at 18 h. Negative regulation of *nfs* by FruA was observed previously by comparing fluorescence intensity from a $P_{nfsA}$-*mCherry* fusion in a WT strain versus a *fruA* mutant during development [23].

Negative regulation by unactivated FruA appears to reduce transcription of late genes important for spore coat biogenesis before their products are needed (Fig. 7). Under our conditions of submerged culture development, the WT strain forms compact mounds by 18 h [35] (Fig. 1), but cells are not yet changing shape (Fig. S1B). Transcript levels from *exo, nfs*, and

*MXAN_3259* rise by 24 h (Fig. 3 and 5), coincident with the beginning of detectable cellular shape change (Fig. S1B). Relative to the transcript level at 6 h, the *exo* and *nfs* levels, but not the *MXAN_3259* level, rose at 18 h (Fig. 6 and Table S2), so temporal regulation of these genes differs slightly. Using a fluorescent membrane stain and confocal laser scanning microscopy, some cells in mounds of the WT strain begin to change shape by 21 h, but not by 18 h (Y Hoang and Lee Kroos, unpublished data). We did not detect cells changing shape at 21 h (Fig. S1B). In any case, *exo* and *nfs* transcript levels rose by 18 h, and the *MXAN_3259* level rose later, between 18 and 30 h (Fig. 3 and 5, and Table S2), close to the time cellular shape change begins.

Negative regulation by MrpC independently of unactivated FruA appears to further differentiate transcription of late genes that play a role in spore coat biogenesis (Fig. 7). Negative regulation by MrpC was strongest for *exo*. The *exo* transcript level was on average elevated in the *mrpC* mutant compared with the *fruA* mutant at all times and the differences yielded $p < 0.05$ in a test of statistical significance at 6, 18, and 30 h (Fig. 5A and 6A). This comparison suggests that MrpC negatively regulates the *exo* transcript level during the entire period leading up to and including the time that many cells commit to spore formation [35]. Negative regulation by MrpC independently of unactivated FruA was weaker for *MXAN_3259* than for *exo*. The *MXAN_3259* transcript level was on average elevated in the *mrpC* mutant relative to the *fruA* mutant only at 12 and 18 h (Fig. 5C and 6C). Although the differences did not yielded $p < 0.05$ in a test of statistical significance, the average was elevated about threefold in the *mrpC* mutant relative to the *fruA* mutant at 18 h in both experiments. Interestingly, MrpC appeared to regulate *MXAN_3259* transcription positively at 24 and 30 h

(Fig. 5C), in clear contrast to the persistent negative regulation of *exo* transcription by MrpC (Fig. 5A and 7). MrpC did not appear to regulate *nfs* transcription negatively at any time tested, but rather MrpC appeared to regulate *nfs* transcription positively at 18-30 h (Fig. 5B, 6B, and 7).

***Potential mechanisms of differential regulation of spore coat biogenesis genes by MrpC, FruA***

The negative regulation of *exo* and *MXAN_3259* transcript levels by MrpC, and the independent negative regulation of these transcript levels and the *nfs* transcript level by unactivated FruA (Fig. 7), raised the question whether increased transcript levels in the WT strain could be explained solely by relief from negative regulation. In the case of *nfs*, this scenario would not explain the low transcript level in the *mrpC* mutant (which lacks MrpC and FruA) compared with the WT strain at 24 and 30 h (Fig. 5B). Nor would the scenario explain the low *nfs* transcript level in the *fruA* mutant relative to the WT strain at 27 and 30 h (Fig. 3B and 5B). Rather, both MrpC and activated FruA appear to positively regulate *nfs* transcription (Fig. 7). The effect of MrpC could be indirect since binding *in vitro* of purified MrpC was very weak and there was no indication of cooperative binding with FruA (Fig. S9). On the other hand, ChIP-seq analysis suggested that MrpC binds to the *nfs* upstream region *in vivo* [42], so a direct effect of MrpC is possible. A direct effect of FruA is supported by binding to an *nfs* upstream DNA fragment *in vitro* (Fig. S9). Positive regulation by activated FruA in the absence of MrpC *in vivo* is supported by the slightly elevated *nfs* transcript level in the *mrpC* $P_{van}$-*fruA* strain relative to the WT strain at 6 h and relative to the *mrpC* mutant at 6-18 h (Fig. 6B). The *mrpC* $P_{van}$-*fruA* strain produces FruA ectopically at a three-fold elevated level relative to the WT strain by 6 h (Fig. S4A). Relative to the *mrpC* mutant, the *mrpC* $P_{van}$-*fruA* strain forms nascent mounds earlier (Fig. S5), suggestive of ongoing C-signaling, although the mounds fail to become compact by 18 h or

later, as they do in the WT strain (Fig. S5 and S6), so short-range C-signaling is likely impaired. As a result, the level of activated FruA in the *mrpC* $P_{van}$-*fruA* strain may only be sufficient to elevate *nfs* transcription slightly (Fig. 6B).

Relief from negative regulation by MrpC and unactivated FruA could explain the increasing *exo* and *MXAN_3259* transcript levels in the WT strain at 24 and 30 h PS, since the levels of these transcripts in the *mrpC* and *fruA* mutants are comparable or elevated relative to the WT strain at 18-30 h (Fig. 3A, 3C, 5A, and 5C). The only exceptions were that on average the *exo* transcript level was lower in the *fruA* mutant than in the WT strain at 30 h, which we initially considered weak evidence that activated FruA increases *exo* transcription (since one biological replicate of the WT strain had a much greater transcript level than the other three replicates) (Fig. 3A), but the evidence was strengthened by a second experiment (Fig. 5A). Moreover, the *exo* transcript level was elevated in the *mrpC* $P_{van}$-*fruA* strain relative to both the WT strain and the *mrpC* mutant at 6-18 h (Fig. 6A), suggesting that activated FruA can greatly increase *exo* transcription in the absence MrpC. We propose that in the WT strain negative regulation by MrpC is partly relieved and negative regulation by unactivated FruA is switched to positive regulation by activated FruA, increasing *exo* transcription at 18-30 h (Fig. 7). The effect of MrpC is likely indirect, since neither binding to an *exo* upstream DNA fragment *in vitro* (Fig. S9) nor binding to the *exo* upstream region *in vivo* [42] was detected. On the other hand, FruA likely exerts its effects directly, since binding was observed *in vitro* [41] (Fig. S9). Presumably, recombinant FruA purified from *E. coli* represents unactivated FruA in *M. xanthus.* How C-signaling activates FruA is unknown. The answer is key to understanding the switch from

negative regulation by unactivated FruA to positive regulation by activated FruA, which our results suggest occurs for both *exo* and *nfs* transcription (Fig. 7).

Although relief from negative regulation by MrpC and unactivated FruA could explain the increasing *MXAN_3259* transcript level in the WT strain at 24 and 30 h PS for the reasons mentioned above, our data suggest that both MrpC and FruA switch from negative to positive regulation of *MXAN_3259* transcription (Fig. 7). The *MXAN_3259* transcript level is elevated in the *fruA* mutant relative to the *mrpC* mutant at 30 h (Fig. 5C), suggesting positive regulation by MrpC. Positive regulation by activated FruA is supported by the elevated *MXAN_3259* transcript level in the *mrpC* $P_{van}$-*fruA* strain relative to both the WT strain at 6-18 h and the *mrpC* mutant on average at 6 and 12 h (Fig. 6C). Therefore, we propose that in the WT strain negative regulation by MrpC and unactivated FruA during mound formation is relieved, and switches to positive regulation by MrpC and activated FruA during spore formation (Fig. 7). The effects of MrpC may be indirect since binding to the *MXAN_3259* upstream region was not observed in ChIP-seq analysis at 18 h [42]. Binding of FruA remains to be tested and the transcriptional start site remains to be identified.

***Roles of Nla6 and Dev proteins in late gene regulation***

Our results implicate Nla6 as a positive regulator of late gene transcript levels during mound formation (Fig. 7). Late gene transcript levels remained very low in *nla6* mutants (Fig. S7). Since the DNA-binding domain of Nla6 binds to the *exo* and *MXAN_3259* promoter regions *in vitro* [25], Nla6 may directly activate transcription of these genes. One of the two Nla6 binding sites in the *exo* promoter region partially overlaps with the FruA-binding site [41], so negative regulation by unactivated FruA could involve competition for binding with Nla6. Later, during

spore formation, positive regulation by activated FruA could depend on a diminished Nla6 level. This potential mechanism would explain the elevated *exo* transcript level observed in an *nla6* mutant compared with the WT strain at 24 h PS [25], since Nla6 would be absent from the *nla6* mutant but perhaps only diminished in the WT strain. The *nfs* and *fadI* upstream regions were not identified as potential targets of Nla6 binding using bioinformatics [25], so perhaps positive regulation by Nla6 is indirect for *nfsA-H* and *fadIJ.* Since we discovered that MrpC and unactivated FruA negatively regulate certain late genes during mound formation (Fig. 3, 5, 6, and 7), we predicted that transcript levels of those late genes would remain low in *mrpC nla6* and *fruA nla6* double mutants. However, we were unable to construct the double mutants in order to test our prediction. Unexpectedly, a null mutation in *nla6* appeared to create a synthetic lethal phenotype in combination with a null mutation in *mrpC* or *fruA*, suggesting that Nla6 functions redundantly with MrpC and FruA to express genes required for growth. This outcome was unexpected since none of the three transcription factors have been reported to function during growth, although MrpC has been shown to be present [15].

Our results implicate DevI as a negative regulator of late gene transcript levels during spore formation (Fig. 7). In the absence of DevI, sporulation occurs about 6 h earlier [20] and late gene transcript levels are slightly elevated relative to the WT strain at most times from 18-30 h PS (Fig. S8). In the absence of DevS (or DevR or DevT), DevI is overproduced and strongly inhibits sporulation [19, 20] and late gene transcription [20, 23, 30] (Fig. S8). Given the similarities mentioned above between *fadI* and *fmg* genes with respect to positive regulation by MrpC and activated FruA, and given that the *fadI* transcript level was slightly elevated in the *devI* mutant and low in the *devS* mutant compared with the WT strain (Fig. S8), it would be

interesting to determine whether mutations in *devI* and *devS* have similar effects on *fmg* transcript levels as on *fadI* and the other late genes. Perhaps DevI overproduction broadly inhibits transcription of genes positively regulated by MrpC and activated FruA, and among those genes are one or more required for cellular shape change, since DevI overproduction greatly delays and reduces the shape change associated with sporulation [19, 20].

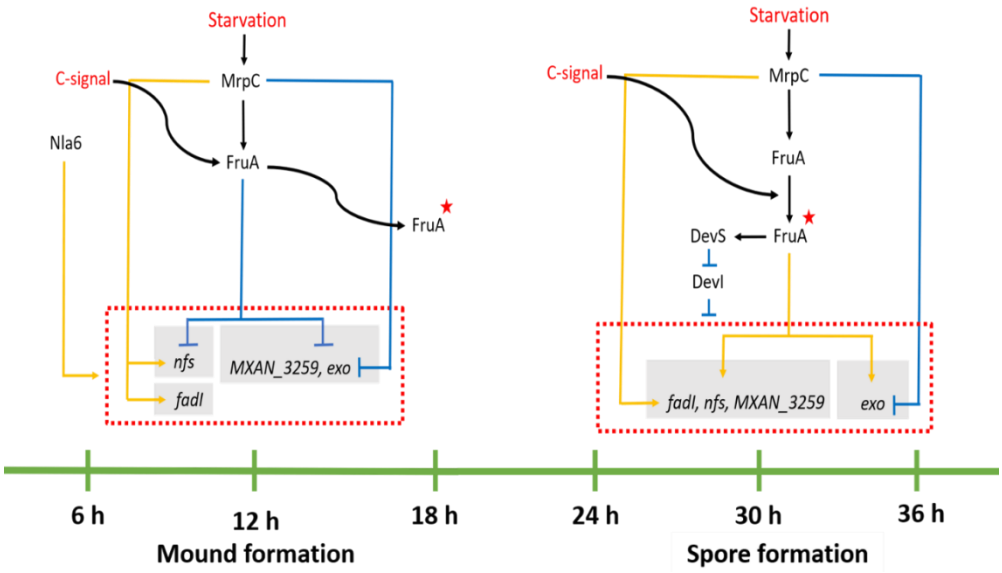


**Figure 3.7 Model of differential late gene regulation.** Starvation increases the MrpC level which in turn increases the FruA level. C-signal activates FruA to FruA*. Positive regulation (yellow arrows) and negative regulation (blue line with blunt) of late genes (gray boxes) is indicated. During mound formation between 6 and 18 h poststarvation, Nla6 positively regulates transcription of all four late genes (dashed box), but unactivated FruA and MrpC negatively regulate certain late genes as indicated. During spore formation between 24 and 36 h, activated FruA* induces transcription of the dev operon gene. DevS (and DevT and DevR, which are not shown) negatively autoregulates transcription of *devI*. *DevI* negatively regulates all four late genes (dashed box), but FruA* positively regulates their transcription, while MrpC positively or negatively regulates certain late genes as indicated.

***Differential regulation of late genes***

Nla6 and Dev proteins regulated all four late genes similarly, whereas MrpC and FruA mediated differential regulation (Fig. 7). C-signaling appears to switch FruA from negative regulation of certain late genes during mound formation to positive regulation of all the late genes during sporulation. FruA and MrpC did not bind cooperatively to *exo* or *nfs* upstream DNA fragments, as observed for *dev* (Fig. S9) [37] and *fmg* [36, 38, 39, 45] genes. Systematic experimental and computational analyses of *dev* transcript levels support a model in which C-signaling activates FruA at least ninefold by 18 h PS [1], and different arrangements and affinities of cooperative binding sites for activated FruA and MrpC have been proposed to explain differential dependence on C-signaling and timing of transcription of *dev* and individual *fmg* genes [1, 36-39, 45]. Cooperative binding of activated FruA and MrpC may likewise explain the C-signal-dependence (Fig. 3) and timing of *fadI* transcription (Table S2).

The late genes implicated in spore coat biogenesis appear to be regulated uniquely. Most of the evidence so far points to indirect regulation by MrpC (Fig. S9), which can be positive (*nfs*), negative (*exo*), or switching from negative to positive during mound formation and sporulation, respectively (*MXAN_3259*) (Fig. 5, 6, and 7). Regulation by FruA appears to be direct (*nfs*, *exo*) (Fig. S9), although binding remains to be tested in the *MXAN_3259* upstream region. Unactivated FruA acts negatively during mound formation and activated FruA acts positively during sporulation (Fig. 3, 5, 6, and 7). Different arrangements and affinities of binding sites for the two forms of FruA, and for Nla6 acting positively during mound formation (Fig. S7 and 7) and negatively during spore formation [25] (not shown in Fig. 7 since we only measured late

gene transcript levels at 6-18 h), may account for differential transcription of the late genes implicated in spore coat biogenesis (Table S2).

In summary, multiple signals and transcription factors appear to act in concert to differentially control late genes. This strategy presumably prevents starving cells from wasting resources during mound formation and finely-tunes expression of genes involved in metabolism, spore coat biogenesis, and other functions during spore formation. Multiple transcription factors likewise positively and negatively fine-tune the expression of hundreds of genes during *Bacillus subtilis* endospore formation [51] [52] [53], ensuring that the resulting spores are endowed with resistance and surface properties tailored for their environment [54-56]. MrpC and/or FruA likely regulate hundreds of genes during *M. xanthus* development, including genes involved in protein phosphorylation and fate, transcription, signal production, and motility, as well as other proteins important for spore formation inch addition to those studied here [42]. Identifying the key genes for mound formation and the cellular shape change associated with sporulation, and elucidating the molecular mechanisms of regulation by MrpC and FruA for those genes, including the mechanism by which C-signaling activates FruA, are important goals for the future.

## Materials and methods

### *Bacterial strains, plasmids and primers*

The strains, plasmids and primers used in this study are listed in Table S3. *E. coli* strain DH5α was used for cloning. *M. xanthus* strains with ectopically integrated $P_{van}$-*fruA* and $P_{van}$-*fruA D59E* were constructed by electroporation [57] followed by selection of transformants on CTT agar with 15 μg/mL tetracycline [58]. To construct pSS11, primer pair Nla6 Fwd and Nla6 Rev

was used to generate a PCR product using chromosomal DNA from *M. xanthus* strain DK1622 as a template. The product was combined with DNA amplified from pMR3487 using PMR3487G Fwd and PMR3487G Rev primers, and a Gibson assembly reaction was used to enzymatically join the overlapping DNA fragments [59]. The cloned DNA sequence was verified using primers 3487 seq Fwd1, 3487 seq Fwd2, 3487 seq Fwd3, 3487 seq Fwd4, and 3487 seq Fwd5. *M. xanthus* strain MSS10 was created by electroporating pSS11 into strain DK1622. The transformants were selected on CTT agar with tetracycline (15 μg/mL) followed by verification by colony PCR using PMR3487 Rev, Nla6 Fwd4, and Nla6 Fwd5 primers. To create pSS13 and pSS14, 315 bp and 373 bp DNA fragments were amplified from *M. xanthus* strain DK1622 genomic DNA using primer pairs Exo -267G and Exo +108G, and Nfs -290G and Nfs +83G, respectively. The products were combined with DNA amplified from pMR3487 using PMR3487G Fwd and PMR3487G Rev primers, and joined using a Gibson assembly reaction [59]. The cloned DNA sequences were verified using the same primers as for pSS11.

***Growth and development***

*E. coli* strains containing plasmids were grown at 37°C in Luria Burtani broth supplemented with 15 μg/mL of tetracycline or 50 μg/mL of kanamycin sulfate as needed. Strains of *M. xanthus* were grown at 32°C in CTTYE liquid medium (1% Casitone, 0.2% yeast extract, 10 mM Tris-HCl [pH 8.0], 1 mM $KH_2PO_4$-$K_2HPO_4$, 8 mM $MgSO_4$ [final pH 7.6]) with shaking at 350 rpm. CTT agar (CTTYE without yeast extract and solidified with 1.5% agar) was used for growth on solid medium and was supplemented with 40 μg/mL of kanamycin sulfate or 15 μg/mL of tetracycline as required. Fruiting body development under submerged culture conditions was performed using MC7 (10 mM morpholinepropanesulfonic acid [MOPS; pH 7.0], 1 mM $CaCl_2$) as

the starvation buffer as described previously [5]. Briefly, at mid-exponential growth, cells were collected by centrifugation CTTYE medium was removed. The cell pellet was resuspended in MC7 buffer at a density of approximately 1,000 Klett units and fruiting body development was initiated in submerged culture. Upon incubation at 32°C, cells adhere to the bottom of the plate and undergo development. A 96-μL sample (designated $T_0$) was removed and was stored at 4°C for at least 24 h with glutaraldehyde (2% final concentration) to fix cells, followed by quantification of cells by counting microscopically as described previously [1]. For each developmental sample, 1.5 mL of the cell suspension plus 10.5 mL of MC7 buffer was added to an 8.5-cm-diameter plastic petri plate. At the indicated times, developing populations were photographed using a Leica Wild M8 microscope equipped with an Olympus E-620 digital camera.

***Sample collection***

At the indicated times PS, the MC7 buffer overlay was replaced with 5 mL of fresh MC7 buffer with or without inhibitors as required. Developing cells were scraped from the bottom of the plates, the entire contents were collected in a 15-mL centrifuge tube, and samples were mixed thoroughly as described previously [1]. For quantification of rods and cells changing shape, 96 μL of the mixture was removed and 4 μL of glutaraldehyde was added from a 50% stock solution to achieve a 2% final concentration in order to fix the developing cells. The sample was stored at 4°C for at least 24 h before counting as described below. For measurement of sonication-resistant spores, 400 μL of the mixture was removed and stored at -20°C. Immediately after collecting the two samples just described, the remaining 4.4 mL of the developing population was mixed with 0.5 mL of RNase stop solution (5% phenol [pH < 7] in

ethanol), followed by rapid cooling in liquid nitrogen until almost frozen, centrifugation at 8,700 × *g* for 10 min at 4°C, removal of the supernatant, freezing of the cell pellet in liquid nitrogen, and storage at -80°C until RNA extraction.

***Quantification of total cells, sonication-resistant spores, and cells changing shape***

During starvation-induced development a small percentage of the rod-shaped cells convert to round spores that become sonication-resistant. The number of sonication-resistant spores in developmental samples was quantified as described previously [5]. Each 400-µL sample was also used for determination of total protein concentration as described earlier [1]. The total number of cells, including rod-shaped cells and round spores, as well as cells that appeared to be in transition between the two, was determined using the glutaraldehyde-fixed samples collected as described above. Each sample was thawed and mixed by vortexing and pipetting, diluted with MC7 buffer, sonicated once for 10 s, and then all cells were counted microscopically as described previously [1], except taking note of the number of cells that were not rod-shaped (i.e. cells changing shape plus round spores). The total cell number minus the number of sonication-resistant spores was designated the number of sonication-sensitive cells (consisting primarily of rod-shaped cells) and was expressed as a percentage of the total cell number in the corresponding $T_0$ sample (consisting only of rod-shaped cells). The number of cells that were not rod-shaped minus the number of sonication-resistant spores was designated the number of cells changing shape and was also expressed as a percentage of the total cell number in the corresponding $T_0$ sample.

***RNA extraction and analysis***

Total RNA was extracted using the hot-phenol method followed by digestion with DNase I (Roche) as described previously [60]. Total RNA (1 μg) was subjected to cDNA synthesis using Superscript III reverse transcriptase (Invitrogen) and random primers (Promega), as instructed by the manufacturers. In parallel, total RNA (1 μg) was subjected to cDNA synthesis reaction conditions without Superscript III reverse transcriptase, as a control. One μl of cDNA at the appropriate dilution (as determined empirically) and 20 pmol of each primer were subjected to qPCR in a 25 μl reaction using 2× reaction buffer as described previously [1]. qPCR was done in quadruplicate for each cDNA using a LightCycler® 480 System (Roche). In parallel, a standard curve was generated for each pair of qPCR primers using the genomic DNA of *M. xanthus* WT strain DK1622 and gene expression was quantified using the relative standard curve method (user bulletin 2; Applied Biosystems). 16S rRNA was used as the internal standard for each sample. Transcript levels for the WT strain at each time except 18 h PS, and for mutants at each time, were normalized to the transcript level observed for one replicate of the WT strain at 18 h in the same experiment, as describe previously [1]. For the WT strain at 18 h, the transcript levels of at least three biological replicates from different experiments were normalized to their average, which was set as 1 [1]. RNA stability after addition of rifampicin (50 μg/mL) to inhibit transcription was also determined as described previously [1].

***Preparation of FruA-DBD-His$_8$, FruA-His$_6$ and His$_6$-MrpC***

*E. coli* strain BL21(DE3) (Novagen) was freshly transformed individually with plasmids pET28a/H$_6$-MrpC [4, 61], pET11a/FruA-DBD-H$_8$ [49] and pET11a/FruA-H$_6$ [13]. For each transformation an isolated kanamycin-resistant colony was used to inoculate 10 mL of Luria-

Bertani broth supplemented with kanamycin followed by overnight incubation at 37°C with shaking. The cultures (5 mL) were used to inoculate 500 mL of the same medium, followed by continued incubation at 37°C with shaking until the cultures reached 60-80 Klett units. IPTG (1 mM final concentration) was added to induce synthesis of the recombinant proteins. After 2 h, cells were harvested as reported previously [49] and stored at -80°C until further purification. Each cell pellet was resuspended in 35 ml of lysis buffer (50 mM Na-phosphate buffer [pH 8.0], 500 mM NaCl, 10 mM β-mercaptoethanol) supplemented with protease inhibitor cocktail (Roche Mini EDTA-free tablets) and sonicated 4 times for 1 min to disrupt the cells with intermittent cooling on ice. After centrifugation at 18,000 × *g* for 10 min at 4°C, the supernatant was mixed with lysis buffer supplemented with 10% w/v Triton X-100 to make the volume upto 50 ml. Lysis buffer supplemented with 20 mM imidazole (pH 8.0) was used to wash 3 times and finally resuspend Ni-NTA beads (Qiagen) followed by addition of 1/100 volume to the supernatant for binding on a rotator for 1 h at 4°C. The unbound fraction was collected by centrifugation at 700 × *g* for 3 min at 4°C. The Ni-NTA beads were washed 4 times with 50 mL of wash buffer A (50 mM Na-phosphate buffer [pH 8.0], 500 mM NaCl, 5 mM β-mercaptoethanol, 20 mM imidazole [pH 8.0], 20% v/v glycerol) . Proteins were eluted from the beads with 10 mL of elution buffer (50 mM Na-phosphate buffer [pH 8.0], 500 mM NaCl, 2 mM β-mercaptoethanol, 250 mM imidazole [pH 8.0], 20% v/v glycerol) supplemented with protease inhibitor cocktail (Roche Mini EDTA-free tablets) on a rotator for 30 min at 4°C. Eluates were dialyzed overnight at 4°C against a buffer containing 10 mM Tris-HCL [pH 8.0], 100 mM NaCl, 1 mM β-mercaptoethanol and 10% w/v glycerol. The concentration of each protein preparation was determined using the Bradford method [62].

***EMSA***

$^{32}$P-labelled DNA fragments were generated from the *dev*, *exo* and *nfs* promoter regions using primers labelled with [γ-$^{32}$P]ATP using T4 polynucleotide kinase as mentioned previously [17]. A DNA fragment from the *dev* promoter region from bp -19 to -114 was generated by PCR using primers LK1298 and LK1331 and plasmid pPV391 as template [17]. Plasmids pSS13 and pSS14 were used as templates to generate DNA fragments spanning the *exo* and *nfs* promoter regions, respectively, from bp +1 to -120 and from bp +1 to -201 by using primer pairs Exo +1 Rev and Exo -120 Fwd, and Nfs +1 Rev and Nfs-201 Fwd. The labeled DNA fragments were purified by electrophoresis on 15% polyacrylamide gels followed by visualization using autoradiography, excision and overnight elution by soaking in TE buffer as described previously [49].

Binding reactions (10 μL) were performed as reported previously [49], except the reaction mixtures were incubated for 10 min at room temperature prior to loading on 8% polyacrylamide gels. Gels were dried and exposed to X-ray film for autoradiography as described earlier [49].

**APPENDIX**

**Table S3.1 Cell and spore numbers counted in chapter 3.**

| Strain | Sonication – sensitive cells at $T_0$ ($10^7$ / ml) | Sonication – resistant spores at 48 h PS ($10^7$ / ml) | Mature spores at 72 h PS ($10^6$ / ml) |
|---|---|---|---|
| Wild type | $140 \pm 7.4$ | $2.3 \pm 1.1$ | $2 \pm 0.1$ |
| *exoC* | $140 \pm 8.9$ | < 0.05 | $0 \pm 0$ |
| *NfsA-H* | $142 \pm 7.1$ | $1.42 \pm 0.1$ | $0.3 \pm 0.1$ |
| *MXAN_3259* | $160 \pm 14$ | < 0.05 | $0 \pm 0$ |
| *MXAN_5372* | $142 \pm 5.9$ | $4.27 \pm 0.2$ | $2 \pm 1.3$ |
| *mrpC* ($P_{van}$-*fruA*) | $120 \pm 22$ | < 0.05 | $0 \pm 0$ |
| Km$^r$ *nla6* | $120 \pm 15$ | < 0.05 | $0 \pm 0$ |
| *Tc$^r$ nla6* | $110 \pm 16$ | < 0.05 | $0 \pm 0$ |

Wild-type DK1622 and its indicated mutant derivatives were subjected to starvation under submerged culture conditions. Rod-shaped sonication-sensitive cells at $T_0$ and sonication-resistant spores at 48 h PS were counted microscopically using a Neubauer chamber. Mature spores at 72 h PS were quantified by subjecting samples to heat- and sonication-treatments followed by plating on nutrient agar medium and counting of colonies after 5 days. Values indicate average of at least 3 biological replicates and one standard deviation.

**Table S3.2 Changes in transcript levels during development.**

| Transcript level | Ratio 18/6 h PS[a] | Ratio 30/18 h PS[b] |
|---|---|---|
| *exo* | 73 | 14 ± 9 |
| *nfs* | 10 | 3.4 ± 0.6 |
| *MXAN_3259* | 0.85 | 53 ± 21 |
| *fadI* | 2.7 | 3.0 ± 0.8 |

[a]The ratio of average transcript levels at 18 and 6 h PS from Fig. 6. [b]The ratio of average transcript levels at 30 and 18 h PS from Fig. 3.3, 3.5, and S3.2 is reported as the average and standard deviation of the three experiments.

**Table S3.3 Plasmids, strains and primers used in chapter 3.**

| Plasmids | Description | Source |
|---|---|---|
| pSS10 | $Tc^r$; pMR3691 with *fruA* inserted at MCS_G | [34] |
| pSS9 | $Tc^r$; pMR3691 with *fruA (D59E)* inserted at MCS_G | [34] |
| pMR3691 | $Tc^r$; *M. xanthus* MXAN_0018-MXAN_0019-$P_{R3-4}$::*vanR*-$P_{van}$-MCS_G | [58] |
| pMR3487 | $Tc^r$; *M. xanthus* 1.38-kb-$P_{IPTG}$- MCS_A-PR4::*lacI* | [58] |
| pSS11 | $Tc^r$; ColE1 amplified from pMR3487 using PMR3487G Fwd and PMR3487G Rev combined with 600 bp *nla6* fragment starting from +81 till + 699 of Nla6 ORF. | [34] |
| pSS13 | $Tc^r$; ColE1 amplified from pMR3487 using PMR3487G Fwd and PMR3487G Rev combined with 315 bp fragment starting from the upstream region of <u>*exo*</u> promoter (bp -207 to bp +108). | This study |
| pSS14 | $Tc^r$; ColE1 amplified from pMR3487 using PMR3487G Fwd and PMR3487G Rev combined with 373 bp fragment starting from the upstream region of *nfs* promoter (bp -290bp to bp +83) | This study |
| pPV391 | pCR 2.1 TOPO with *dev* DNA spanning bp -321 to +71 generated by PCR | [17] |
| **Strains** | **Description** | **Source** |
| LS3950 | DK1622::*Mxan_5372* ($Km^{40}$) (note that *MXAN_5372* is referred to as *fadI* herein, although *M. xanthus* has a *fadI* paralog that is not up-regulated during development. | [64] |
| AG1152 | DK1622::*Mxan_3259* ($Km^{40}$) | [65] |
| DK10524 | DK1622:: Tn*5 lac* Ω7536 *exoC* ($Km^{40}$) | [26] |
| PH1200 | DK1622::*Δ*(*nfsA-H*) | [23] |
| AG306 | DK1622::*nla6* ($Km^{40}$) | [66] |
| MSS2 | *mrpC*::pRR028 ($Km^r$) MXAN_0018-MXAN_0019::pSS10 ($Tc^r$) | This study |
| MSS3 | *csgA*::pRR028 ($Km^r$) MXAN_0018-MXAN_0019:: pSS10 ($Tc^r$) | [34] |
| MSS5 | *csgA*::pRR028 ($Km^r$) MXAN_0018-MXAN_0019::pSS9 ($Tc^r$) | [34] |
| MSS7 | *fruA*::Tn*5 lac* Ω4491 ($Km^r$) MXAN_0018-MXAN_0019::pSS9 ($Tc^r$) | [34] |
| MSS10 | DK1622::pSS11 | This study |
| DK1622 | Laboratory strain | [67] |

**Table 3.3 (cont'd)**

| Strains | Description | Source |
|---|---|---|
| DK5208 | *csgA*::Tn*5-132* Ω 205 (Tc$^r$) | [68] |
| SW2808 | Δ*mrpC* | [69] |
| DK5285 | *fruA*::Tn*5 lac* Ω4491 (Km$^r$) | [70] |
| DK11209 | Δ*devS* | [71] |
| MRR7 | Δ*devI* | [72] |
| DK5285 | *fruA*::Tn*5 lac* Ω4491 (Km$^r$) | [70] |
| **Primers** | **Description** | **Source** |
| Nla6 Fwd | ATTGATTCCATTTTTACACTGATGAGGTACCGAATTCTGACACAAGG TCGAGAT CGCATT | This study |
| Nla6 Rev | TCTCCTTACGCATCTGTGCGGTATTCTCGAGCCCGGGTCACATCTCG AACACG CCGGG | This study |
| PMR3487 G Fwd | AATACCGCACAGATGCGTAA | This study |
| PMR3487 G Rev | TCATCAGTGTAAAAATGGAATCAATAAA | This study |
| 3487 seq Fwd1 | GTAAAAAGGCCGCGTTGCTGG | This study |
| 3487 seq Fwd2 | CCTTTGATCTTTTCTACGGGG | This study |
| 3487 seq Fwd3 | GTCCATTCCGACAGCATCGCC | This study |
| 3487 seq Fwd4 | ACCAAACGTTTCGGCGAGAAG | This study |
| 3487 seq Fwd5 | CTGGATACCGCGCGGCTCAAG | This study |
| LK1298 | CGAGGACCAGCGCTCGTC | This study |
| LK1331 | CCAAGCTTGCTCACGTTGCAGACGGGG | This study |
| exo -120 fwd | CCTGCTCAGAGCAATGCCTG | This study |
| exo + 1 rev | CCTTGGATCGCAGTGGGTTAC | This study |
| Exo -14 | TGGGTTACGAAGTGCCCTTC | This study |
| Exo -161 | AAATGGGAAGCGGGAGGGGC | This study |
| nfs -201 fwd | CTGCCCCGCGTGACGACC | This study |
| nfs + 1 rev | CTGCCCCGCGTGACGACC | This study |

**Table 3.3 (cont'd)**

| Primers | Description | Source |
|---|---|---|
| Exo -267G | ATTGATTCCATTTTTACACTGATGAGGTACCGAATTCCTTCCT CATCCGACCATCCCC | This study |
| Exo +108G | TCTCCTTACGCATCTGTGCGGTATTCTCGAGCCCGGGCTCGT CTTGCCCATCGTCAGC | This study |
| Nfs -290G | ATTGATTCCATTTTTACACTGATGAGGTACCGAATTCCGCTTC CGGGCCCGATTCCTC | This study |
| Nfs +83G | TCTCCTTACGCATCTGTGCGGTATTCTCGAGCCCGGGGACGG CCAACGAAGCAAAGACG | This study |
| D59E (F) | CCGCAGGTCGCGGTGATGGAGGTGGAGGGCGACAGCGAG | [34] |
| D59E (R) | CTCGCTGTCGCCCTCCACCTCCATCACCGCGACCTGCGG | [34] |
| ExoA-NF4 | CAGCAAGGGCGGACAGAT | This study |
| ExoA-NR4 | CGGAGCATGACCTCGTGT | This study |
| NfsA-NF | TTCTTCATCCTGGACAAGCAC | This study |
| NfsA-NR | TCCAGGTTGACGCGGTAG | This study |
| Mxan_5372 F1 | CTGGAGTCTTCACGGACGAT | This study |
| Mxan_5372 R1 | TCTGTTCGACAACGAGGTCA | This study |
| Mxan_3259 F3 | TCCTCTCCGGGCAGAAGAC | This study |
| Mxan_3259 R3 | GCATCGATGATCTCCGTCA | This study |
| 16S rRNA fwd | CAAGGGAACTGAGAGACAGG | [73] |
| 16S rRNA rev | CTCTAGAGATCCACTACTTGCG | [73] |
| pMR3691MCS G-F | CACGATGCGAGGAAACGCA | [34] |
| pMR3691 MCS G-R | CACCGGTACGCGTAACGTTC | [34] |

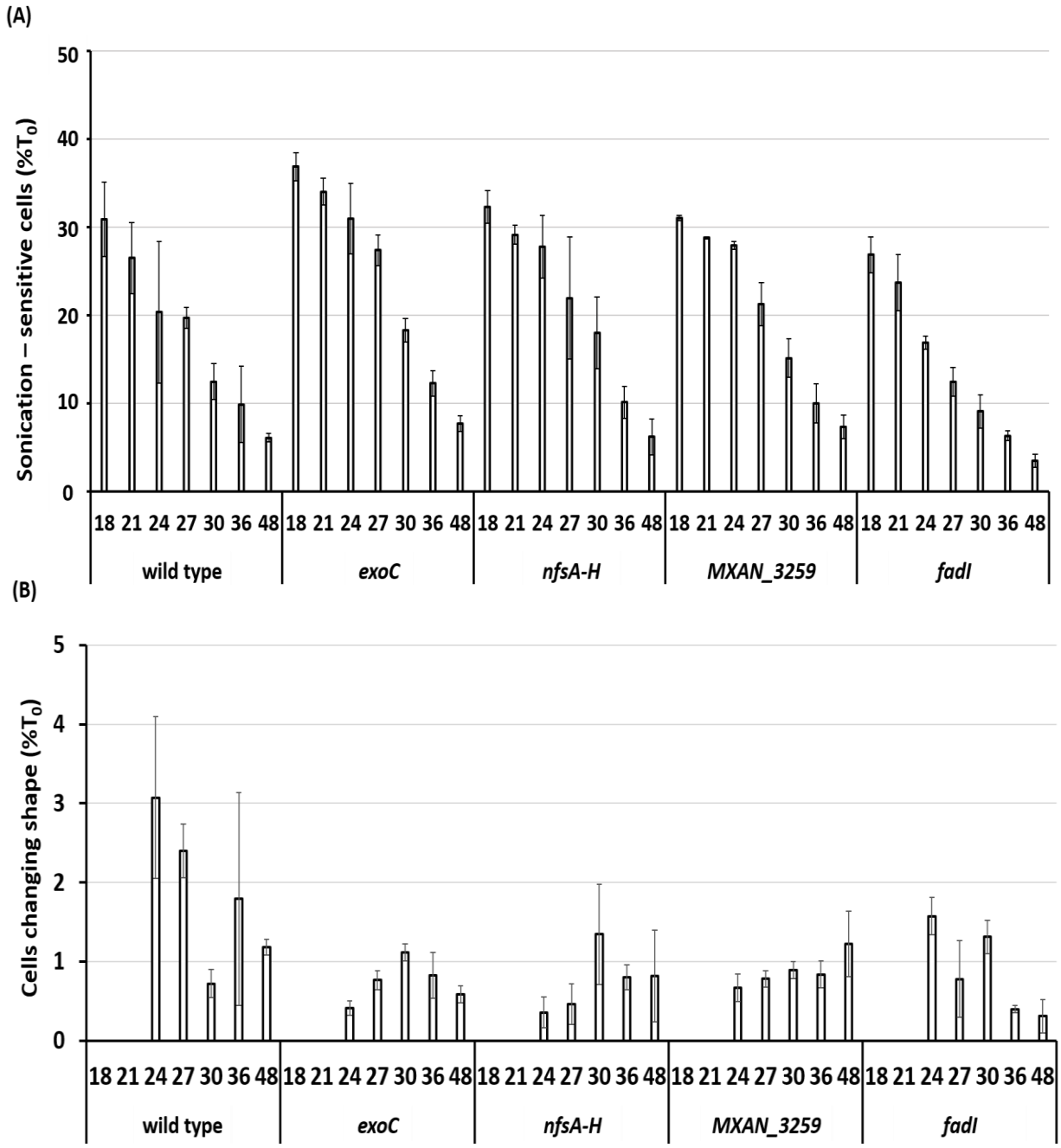


**Figure S3.1 Cellular changes during *M. xanthus* development.** Wild-type strain DK1622 and its mutant derivatives were subjected to starvation under submerged culture conditions. Samples were collected at the indicated hours post-starvation for quantification of (A) sonication-sensitive cells and (B) cells changing shape. Values are expressed as percentage of the number of rod-shaped cells present at the time when starvation-initiated development ($T_0$) (Table S1). Bars show the average of three biological replicates and error bars indicate one standard deviation.

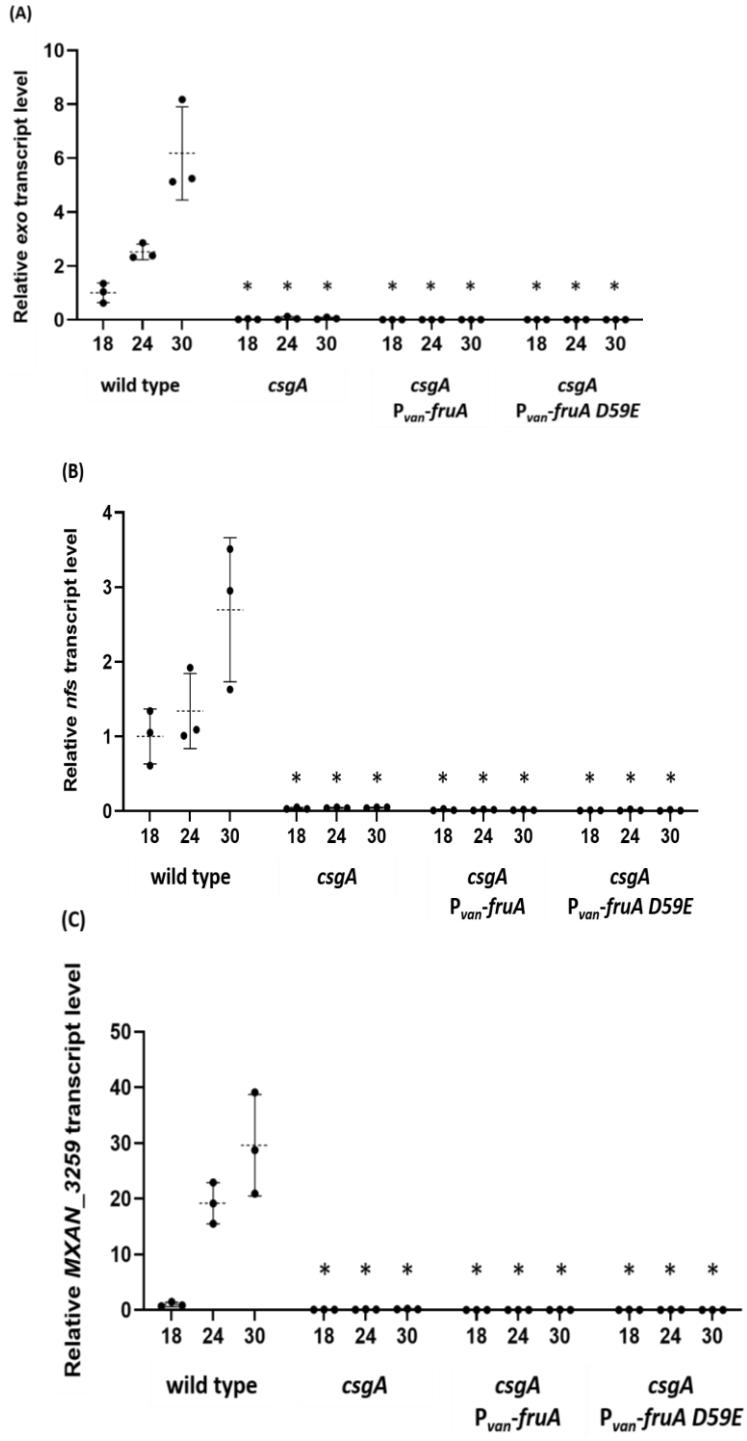


**Figure S3.2 Transcript levels in wild type*, csgA mutant, csgA (P*$_{van}$**-fruA*) mutant, csgA (P*$_{van}$**-f*ruAD59E*) during *M. xanthus* development.**

**Figure S3.2 (cont'd)**

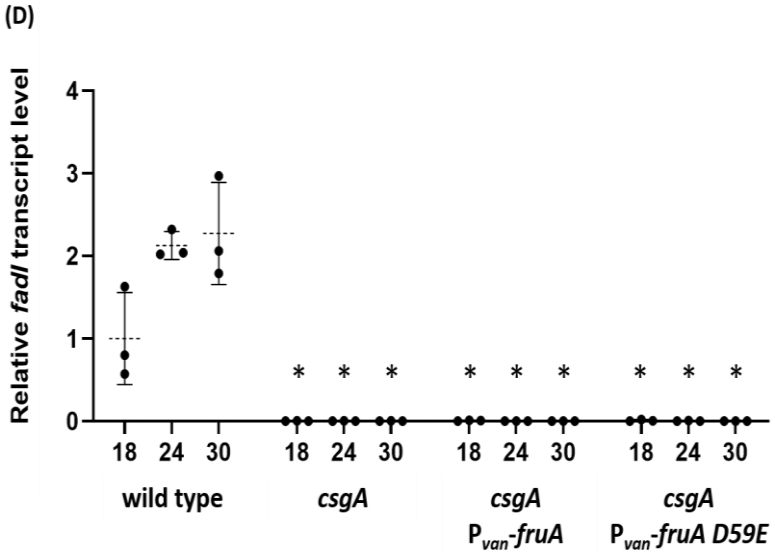


Wild-type strain DK1622 and its indicated mutant derivatives were subjected to starvation under submerged culture conditions and samples were collected at the indicated number of hours poststarvation for measurement of (A) *exo*, (B) *nfs,* (C) *MXAN_3259* and (D) *fadI* transcript levels by RT-qPCR. Induction of $P_{van}$ with vanillate (0.5 mM) during growth and development was as described previously [1]. Graphs show the data points and average of three biological replicates, relative to the wild-type strain at 18 h, and error bars indicate one standard deviation. Asterisks indicate a significant difference ($p < 0.05$ in Student's two-tailed t-tests) from the wild-type strain at the corresponding time poststarvation.

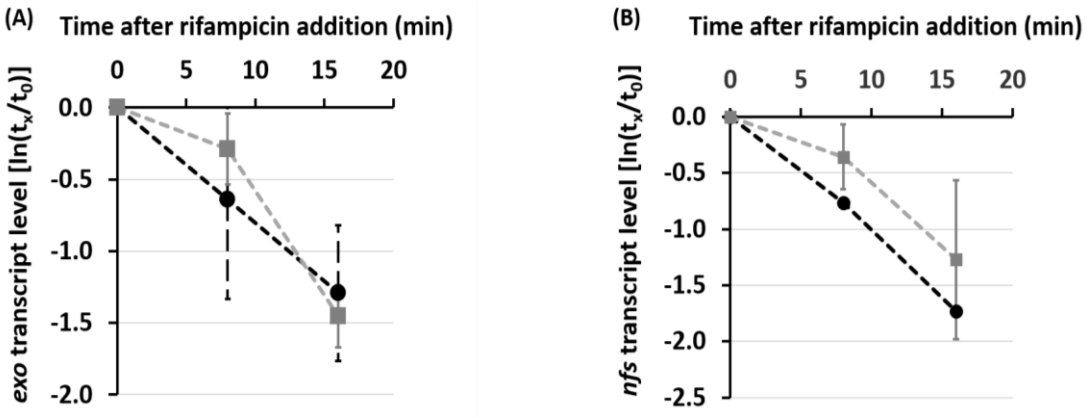


**Figure S3.3 Transcript stability in wild type and *mrpC* mutant.**

**Figure S3.3 (cont'd)**

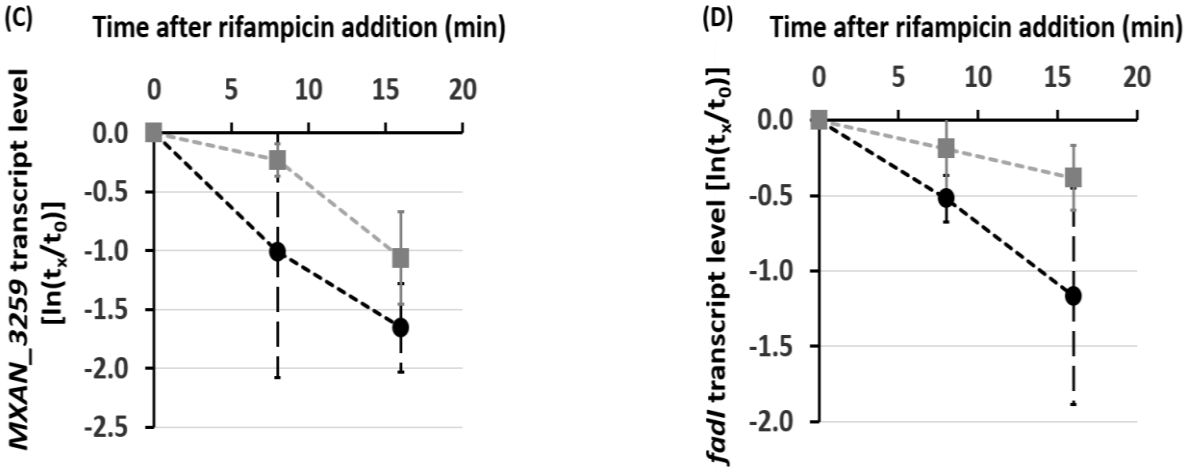


**(E)**

| Transcript | Half-life in the wild-type strain (min) | Half-life in the *mrpC* mutant (min) | *p* value comparing the wild-type strain to the *mrpC* mutant |
|---|---|---|---|
| *exo* | $6 \pm 4$ | $11 \pm 5$ | $p = 0.35$ |
| *nfs* | $7 \pm 0.4$ | $7 \pm 1$ | $p = 0.21$ |
| *MXAN_3259* | $8 \pm 2$ | $12 \pm 5$ | $p = 0.20$ |
| *fadI* | $8 \pm 2$ | $12 \pm 5$ | $p = 0.20$ |

Wild-type strain DK1622 and the *mrpC* mutant were subjected to starvation under submerged culture conditions for 18 h. The overlay was replaced with fresh starvation buffer containing rifampicin (50 mg/mL) and samples were collected immediately ($t_0$) and at the times indicated ($t_x$) for measurement of the *exo* (A), *nfs* (B), *MXAN_3259* (C) and *fadI* (D) transcript level by RT-qPCR. Transcript levels at $t_x$ were normalized to that at $t_0$ for each of three biological replicates and used to determine the transcript half-life for each replicate. The graph shows the average $\ln(t_x/t_0)$ and one standard deviation for the three biological replicates of the wild-type strain and the *mrpC* mutant [2]. The average half-life and one standard deviation, as well as p values from Student's two-tailed *t*-tests, are reported in (E).

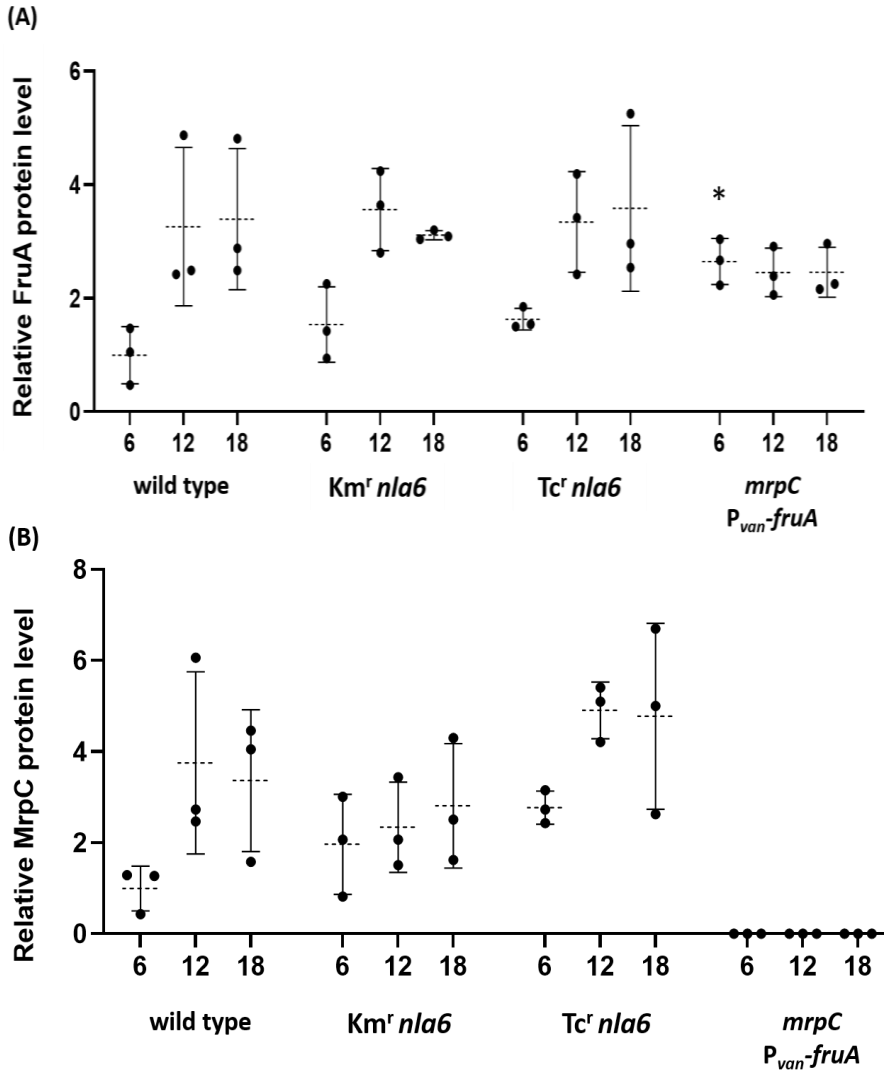


**Figure S3.4 Protein levels in wild type, *nla6*$^{kmR}$ mutant, *nla6*$^{tetR}$ mutant and *mrpC* ($P_{van}$-*fruA*) mutants during early time points.** Wild-type strain DK1622 and its indicated mutant derivatives were subjected to starvation under submerged culture conditions and samples were collected at the indicated number of hours poststarvation for immunoblot analysis as described previously [1] to measure (A) MrpC and (B) FruA levels. Graphs show the data points and average of three biological replicates, relative to the wild-type strain at 6 h, and error bars indicate one standard deviation. The asterisk in panel A indicates a significant difference ($p < 0.05$ in a Student's two-tailed t-test) from the wild-type strain at the corresponding time poststarvation.

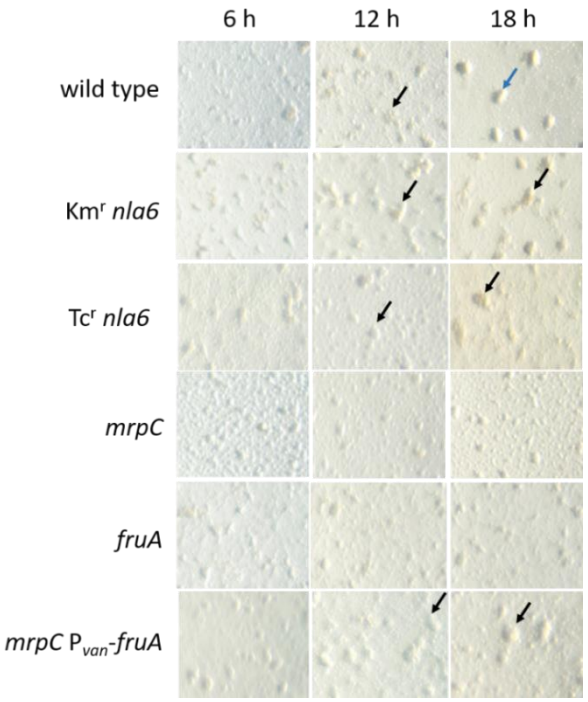


**Figure S3.5 Development of *M. xanthus* strains at early times.** Wild-type strain DK1622 and its indicated mutant derivates were subjected to starvation under submerged culture conditions and images were obtained at the indicated number of hours poststarvation. The wild-type strain, both *nla6* mutants, and the *mrpC* P$_{van}$-*fruA* strain formed nascent mounds by 12 h (black arrows); however, only the wild-type strain formed compact mounds by 18 h (blue arrow). The *mrpC* and *fruA* mutants failed to form mounds.

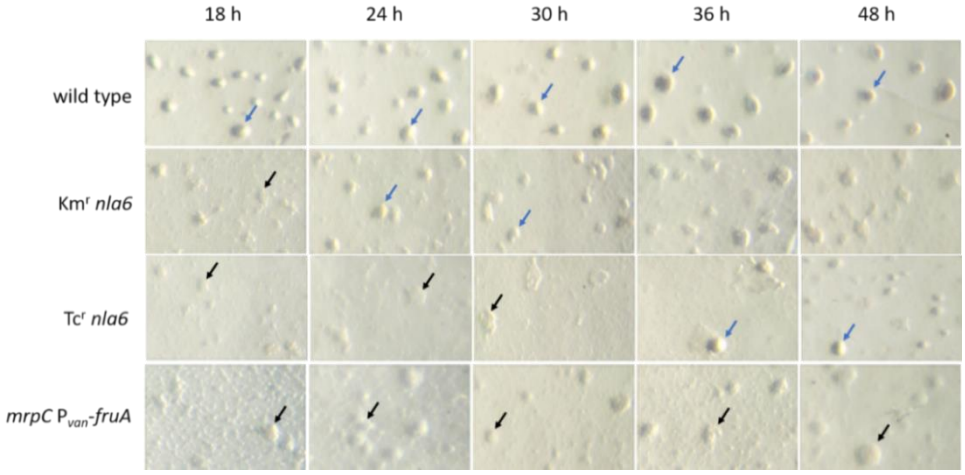


**Figure S3.6 Developmental phenotype of wild type, *nla6*$^{kmR}$ mutant, *nla6*$^{tetR}$ mutant, *mrpC* (P$_{van}$-*fruA*) mutant.**

**Figure S3.6 (cont'd)**

Wild-type strain DK1622 and its indicated mutant derivates were subjected to starvation under submerged culture condition and images were obtained at the indicated number of hours poststarvation. The wild-type strain formed compact mounds (blue arrows) by 18 h, which darkened by 36 h. The Km$^r$ *nla6* mutant formed nascent mounds (black arrows) at 18 h and compact mounds at 24 and 30 h, but the mounds failed to darken and became less compact at 36 and 48 h. The Tc$^r$ nla6 mutant formed nascent mounds by 18 h, but the mounds did not become compact until 36 h and did not darken by 48 h. The *mrpC* P$_{van}$-*fruA* strain formed nascent mounds by 18 h, but the mounds did not become compact and did not darken bv 48 h.

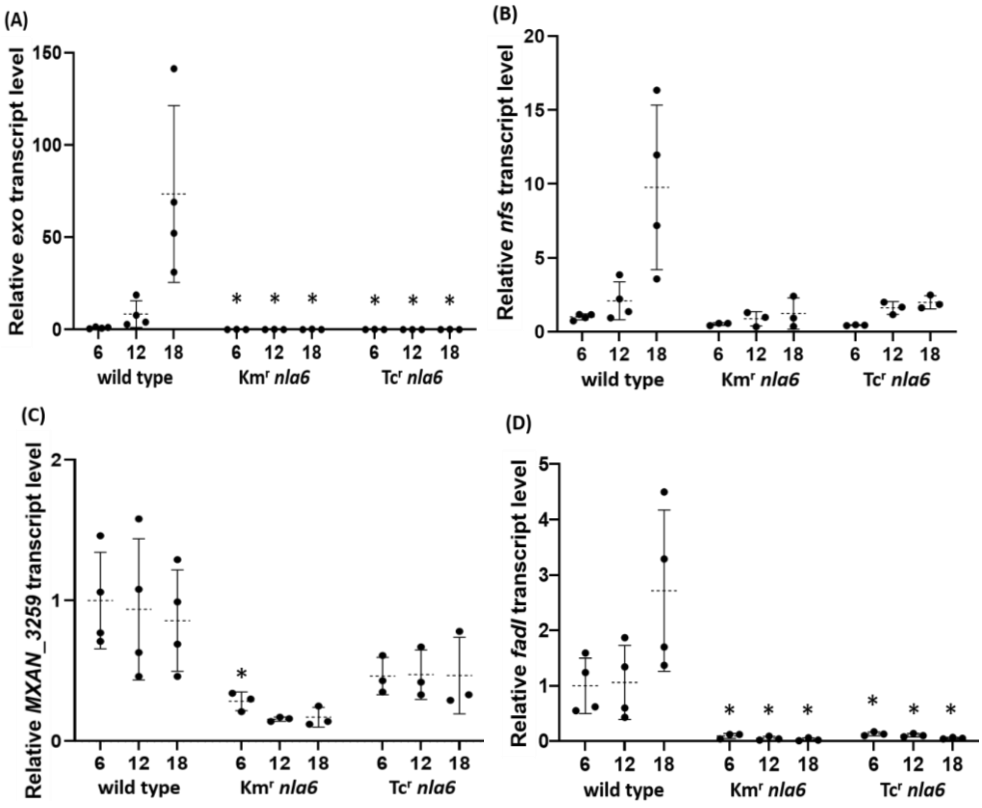


**Figure S3.7 Transcript levels in wild type, *nla6*$^{kmR}$ mutant and *nla6*$^{tetR}$ mutant during early time points.** Wild-type strain DK1622 and its indicated mutant derivatives were subjected to starvation under submerged culture conditions and samples were collected at the indicated number of hours poststarvation for measurement of (A) *exo*, (B) *nfs,* (C) *MXAN_3259* and (D) *fadI* transcript levels by RT-qPCR. Graphs show the data points and average of at least three biological replicates, relative to the wild-type strain at 6 h, and error bars indicate one standard deviation. Asterisks indicate a significant difference ($p$ < 0.05 in Student's two-tailed *t*-tests) from wild type at the corresponding time poststarvation.

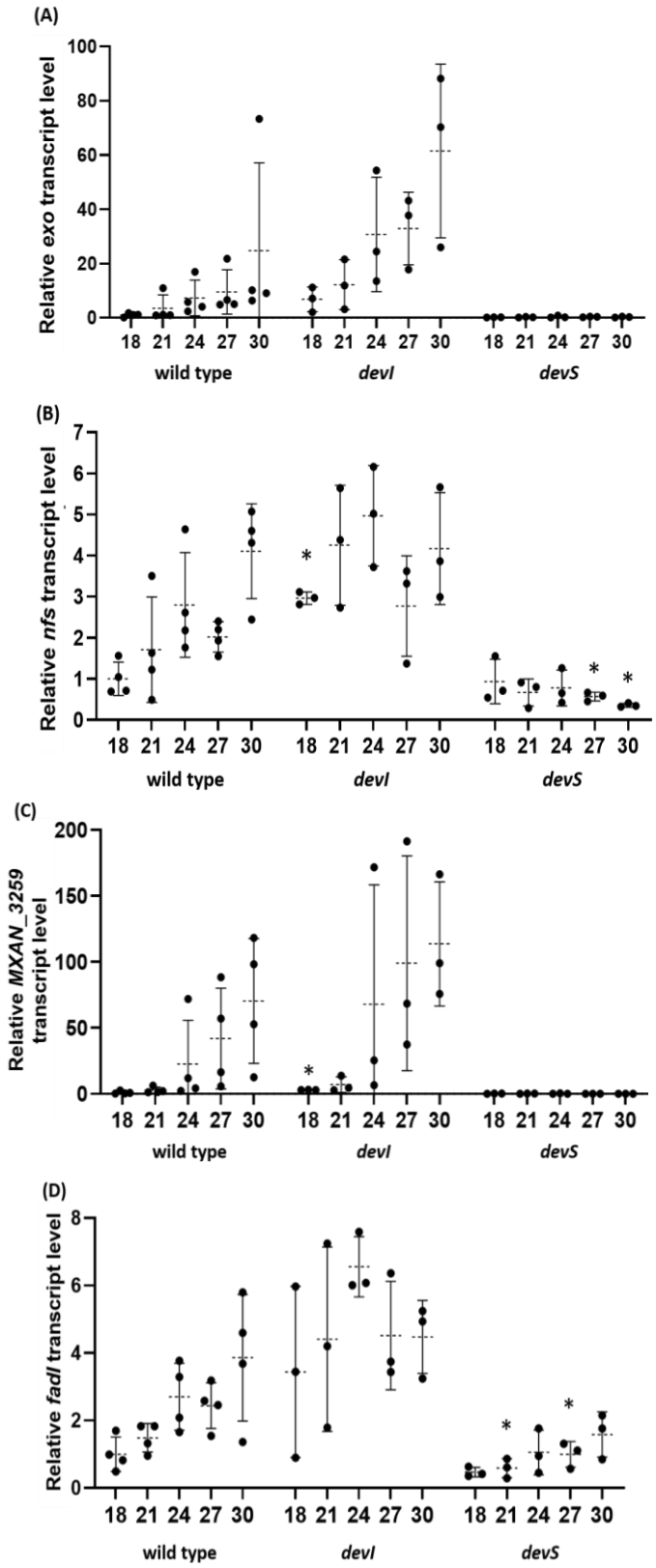


**Figure S3.8 Transcript levels in wild type, *devI* and *devS* mutants.**

**Figure S3.8 (cont'd)**

Wild-type strain DK1622 and its indicated mutant derivatives were subjected to starvation under submerged culture conditions and samples were collected at the indicated number of hours poststarvation for measurement of (A) *exo*, (B) *nfs*, (C) *MXAN_3259* and (D) *fadI* transcript levels by RT-qPCR. Graphs show the data points and the average of at least three biological replicates, relative to the wild-type strain at 18 h, and error bars indicate one standard deviation. Asterisks indicate a significant difference ($p < 0.05$ in Student's two-tailed *t*-tests) from wild type at the corresponding time poststarvation.

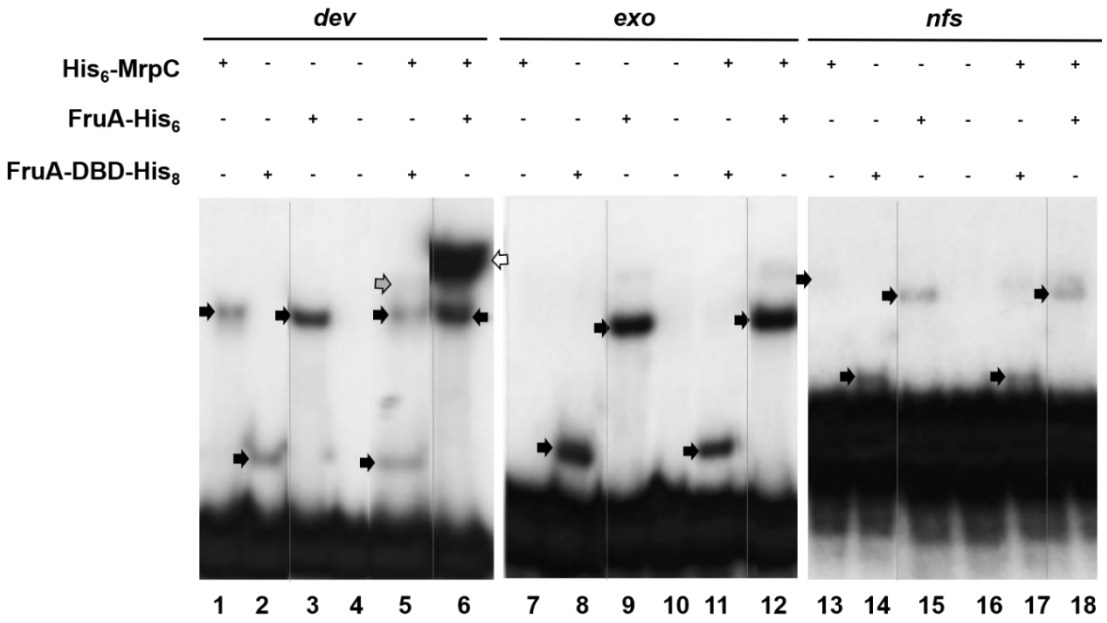


**Figure S3.9 Binding of FruA and MrpC to the *dev, exo* and *nfs* upstream regions.** EMSAs with $^{32}$P-labeled DNA fragments (2 nM) of the dev (-119 to + 1), exo (-120 to + 1) and nfs (-201 to +1) promoter regions and $H_6$-MrpC (1 mM), FruA-$H_6$ (3 mM) and FruA-DBD-$His_8$ (3 mM) as indicated. Black arrows indicate shifted complexes produced by the individual proteins. The gray arrow points to a faint complex indicative of non-cooperative binding by both proteins, whereas the white arrow points to and abundant complex indicative of cooperative binding of the two proteins.

**REFERENCES**

## REFERENCES


1. Saha S, Patra P, Igoshin O, Kroos L: Systematic analysis of the *Myxococcus xanthus* developmental gene regulatory network supports posttranslational regulation of FruA by C-signaling. *Mol Microbiol* 2019, 111:1732-1752.

2. Bui NK, Gray J, Schwarz H, Schumann P, Blanot D, Vollmer W: The peptidoglycan sacculus of *Myxococcus xanthus* has unusual structural features and is degraded during glycerol-induced myxospore development. *J Bacteriol* 2009, 191(2):494-505.

3. O'Connor KA, Zusman DR: Behavior of peripheral rods and their role in the life cycle of *Myxococcus xanthus*. *J Bacteriol* 1991, 173(11):3342-3355.

4. Lee B, Holkenbrink, C, Treuner-Lange, A, Higgs, P. I.: Myxococcus xanthus developmental cell fate production: heterogeneous accumulation of developmental regulatory proteins and reexamination of the role of MazF in developmental lysis. *Journal of bacteriology* 2012, 194(12):3058-3068.

5. Rajagopalan R, Kroos, L.: Nutrient-regulated proteolysis of MrpC halts expression of genes important for commitment to sporulation during Myxococcus xanthus development. *J Bacteriol* 2014, 196(15):2736-2747.

6. Kroos L: Highly signal-responsive gene regulatory network governing *Myxococcus* development. *Trends Genet* 2017, 33:3-15.

7. Crawford EW, Shimkets LJ: The stringent response in *Myxococcus xanthus* is regulated by SocE and the CsgA C-signaling protein. *Genes Dev* 2000, 14(4):483-492.

8. Garza AG, Pollack JS, Harris BZ, Lee A, Keseler IM, Licking EF, Singer M: SdeK is required for early fruiting body development in *Myxococcus xanthus*. *J Bacteriol* 1998, 180(17):4628-4637.

9. Lobedanz S, Sogaard-Andersen L: Identification of the C-signal, a contact-dependent morphogen coordinating multiple developmental responses in *Myxococcus xanthus*. *Genes Dev* 2003, 17(17):2151-2161.

10. Boynton TO, Shimkets LJ: *Myxococcus* CsgA, *Drosophila* Sniffer and human HSD17B10 are cardiolipin phospholipases. *Genes Dev* 2015, 29:1903-1914.

11. Ellehauge E, Norregaard-Madsen M, Sogaard-Andersen L: The FruA signal transduction protein provides a checkpoint for the temporal co-ordination of intercellular signals in *Myxococcus xanthus* development. *Mol Microbiol* 1998, 30:807-817.

12. Ogawa M, Fujitani, S, Mao, X, Inouye, S, Komano, T.: FruA, a putative transcription factor essential for the development of Myxococcus xanthus. *Molecular microbiology* 1996, 22(4):757-767.

13. Mittal S, Kroos, L.: A combination of unusual transcription factors binds cooperatively to control Myxococcus xanthus developmental gene expression. *Proceedings of the National Academy of Sciences of the United States of America* 2009, 106(6):1965-1970.

14. Ueki T, Inouye S: Identification of an activator protein required for the induction of *fruA*, a gene essential for fruiting body development in *Myxococcus xanthus*. *Proc Natl Acad Sci USA* 2003, 100(15):8782-8787.

15. Nariya H, Inouye S: A protein Ser/Thr kinase cascade negatively regulates the DNA-binding activity of MrpC, a smaller form of which may be necessary for the *Myxococcus xanthus* development. *Mol Microbiol* 2006, 60(5):1205-1217.

16. Hoang Y, Kroos L: Ultrasensitive response of developing *Myxococcus xanthus* to the addition of nutrient medium correlates with the level of MrpC. *J Bacteriol* 2018, 200:e00456-00418.

17. Campbell A, Viswanathan, P, Barrett, T, Son, B, Saha, S, Kroos, L.: Combinatorial regulation of the dev operon by MrpC2 and FruA during Myxococcus xanthus development. *Journal of bacteriology* 2015, 197(2):240-251.

18. Viswanathan P, Murphy K, Julien B, Garza AG, Kroos L: Regulation of *dev*, an operon that includes genes essential for *Myxococcus xanthus* development and CRISPR-associated genes and repeats. *J Bacteriol* 2007, 189:3738-3750.

19. Rajagopalan R, Wielgoss S, Lippert G, Velicer GJ, Kroos L: *devI* is an evolutionarily young negative regulator of *Myxococcus xanthus* development. *J Bacteriol* 2015, 197(7):1249-1262.

20. Rajagopalan R, Kroos L: The *dev* operon regulates the timing of sporulation during *Myxococcus xanthus* development. *J Bacteriol* 2017, 199(10):e00788-00716.

21. Holkenbrink C, Hoiczyk E, Kahnt J, Higgs PI: Synthesis and assembly of a novel glycan layer in *Myxococcus xanthus* spores. *J Biol Chem* 2014, 289(46):32364-32378.

22. Muller FD, Schink CW, Hoiczyk E, Cserti E, Higgs PI: Spore formation in *Myxococcus xanthus* is tied to cytoskeleton functions and polysaccharide spore coat deposition. *Mol Microbiol* 2012, 83(3):486-505.

23. Muller FD, Treuner-Lange A, Heider J, Huntley SM, Higgs PI: Global transcriptome analysis of spore formation in *Myxococcus xanthus* reveals a locus necessary for cell differentiation. *BMC Genomics* 2010, 11:264.

24. Bullock HA, Shen H, Boynton TO, Shimkets LJ: Fatty acid oxidation is required for *Myxococcus xanthus* development. *J Bacteriol* 2018, 200(10):e00572-00517.

25. Giglio KM, Zhu C, Klunder C, Kummer S, Garza AG: The enhancer binding protein Nla6 regulates developmental genes that are important for *Myxococcus xanthus* sporulation. *J Bacteriol* 2015, 197(7):1276-1287.

26. Licking E, Gorski, L, Kaiser, D.: A common step for changing cell shape in fruiting body and starvation-independent sporulation of Myxococcus xanthus. *Journal of bacteriology* 2000, 182(12):3553-3558.

27. Ueki T, Inouye, S.: Identification of a gene involved in polysaccharide export as a transcription target of FruA, an essential factor for Myxococcus xanthus development. *The Journal of biological chemistry* 2005, 280(37):32279-32284.

28. Bush M, Dixon R: The role of bacterial enhancer binding proteins as specialized activators of $\sigma^{54}$-dependent transcription. *Microbiol Mol Biol Rev* 2012, 76(3):497-529.

29. Higgs P, Hartzell PL, Holkenbrink C, Hoiczyk E: *Myxococcus xanthus* vegetative and developmental cell heterogeneity. In: *Myxobacteria: genomics, cellular and molecular biology.* Edited by Yang Z, Higgs P. Norfolk, UK: Caister Academic Press; 2014: 51-77.

30. Licking E, Gorski L, Kaiser D: A common step for changing cell shape in fruiting body and starvation-independent sporulation of *Myxococcus xanthus*. *J Bacteriol* 2000, 182(12):3553-3558.

31. Blaylock B, Jiang X, Rubio A, Moran CP, Jr., Pogliano K: Zipper-like interaction between proteins in adjacent daughter cells mediates protein localization. *Genes Dev* 2004, 18(23):2916-2928.

32. Bhat S, Ahrendt T, Dauth C, Bode HB, Shimkets LJ: Two lipid signals guide fruiting body development of *Myxococcus xanthus*. *MBio* 2014, 5(1):e00939-00913.

33. Cavicchioli R, Ripple WJ, Timmis KN, Azam F, Bakken LR, Baylis M, Behrenfeld MJ, Boetius A, Boyd PW, Classen AT *et al*: Scientists' warning to humanity: microorganisms and climate change. *Nat Rev Microbiol* 2019, 17(9):569-586.

34. Saha S, Patra, P, Igoshin, O, Kroos, L.: Systematic analysis of the Myxococcus xanthus developmental gene regulatory network supports posttranslational regulation of FruA by C-signaling. *Molecular microbiology* 2019, 111(6):1732-1752.

35. Rajagopalan R, Kroos L: Nutrient-regulated proteolysis of MrpC halts expression of genes important for commitment to sporulation during *Myxococcus xanthus* development. *J Bacteriol* 2014, 196:2736-2747.

36. Mittal S, Kroos L: A combination of unusual transcription factors binds cooperatively to control *Myxococcus xanthus* developmental gene expression. *Proc Natl Acad Sci USA* 2009, 106:1965-1970.

37. Campbell A, Viswanathan P, Barrett T, Son B, Saha S, Kroos L: Combinatorial regulation of the *dev* operon by MrpC2 and FruA during *Myxococcus xanthus* development. *J Bacteriol* 2015, 197:240-251.

38. Mittal S, Kroos L: Combinatorial regulation by a novel arrangement of FruA and MrpC2 transcription factors during *Myxococcus xanthus* development. *J Bacteriol* 2009, 191:2753-2763.

39. Lee J, Son B, Viswanathan P, Luethy P, Kroos L: Combinatorial regulation of *fmgD* by MrpC2 and FruA during *Myxococcus xanthus* development. *J Bacteriol* 2011, 193:1681-1689.

40. Ueki T, Inouye, S.: Identification of an activator protein required for the induction of fruA, a gene essential for fruiting body development in Myxococcus xanthus. *Proceedings of the National Academy of Sciences of the United States of America* 2003, 100(15):8782-8787.

41. Ueki T, Inouye S: Identification of a gene involved in polysaccharide export as a transcription target of FruA, an essential factor for *Myxococcus xanthus* development. *J Biol Chem* 2005, 280(37):32279-32284.

42. Robinson M, Son B, Kroos L: Transcription factor MrpC binds to promoter regions of many developmentally-regulated genes in *Myxococcus xanthus*. *BMC Genomics* 2014, 15:1123.

43. Caberoy NB, Welch RD, Jakobsen JS, Slater SC, Garza AG: Global mutational analysis of NtrC-like activators in *Myxococcus xanthus*: identifying activator mutants defective for motility and fruiting body development. *J Bacteriol* 2003, 185(20):6083-6094.

44. Huntley S, Hamann N, Wegener-Feldbrugge S, Treuner-Lange A, Kube M, Reinhardt R, Klages S, Muller R, Ronning CM, Nierman WC *et al*: Comparative genomic analysis of fruiting body formation in Myxococcales. *Mol Biol Evol* 2010, 28:1083-1097.

45. Son B, Liu Y, Kroos L: Combinatorial regulation by MrpC2 and FruA involves three sites in the *fmgE* promoter region during *Myxococcus xanthus* development. *J Bacteriol* 2011, 193:2756-2766.

46. Kroos L, Kaiser D: Expression of many developmentally regulated genes in *Myxococcus* depends on a sequence of cell interactions. *Genes Dev* 1987, 1:840-854.

47. Viswanathan P, Ueki T, Inouye S, Kroos L: Combinatorial regulation of genes essential for *Myxococcus xanthus* development involves a response regulator and a LysR-type regulator. *Proc Natl Acad Sci USA* 2007, 104:7969-7974.

48. Viswanathan K, Viswanathan P, Kroos L: Mutational analysis of the *Myxococcus xanthus* Ω4406 promoter region reveals an upstream negative regulatory element that mediates C-signal dependence. *J Bacteriol* 2006, 188:515-524.

49. Yoder-Himes D, Kroos L: Regulation of the *Myxococcus xanthus* C-signal-dependent Ω4400 promoter by the essential developmental protein FruA. *J Bacteriol* 2006, 188:5167-5176.

50. Ogawa M, Fujitani S, Mao X, Inouye S, Komano T: FruA, a putative transcription factor essential for the development of *Myxococcus xanthus*. *Mol Microbiol* 1996, 22(4):757-767.

51. Eichenberger P, Fujita M, Jensen ST, Conlon EM, Rudner DZ, Wang ST, Ferguson C, Haga K, Sato T, Liu JS *et al*: The program of gene transcription for a single differentiating cell type during sporulation in *Bacillus subtilis*. *PLoS Biol* 2004, 2(10):1664-1683.

52. Kroos L: The *Bacillus* and *Myxococcus* developmental networks and their transcriptional regulators. *Ann Rev Genet* 2007, 41:13-39.

53. Arrieta-Ortiz ML, Hafemeister C, Bate AR, Chu T, Greenfield A, Shuster B, Barry SN, Gallitto M, Liu B, Kacmarczyk T *et al*: An experimentally supported model of the *Bacillus subtilis* global transcriptional regulatory network. *Mol Syst Biol* 2015, 11(11):839.

54. McKenney PT, Driks A, Eichenberger P: The *Bacillus subtilis* endospore: assembly and functions of the multilayered coat. *Nat Rev Microbiol* 2013, 11(1):33-44.

55. Shuster B, Khemmani M, Abe K, Huang X, Nakaya Y, Maryn N, Buttar S, Gonzalez AN, Driks A, Sato T *et al*: Contributions of crust proteins to spore surface properties in *Bacillus subtilis*. *Mol Microbiol* 2019, 111(3):825-843.

56. Shuster B, Khemmani M, Nakaya Y, Holland G, Iwamoto K, Abe K, Imamura D, Maryn N, Driks A, Sato T *et al*: Expansion of the spore surface polysaccharide layer in *Bacillus subtilis* by deletion of genes encoding glycosyltransferases and glucose modification enzymes. *J Bacteriol* 2019, 201(19):e00321-00319.

57. Kashefi K, Hartzell P: Genetic supression and phenotypic masking of a *Myxococcus xanthux frzF*$^-$ defect. *Molec Microbiol* 1995, 15:483-494.

58. Iniesta AA, Garcia-Heras, F, Abellon-Ruiz, J, Gallego-Garcia, A, Elias-Arnanz, M.: Two systems for conditional gene expression in Myxococcus xanthus inducible by isopropyl-beta-D-thiogalactopyranoside or vanillate. *Journal of bacteriology* 2012, 194(21):5875-5885.

59. Gibson DG, Young, L, Chuang, R. Y, Venter, J. C, Hutchison, C. A., 3rd, Smith HO: Enzymatic assembly of DNA molecules up to several hundred kilobases. *Nature methods* 2009, 6(5):343-345.

60. Higgs PI, Jagadeesan, S, Mann, P, Zusman, D. R.: EspA, an orphan hybrid histidine protein kinase, regulates the timing of expression of key developmental proteins of Myxococcus xanthus. *Journal of bacteriology* 2008, 190(13):4416-4426.

61. McLaughlin PT, Bhardwaj, V, Feeley, B. E, Higgs, P. I.: MrpC, a CRP/Fnr homolog, functions as a negative autoregulator during the Myxococcus xanthus multicellular developmental program. *Molecular microbiology* 2018.

62. Bradford M: A rapid and sensitive method for the quantitation of microgram quantities of protein utilizing the principle of protein-dye binding. *Anal Biochem* 1976, 72:248-254.

63. Britton RA, Eichenberger P, Gonzalez-Pastor JE, Fawcett P, Monson R, Losick R, Grossman AD: Genome-wide analysis of the stationary-phase sigma factor (sigma-H) regulon of Bacillus subtilis. *J Bacteriol* 2002, 184(17):4881-4890.

64. Bullock HA, Shen, H, Boynton, T. O, Shimkets, L. J.: Fatty Acid Oxidation Is Required for Myxococcus xanthus Development. *Journal of bacteriology* 2018, 200(10).

65. Giglio KM, Zhu, C, Klunder, C, Kummer, S, Garza, A. G.: The enhancer binding protein Nla6 regulates developmental genes that are important for Myxococcus xanthus sporulation. *Journal of bacteriology* 2015, 197(7):1276-1287.

66. Caberoy NB, Welch, R. D, Jakobsen, J. S, Slater, S. C, Garza, A. G.: Global mutational analysis of NtrC-like activators in Myxococcus xanthus: identifying activator mutants defective for motility and fruiting body development. *Journal of bacteriology* 2003, 185(20):6083-6094.

67. Kaiser D, Manoil C: Myxobacteria: cell interactions, genetics and development. *Ann Rev Microbiol* 1979, 33:595-639.

68. Shimkets LJ, Asher, S. J.: Use of recombination techniques to examine the structure of the csg locus of Myxococcus xanthus. *Molecular & general genetics : MGG* 1988, 211(1):63-71.

69. Sun H, Shi, W.: Genetic studies of mrp, a locus essential for cellular aggregation and sporulation of Myxococcus xanthus. *Journal of bacteriology* 2001, 183(16):4786-4795.

70. Kroos L, Kaiser, D.: Expression of many developmentally regulated genes in Myxococcus depends on a sequence of cell interactions. *Genes & development* 1987, 1(8):840-854.

71. Viswanathan P, Murphy, K, Julien, B, Garza, A. G, Kroos, L.: Regulation of dev, an operon that includes genes essential for Myxococcus xanthus development and CRISPR-associated genes and repeats. *Journal of bacteriology* 2007, 189(10):3738-3750.

72. Rajagopalan R, Wielgoss, S, Lippert, G, Velicer, G. J, Kroos, L.: devI is an evolutionarily young negative regulator of Myxococcus xanthus development. *Journal of bacteriology* 2015, 197(7):1249-1262.

73. Ossa F, Diodati, M. E, Caberoy, N. B, Giglio, K. M, Edmonds, M, Singer, M, Garza, A. G.: The Myxococcus xanthus Nla4 protein is important for expression of stringent response-associated genes, ppGpp accumulation, and fruiting body development. *Journal of bacteriology* 2007, 189(23):8474-8483.

## CHAPTER 4: Conclusion and future directions

Studies of bacterial gene regulatory networks (GRNs) have significantly progressed in the recent past. By understanding the mechanisms of gene regulation, this work is not only building a base of fundamental knowledge, but in the case of genes critical for pathogenesis, is elucidating potential targets for the advancement of therapeutic strategies. Additionally, understanding of GRNs governing bacterial sporulation aids elucidation of mechanisms underlying disease transmission [1] and resistance against host immunity [2]. With the advancement of interdisciplinary research, systems biology combining experimental and computational methods has emerged as a powerful approach to study GRNs [3]. By using *Myxococcus xanthus* as a model system, my work has involved the first such systematic approach to elucidate the dynamics of the GRN governing a bacterial multicellular developmental process that culminates in commitment to sporulation. Our systematic analysis uncovered a novel role of the long-known transcriptional activator FruA in negatively regulating expression of network output genes before FruA is activated by C-signaling. From the systematic analysis, the project progressed to mechanistic approaches (i.e. DNA-binding studies) aimed at further elucidating the differential role of upstream transcription factors (MrpC and FruA) in regulating the network output genes. In this chapter, the key findings of the work will be discussed in the context of the outstanding questions and potential future directions.

### *The GRN governing multicellular development of M. xanthus can be studied systematically*

Significant progress was made toward establishing systematic and quantitative methods to study the GRN governing multicellular development of *M. xanthus* [4]. One major accomplishment was the establishment of a higher-throughput, robotic platform for qRT-PCR

analysis to measure RNA levels of large numbers of sample [4]. Reproducibility of the qRT-PCR analysis was tested between biological and technical replicates. In the field of *M. xanthus* development, 16S rRNA has been commonly used as an internal standard for mRNA measurements. By reporting that the yield of total RNA per cell (which is primarily rRNA) remains unchanged during the commitment period, we validated 16S rRNA as a reliable internal control to be used to measure mRNA transcript levels. Another significant accomplishment was the establishment of systematic methods to quantify cellular changes during the commitment period. These methods involve quantification of cell numbers and types followed by computation of the percentage of the starving population committing to the three developmental cell fates (lysis, peripheral rods and spores) [4]. Systematically collected data on transcript and protein levels was used to build a computational model of part of the GRN, which was used to make predictions about experimentally testable hypotheses. A potential extension of the work would be refinement of the computational model by implementing the cell fate data reported in Chapter 2. The magnitude of the molecular changes predicted by the computational model can perhaps be refined by incorporating the percentages of cells in the developing population adopting different cell fates.

***Systematic analysis of the M. xanthus GRN supports C-signal-dependent posttranslational activation of FruA resulting in commitment to form spores***

A significant finding from the systematic analysis was support for a model in which C-signaling posttranslationally activates FruA at least ninefold in order to increase *dev* transcription and commit cells to form spores [4]. C-signaling was earlier suggested to posttranslationally activate FruA by phosphorylation [5]. However, we found that boosting the level of native FruA or a phosphomimetic form of FruA by ectopic expression from a vanillate-inducible promoter in a

mutant defective of C-signaling, did not increase the *dev* transcript level (Chapter 2) [4]. This finding perhaps rules out phosphorylation to be the mechanism by which FruA is activated in response to C-signal. A fascinating extension of this work would be to elucidate the mechanism by which C-signaling activates FruA. Investigations of C-signaling have led to two models discussed in Chapter 1 [6, 7]. One of those models suggests that phospholipase activity of CsgA releases diacylglycerols (DAGs) from the inner membrane, which serve as the C-signal and account for cell shortening during development [7]. DAGs released by CsgA are eventually converted to triacylglycerols (TAGs) by acyltransferases, resulting in formation of cytosolic lipid bodies that may store energy for use later during development [7]. It is possible that β-oxidation of fatty acids released from TAGs elevates cellular acetyl-CoA and FruA is activated by acetylation. In order to test whether FruA gets activated by acetylation, FruA expressed in and purified from *E. coli* could be subjected to *in vitro* acetylation [8]. The DNA-binding ability of acetylated FruA alone and or in combination with MrpC would be tested in EMSA with $^{32}$P-labelled *dev* DNA, and compared with non-acetylated FruA. Greater affinity of acetylated FruA for *dev* DNA would suggest that acetylation of one or more lysine residues of FruA is the mechanism of activation by C-signaling.

If it appears that C-signaling activates FruA by acetylation, the investigation could be further extended by measuring the levels of CsgA and activated FruA (FruA$^{*}$) during development by immunoblot. Commercially available acetylation-specific antibody would be used to determine the level FruA$^{*}$. Anti-FruA antibody would be used to quantify the level of total FruA (activated and unactivated). Using a method devised by Tye Boynton and Larry Shimkets (University of Georgia), I purified CsgA and it was used to generate polyclonal antibodies in rabbits. By

quantifying the levels of CsgA, total FruA and FruA$^*$ during development, the ratio of FruA$^*$ to total FruA as a function of the CsgA could be determined. It would be exciting to observe a steady increase in the FruA$^*$/total FruA ratio, perhaps correlating with an increasing level of CsgA, during the period leading up to and including commitment to spore formation.

If it appears that C-signaling does not activate FruA by acetylation, other approaches to investigate the mechanism of FruA activation could be tried. For example, native FruA has been substituted by a functional histidine-tagged version in *M. xanthus*, both in the wild-type strain and in a *csgA* mutant. Purification of the recombinant protein from both strains followed by mass spectrometry approaches identify a modification and its precise location in the protein from the wild-type strain that is not present in the protein from the *csgA* mutant. Understanding of the mechanism of C-signal-dependent posttranslational modification of FruA would solve a long-standing mystery in the field of *M. xanthus* development and would open up avenues to test the effect of FruA activation on gene expression.

Our systematic analysis in combination with computational modeling suggests that C-signaling activates FruA at least ninefold for cells to increase *dev* transcription and commit to spore formation [4]. It would be fascinating to determine the minimum level of activated FruA required to induce *dev* expression in individual cells committing to form spores. In order to accomplish this, methods to measure gene expression and visualize cellular shape change at the single-cell level are being developed. A functional mNeonGreen-FruA fusion expressed from the native promoter in *M. xanthus* has been created and studied by Y Hoang in our group. Y has also fused the *dev* promoter region and the *fmgE* promote region (which appears to require a higher level of activated FruA for expression) to tdTomato. Both the wild-type strain and a *csgA*

mutant bearing both the mNeonGreen-FruA fusion and a promoter-tdTomato fusion have been created. 3D confocal laser scanning microscopy (CLSM) is being used to measure the green and red fluorescence intensity of individual cells in mound during development. Because tdTomato is cytosolic, red fluorescence also indicates cell shape. Based on the data the computational model can be refined where *dev* serves as the reporter of FruA activity in individual cells undergoing shape change.

***FruA is both a negative and a positive regulator of developmental genes in Myxococcus xanthus***

Our systematic analysis revealed a novel role of unactivated FruA in negatively regulating three of the output genes of the network (*exo*, *nfs*, *MXAN_3259*) (Chapter 3). The EBP Nla6 appears to activate developmental genes at the preaggregation stage of *M. xanthus* development [9] and differentially regulate *exo* expression at different times during development [10]. By binding to the *exo* promoter region, Nla6 is proposed to positively and negatively regulate *exo* transcription early and late in development, respectively [10] One of the two Nla6 binding sites in the *exo* promoter region partially overlaps with the FruA-binding site [11], so negative regulation by unactivated FruA could involve competition for binding with Nla6 (Chapter 3). Experiments are planned to test this model using purified MBP fused to the Nla6 DNA-binding domain (MBP-Nla6 DBD) and FruA in EMSAs. Since the patterns of *nfs* and *MXAN_3259* transcript levels in a *fruA* mutant are similar to *exo* (Chapter 3), it would be a worthwhile future direction to test if MBP-Nla6 DBD and FruA interfere with each other to regulate *nfs* and *MXAN_3259.* An additional motivation for pursuing these competition EMSAs is the earlier evidence showing MBP-Nla6 DBD binding to the *MXAN_3259* promoter region *in vitro* [10]. An

added challenge is that neither the *nfs* nor the *MXAN_3259* transcriptional start site has been mapped yet, which will be important for interpretation of binding results.

We propose that during mound formation unactivated FruA negatively regulates all three output genes by interfering with Nla6 binding, whereas later during development, in response to a higher threshold level of C-signaling [11], FruA$^{*}$ activates transcription of these operons, whose products are involved in spore coat biogenesis. To further extend this work it would be fascinating to elucidate the mechanism by which FruA$^{*}$ replaces inactive FruA at the promoter regions of these operons. It is likely that the promoter regions of *exo, nfs* and *MXAN_3259* would differ in their affinities for FruA and FruA$^{*}$. Presumably, a promoter with a relatively high binding affinity for FruA and/or a relatively low binding affinity for FruA$^{*}$ would require a high level of C-signaling and FruA$^{*}$ in order for transcription to occur. It would be intriguing to perform *in vitro* competition EMSAs to determine whether FruA$^{*}$competes with FruA for binding to the same site(s). For example, if acetylation is the mechanism by which C-signaling activates FruA, then acetylated FruA would be used in competition EMSAs with non-acetylated FruA.

Developmental expression of *fadI* was distinct compared to the other three outputs. Evidence provided in Chapter 3 suggests that transcription of *fadI* is not regulated by unactivated FruA, but is positively regulated by FruA$^{*}$ and MrpC. The close proximity between a putative FruA binding site centered at -110 and a putative MrpC binding site centered at -90 (the centers of both sites are relative to the translation start codon since the transcriptional start site has not been mapped) strongly suggests cooperative binding between the two transcription factors, as observed for *dev* [12] and *fmg* genes [13-15]. Alternatively, MrpC may

regulate *fadI* indirectly by activating *fruA* transcription, resulting in FruA$^{*}$ binding to the *fadI* promoter region in response to C-signaling. Hence, it would be an interesting future direction to test whether MrpC and FruA, individually and/or cooperatively bind to the *fadI* promoter region using EMSAs. Upon detection of MrpC and/or FruA binding, smaller DNA fragments would be used to localize the binding sites, then the sites would be examined for sequences matching the consensus binding sites for MrpC and FruA ) [16]. Mutations designed to eliminate binding of each transcription factor would be introduced into *M. xanthus* by allelic exchange, followed by testing the effect *in vivo* on the *fadI* transcript level by RT-qPCR.

Another interesting future direction of this work would be to design an allele of *fruA* that makes FruA unable to be activated by C-signaling. For example, if FruA appears to be activated by acetylation, substitution of one or more lysine residues with a residue that cannot be acetylated (accomplished by allelic exchange of *fruA* in *M. xanthus*), would be tested by measuring transcript levels of the output genes by RT-qPCR during development. Our results presented in Chapter 3 suggest that activated FruA$^{*}$ positively regulates all four output genes, so in a strain making FruA that cannot be activated, output gene transcript levels are predicted to remain low. This approach has potential to provide additional evidence in support the mechanism of FruA activation and in support of our model for regulation of late gene transcription (Chapter 3).

**Closing remarks**

The work presented in this dissertation has relied on the huge amount of fantastic work that was already done on *M. xanthus* development. My work benefited greatly from established genetic and molecular approaches, and knowledge, in publications contributed by many

scientists. In particular, I thank the scientists who provided us with antibodies, strains and advice, which was important for my work. Our findings have contributed systematic methods and a better understanding of commitment to spore formation in *M. xanthus*. We both elucidated the dynamics of the GRN and discovered a novel role of the previously known transcriptional activator FruA in negatively regulating transcription of network output genes. In the future, there is tremendous potential to extend my work toward a deeper mechanistic understanding of the role of MrpC and FruA in differentially regulating the output genes. I look forward to the discovery of additional novel mechanisms that will advance the fields of signal transduction and gene regulation.

**REFERENCES**

## REFERENCES


1. Shen A, Edwards, A. N, Sarker, M. R, Paredes-Sabja, D.: Sporulation and Germination in Clostridial Pathogens. *Microbiology spectrum* 2019, 7(6).

2. Manganelli R, Provvedi, R.: An integrated regulatory network including two positive feedback loops to modulate the activity of sigma(E) in mycobacteria. *Molecular microbiology* 2010, 75(3):538-542.

3. Durmus S, Cakir, T, Ozgur, A, Guthke, R.: A review on computational systems biology of pathogen-host interactions. *Frontiers in microbiology* 2015, 6:235.

4. Saha S, Patra, P, Igoshin, O, Kroos, L.: Systematic analysis of the Myxococcus xanthus developmental gene regulatory network supports posttranslational regulation of FruA by C-signaling. *Molecular microbiology* 2019, 111(6):1732-1752.

5. Ellehauge E, Norregaard-Madsen, M, Sogaard-Andersen, L.: The FruA signal transduction protein provides a checkpoint for the temporal co-ordination of intercellular signals in Myxococcus xanthus development. *Molecular microbiology* 1998, 30(4):807-817.

6. Lobedanz S, Sogaard-Andersen, L.: Identification of the C-signal, a contact-dependent morphogen coordinating multiple developmental responses in Myxococcus xanthus. *Genes & development* 2003, 17(17):2151-2161.

7. Boynton TO, Shimkets, L. J.: Myxococcus CsgA, Drosophila Sniffer, and human HSD10 are cardiolipin phospholipases. *Genes & development* 2015, 29(18):1903-1914.

8. Christensen DG, Baumgartner, J. T, Xie, X, Jew, K. M, Basisty, N, Schilling, B, Kuhn, M. L, Wolfe, A. J.: Mechanisms, Detection, and Relevance of Protein Acetylation in Prokaryotes. *mBio* 2019, 10(2).

9. Giglio KM, Caberoy, N, Suen, G, Kaiser, D, Garza, A. G.: A cascade of coregulating enhancer binding proteins initiates and propagates a multicellular developmental program. *Proceedings of the National Academy of Sciences of the United States of America* 2011, 108(32):E431-439.

10. Giglio KM, Zhu, C, Klunder, C, Kummer, S, Garza, A. G.: The enhancer binding protein Nla6 regulates developmental genes that are important for Myxococcus xanthus sporulation. *Journal of bacteriology* 2015, 197(7):1276-1287.

11. Ueki T, Inouye, S.: Identification of a gene involved in polysaccharide export as a transcription target of FruA, an essential factor for Myxococcus xanthus development. *The Journal of biological chemistry* 2005, 280(37):32279-32284.

12. Campbell A, Viswanathan, P, Barrett, T, Son, B, Saha, S, Kroos, L.: Combinatorial regulation of the dev operon by MrpC2 and FruA during Myxococcus xanthus development. *Journal of bacteriology* 2015, 197(2):240-251.

13. Lee JS, Son, B, Viswanathan, P, Luethy, P. M, Kroos, L.: Combinatorial regulation of fmgD by MrpC2 and FruA during Myxococcus xanthus development. *Journal of bacteriology* 2011, 193(7):1681-1689.

14. Mittal S, Kroos, L.: A combination of unusual transcription factors binds cooperatively to control Myxococcus xanthus developmental gene expression. *Proceedings of the National Academy of Sciences of the United States of America* 2009, 106(6):1965-1970.

15. Mittal S, Kroos, L.: Combinatorial regulation by a novel arrangement of FruA and MrpC2 transcription factors during Myxococcus xanthus development. *Journal of bacteriology* 2009, 191(8):2753-2763.

16. Robinson M, Son, B, Kroos, D, Kroos, L.: Transcription factor MrpC binds to promoter regions of hundreds of developmentally-regulated genes in Myxococcus xanthus. *BMC genomics* 2014, 15:1123.